

**INTERFERENCE-FREE SPECTRUM
SHARING IN COGNITIVE RADIO
BASED ON SPACE TIME CODING**

M.Sc. THESIS

Mohammadreza BABAEI

Department of Electrical and Electronic Engineering
Electronics and Communication Engineering Program

JUNE 2016

**INTERFERENCE-FREE SPECTRUM
SHARING IN COGNITIVE RADIO
BASED ON SPACE TIME CODING**

M.Sc. THESIS

**Mohammadreza BABAEI
(504131316)**

**Department of Electrical and Electronic Engineering
Electronics and Communication Engineering Program**

Thesis Advisor: Prof. Dr. H. Ümit AYGÖLÜ

JUNE 2016

**BİLİŞSEL RADYO İÇİN
UZAY ZAMAN KODLAMAYA DAYALI
GİRİŞİMSİZ SPEKTRUM PAYLAŞIMI**

YÜKSEK LİSANS TEZİ

**Mohammadreza BABAEL
(504131316)**

Elektrik-Elektronik Mühendisliği Anabilim Dalı

Elektronik ve Haberleşme Mühendisliği Programı

Tez Danışmanı: Prof. Dr. H. Ümit AYGÖLÜ

HAZİRAN 2016

Mohammadreza BABAEI, a M.Sc. student of ITU Graduate School of Science Engineering and Technology 504131316 successfully defended the thesis entitled “**INTERFERENCE-FR SPECTRUM SHARING IN COGNITIVE RADIO BASED ON SPACE TIME CODING**”, which he/she prepared after fulfilling the requirements specified in the associated legislations, before the jury whose signatures are below.

Thesis Advisor : **Prof. Dr. H. Ümit AYGÖLÜ**
Istanbul Technical University

Jury Members : **Prof. Dr. M. Ertuğrul Çelebi**
Istanbul Technical University

Assist. Prof. Dr. Hacı İlhan
Yildiz Technical University

.....

Date of Submission : **02 May 2016**

Date of Defense : **06 June 2016**

*To My Parents who Have Supported Me Throughout My Life
To My Brothers who Have Always Stood by Me
To My Friends who Have Always Believed That I Could Do It,*

FOREWORD

Firstly, I would like to express my sincere gratitude to my advisor Prof. Dr. Ümit Aygözü for the continuous support of my M.Sc study and related research for his patience and motivation as well as immense knowledge. His guidance helped me in all the time of research and writing of this thesis. The door to Prof. Dr. H. Ümit Aygözü office was always open whenever I ran into a trouble spot or had a question about my research or writing. I would like to thank you for encouraging my research and for allowing me to grow as a research scientist. Your advice on research has been priceless.

Besides my advisor, I would also like to thank my committee members, Prof. Dr. M. Ertuğrul Çelebi and Assist. Prof. Dr. Hacı İlhan for their insightful comments and encouragement. I also want to thank you for your brilliant comments and suggestions, thanks to you.

A special thanks to my family. Words cannot express how grateful I am to my parents and my brothers (Alireza - Saeed) for providing me with unfailing support and continuous encouragement throughout my years of study and through the process of researching and writing this thesis.

I would also like to thank all of my friends who supported years, and motivated me to strive towards my goals. This accomplishment would not have been possible without them.

June 2016

Mohammadreza BABAEI
(Telecommunication Eng.)

TABLE OF CONTENTS

	<u>Page</u>
FOREWORD	ix
TABLE OF CONTENTS	xi
ABBREVIATIONS	xiii
LIST OF TABLES	xv
LIST OF FIGURES	xvii
SUMMARY	xix
ÖZET	xxiii
1. INTRODUCTION	1
1.1 Literature Review	1
1.2 Contribution of the Thesis	3
2. WIRELESS COMMUNICATION CHANNELS AND MIMO SYSTEMS ..	5
2.1 Wireless Channel Models	5
2.1.1 Pathloss	6
2.1.2 Shadowing	7
2.1.3 Multipath	7
2.2 MIMO System Models	8
2.2.1 Space time coding.....	10
2.2.1.1 Space time trellis codes	11
2.2.1.2 Space time block codes	11
2.3 Signal Space Diversity.....	14
2.3.1 Coordinate interleaved orthogonal design.....	15
2.4 Cooperative Communication in Wireless Networks	16
2.4.1 Cooperation with relay systems.....	17
2.4.1.1 Decode and forward relaying.....	18
2.4.1.2 Amplify and forward relaying	19
2.4.2 Coded cooperation between users	19
3. COGNITIVE RADIO	21
3.1 Spectrum Sensing	22
3.2 Spectrum Sharing	23
3.2.1 Network architecture	24
3.2.2 Access behavior.....	24
3.2.3 Access technology	24
3.2.3.1 Interweave.....	25
3.2.3.2 Underlay	26
3.2.3.3 Overlay	26
4. SPECTRUM SHARING IN CR USING SIGNAL SPACE DIVERSITY	27
4.1 System Model.....	27

4.2 Outage Analysis.....	30
4.2.1 Primary system outage performance	30
4.2.2 Acceptable distance from primary transmitter	33
4.2.3 Secondary system outage performance	34
4.2.4 Outage performance evaluation.....	35
4.3 Bit Error Probability Analysis	37
4.3.1 Primary system BEP performance.....	37
4.3.1.1 Calculation of $P_{PT \rightarrow ST}^s$	38
4.3.1.2 Calculation of $P_{PT \rightarrow PR}^b$	39
4.3.1.3 Calculation of P_{coop}^b	39
4.3.2 Secondary system BEP performance.....	46
4.3.3 BER performance evaluation.....	46
5. SPECTRUM SHARING IN CR BASED ON COMBINED CIOD AND STBC	51
5.1 System Model and Protocol Description.....	51
5.2 Bit Error Probability Analysis	54
5.2.1 Primary system BEP performance.....	55
5.2.1.1 Calculation of $P_{PT \rightarrow ST}^s$	55
5.2.1.2 Calculation of $P_{PT \rightarrow PR}^b$	56
5.2.1.3 Calculation of P_{coop}^b	56
5.2.2 Secondary system BEP performance.....	62
5.3 BER performance evaluation.....	64
6. CONCLUSIONS	67
REFERENCES.....	69
APPENDICES	73
0.1 Rotated 4-QAM and Irregular 16-QAM.....	74
0.2 Calculation of $P_{PT \rightarrow PR}^b$	74
0.3 Conditional Symbol Error Probability (CSEP) of Irregular 16-QAM in SISO Channel	75
0.4 Maximum Likelihood (ML) Decoding.....	78
0.5 Conditional Pairwise Error Probability (CPEP) Calculation.....	79
CURRICULUM VITAE	81

ABBREVIATIONS

AF	: Amplify and Forward
AWGN	: Additive White Gaussian Noise
BEP	: Bit Error Probability
BER	: Bit Error Rate
CIOD	: Coordinate Interleaved Orthogonal Design
CR	: Cognitive Radio
CSEP	: Conditional Symbol Error Probability
CSI	: Channel State Information
DF	: Decode and Forward
LO	: Local Oscillator
MIMO	: Multiple Input Multiple Output
MISO	: Multiple Input Single Output
MRC	: Maximal Ratio Combining
pdf	: Probability Density Function
PR	: Primary Receiver
PSD	: Power Spectral Density
PSK	: Phase-Shift Keying
PT	: Primary Transmitter
PU	: Primary User
OFDM	: Orthogonal Frequency-Division Multiplexing
QAM	: Quadrature Amplitude Modulation
QoS	: Quality of Service
SEP	: Symbol Error Probability
SER	: Symbol Error Rate
SIMO	: Single Input Multiple Output
SISO	: Single Input Single Output
SNR	: Signal-to-Noise Ratio
SR	: Secondary Receiver
SSD	: Signal Space Diversity
ST	: Secondary Transmitter
STBC	: Space Time Block Code
SU	: Secondary User

LIST OF TABLES

	<u>Page</u>
Table 4.1 : Proposed Protocol Transmission Schedule Using CIOD.....	29
Table 5.1 : Proposed Protocol Transmission Schedule Using both CIOD and STBC.	53

LIST OF FIGURES

	<u>Page</u>
Figure 2.1 : Types of Fading in Wireless Channels.	6
Figure 2.2 : Pathloss, Shadowing and Multipath Effects on Distance and Power.	6
Figure 2.3 : Shadowing Effects on Transmitted Electromagnetic Waves.	7
Figure 2.4 : Multipath Power and Time Effect on Signal.	8
Figure 2.5 : Types of Small-Scale Fading.	9
Figure 2.6 : MIMO with Transmit Diversity and Spatial Multiplexing.	10
Figure 2.7 : Alamouti Scheme.	12
Figure 2.8 : Example of Modulation Diversity.	14
Figure 2.9 : Block Diagram of CIOD.....	15
Figure 2.10 : Wireless Relay Channels.	17
Figure 2.11 : Relay Transmission.	17
Figure 2.12 : Coded Cooperation.....	20
Figure 3.1 : Spectrum Hole Concept.....	22
Figure 3.2 : Cognitive Radio Spectrum Sharing.	22
Figure 3.3 : Spectrum Awareness.....	23
Figure 3.4 : Classification of Spectrum Allocation and Sharing Schemes.	24
Figure 3.5 : Underlay and Interweave Spectrum Sharing Paradigm.....	25
Figure 4.1 : Considered CR Network Model with One Antenna at ST.....	28
Figure 4.2 : Critical Regions for The Proposed Protocol.....	35
Figure 4.3 : Primary System Outage Probability.	36
Figure 4.4 : Secondary System Outage Probability.	37
Figure 4.5 : Irregular 16-QAM Signal Constellation and Its Bit Mapping.....	38
Figure 4.6 : Primary System Bit Error Rate for Irregular 16-QAM ($d_2 = d_4 = 1$ and $d_2 = d_4 = 0.5$).	47
Figure 4.7 : Primary System Bit Error Rate for Irregular 16-QAM ($d_2 = d_4 = 0.75$ and $d_2 = 0.65, d_4 = 0.35$).	48
Figure 4.8 : Secondary System Bit Error Rate for Classical 16-QAM ($d_4 = 1$ and $d_4 = 0.5$).....	49
Figure 4.9 : Secondary System Bit Error Rate for Classical 4-QAM ($d_4 = 1$ and $d_4 = 0.5$).....	49
Figure 5.1 : Considered CR Network Model with Two Antennas at ST.....	52
Figure 5.2 : Primary System Bit Error Performance for Irregular 16-QAM ($d_2 = d_4 = 1$ and $d_2 = d_4 = 0.5$).....	63
Figure 5.3 : Primary System Bit Error Performance for Irregular 16-QAM ($d_2 = d_4 = 0.75$ and $d_2 = 0.65, d_4 = 0.35$).	63
Figure 5.4 : Secondary System Bit Error Performance for Classical 16-QAM ($d_4 = 0.5$ and $d_4 = 1$).....	64

Figure 5.5 : Secondary System Bit Error Performance for Classical 16-QAM
($d_4 = 0.25$ and $d_4 = 0.75$)..... 65

Figure 1 : Rotated 4-QAM. 75

Figure 2 : Signal Constellation of Irregular 16-QAM..... 75

Figure 3 : System Configuration for direct transmission. 75

INTERFERENCE-FREE SPECTRUM SHARING IN COGNITIVE RADIO BASED ON SPACE TIME CODING

SUMMARY

Next generation wireless communications and mobile systems demand higher data rates with maximum bandwidth utilization. Over the past years, some techniques in the literature are provided in various ways where wireless systems should support high data rates. However, this requirement is faced with spectrum scarcity accommodation problem as in spectrum allocation chart where majority of the spectrum is under license. Nevertheless, spectrum measurements show that most of the spectrum is not continuously used based on the frequency, geographical location and time. As a result, this requirement necessitates the efficient use of the available resources by managing spectrum distribution to provide acceptable service quality. Therefore, several approaches in wireless systems are introduced in literature for sharing the available spectrum to overcome the spectrum scarcity problem.

Cognitive Radio (CR) is considered as a potential solution to boost the spectrum utilization and solve the spectrum scarcity in which two different wireless systems could operate in the same frequency band with respect to their priority. CR is an innovative technique and developing area of research for the next wireless generation systems. In CR, to access the licensed bands interweave, underlay and overlay patterns can be used by the Secondary Users (SUs). In the interweave protocol, SUs sense the existence or nonexistence of Primary Users (PUs) to use spectrum holes without causing interference to PUs. In the underlay protocol, SUs are certified to use the licensed spectrum if the interference caused at PUs is below a predetermined interference level. In the overlay protocol, unlicensed users generally pay a price to share a licensed spectrum by cooperating for the benefit of spectrum owners. Different kinds of spectrum sharing model such as hybrid and superposition coding techniques are proposed in the literature. In superposition coding SU combines the PU's and its own signal and then broadcast to both Primary Receiver (PR) and Secondary Receiver (SR). However, this technique causes severe interference in both receivers. Two CR patterns can be combined to approach the hybrid mode where in this case the system has flexibility to operate in different protocols to obtain benefits from the spectrum and cooperate with PU.

One diversity technique that could mitigate the fading channels effect on the transmitted signal is Signal Space Diversity (SSD) also known as modulation diversity. SSD provides performance improvement over fading channels without using extra bandwidth or power. In SSD, constellation points of the modulation are rotated by an angle before the transmission which maximize the minimum product distance of the rotated constellation, and after applying Coordinate Interleaved Orthogonal Design (CIOD) on the rotated constellation an irregular modulation points are acquired. Normally, in cooperative communications overall system spectral efficiency and rate are decreased due to the fact that data takes more than one time slot to be transmitted

to the receiver. However, using SSD and CIOD technique in the system configuration, one can easily enhance the overall spectral efficiency and rate in cooperative systems without adding any complexity to the system.

In this thesis, two different spectrum sharing protocols for cognitive radio operating in overlay mode are proposed. In the first protocol, the primary and secondary system is comprised of PT, PR, ST and SR equipped all with one antenna. SU is allowed to use the shared spectrum band in accordance to cooperate with primary system. We take advantages of the SSD and CIOD concepts in this three-phase overlay protocol to enhance the spectral efficiency, rate and diversity as well as to provide single symbol decoding. In the first transmission time slot, PT broadcasts its signal to PR and ST where ST tries to decode the transmitted signal from PT. If ST correctly decodes the PU's signal, ST forwards the coordinate interleaved signal pair to PR in the second time slot and PR tries to estimate the symbol by received signals from PT and ST. However, in the case that ST could not correctly decode the signal received from PT, PR decodes the symbol only from PT. Finally, SU's signal is transmitted to SR by ST at the third time slot. Due to the fact that a specific time slot is dedicated to SU data transmission, this protocol avoids interference. A critical distance between PT and ST is obtained such that as long as ST is located within that distance the outage probability of PU will be equal or lower than the case that of without spectrum sharing and ST will benefit from the band. The outage probabilities for PU and SU over Rayleigh fading channels are derived in a closed-form expressions and depicted for different target rates. Note that, the theoretic outcomes match perfectly with simulation results. It is shown that a significant performance improvement in the proposed scheme is notable both for PU and SU in comparison to the reference protocol where superposition coding is used at ST. Furthermore, an upper bound on the Bit Error Probability (BEP) of primary system is obtained and supported via simulation results. The simulation results agree well with the theoretical upper bound in the high Signal to Noise Ratio (SNR), respectively. Finally, for the secondary system, BEP performance is the same as classical direct transmission. The BEP performance for 16-QAM and 4-QPSK modulation for different values of the distance between ST and SR are depicted where in both cases simulation. The results confirm the efficiency of the proposed spectrum sharing compared to the reference protocol.

In the second protocol, PU consists of a pair of PT and PR with one antenna and for SU, ST is equipped with two antennas to use the benefits of Maximum Ratio Combining (MRC) and Alamouti techniques and SR has only one antenna. A CR protocol which is configured on overlay mode to share the spectrum of the primary system is presented. SSD, CIOD and Alamouti concepts are used together to benefit from the single symbol decoding, diversity gain and to increase the overall system rate and spectral efficiency. The protocol comprises of three time slots to transmit PU's and SU's data. In the first time slot, PT transmits the primary signal to PR and to both antennas of ST. Then, ST uses the MRC technique to decode the transmitted signal. If ST correctly decodes the transmitted signal from PT, it applies Alamouti coding to transmit the primary and its own symbols to PR and SR in the second and third time slots. Nevertheless, if ST could not correctly decode the signal pair received from PT, PR will estimate the symbol from the direct link $PT \rightarrow PR$. Meanwhile, secondary signal is transmitted in the second and third time slots which provides diversity which enhances SU system performance. This protocol guarantees an interference-free communication for both users by considering the fact that PR and SR could extract their own signal based

on the single symbol decoding technique provided by Alamouti coding. An upper bound for the BEP of the primary system is derived and it is shown that computer simulation results are in perfectly match with the theoretical upper bound in high SNR which validates the theoretical derivations. Results for different values of the distance between PT, ST and PR are obtained where in all cases, they validate the significant improvement in the Bit Error Rate (BER) performance for the proposed protocol. For the secondary system, BEP performance is the same as classical Alamouti code and is depicted for various values of the distance between ST and SR for classical 16-QAM and is compared with the straightforward transmission scheme and with the reference scheme where SU uses nearly all of its power to transmit the PU's signal and SU is in outage in most cases and operates a relay.

BİLİŞSEL RADYO İÇİN UZAY ZAMAN KODLAMAYA DAYALI GİRİŞİMSİZ SPEKTRUM PAYLAŞIMI

ÖZET

Yeni nesil telsiz iletişim sistemleri ve gezgin sistemler daha yüksek veri hızlarının yanında, maksimum bant genişliği kullanımına da gereksinim duyarlar. Son yıllarda, literatürde bazı teknikler telsiz sistemlerin yüksek veri hızlarını destekleyeceği çeşitli şekillerde ortaya konulmuştur. Ancak, yüksek veri hızlarını destekleme gereksinimini karşılamada, spektrumun çoğunun lisanslı kullanıcılara ait olduğu spektrum tahsis tablosunda olduğu gibi spektrum yetersizliği problemiyle karşılaşılır. Bununla birlikte, spektrum ölçümleri frekansa, coğrafi konuma ve zamana bağlı olarak spektrumun büyük bir kısmının sürekli olarak kullanılmadığını göstermektedir. Sonuç olarak, yüksek veri hızlarını desteklemek için spektrum dağılımını kabul edilebilir servis kalitesine göre yöneterek kaynakların verimli bir şekilde kullanılması gerekmektedir. Bu nedenle, telsiz iletişimde mevcut spektrumu paylaşarak spektrum yetersizliği problemini ortadan kaldırmak için pek çok yaklaşım ortaya atılmıştır.

İki farklı telsiz sistemin önceliklerine göre aynı frekans bandında çalıştığı bilişsel radio (CR) spektrum kullanımını arttırmak ve spektrum yetersizliğini çözmek için potansiyel bir yol olarak kabul edilmiştir. CR ilerideki yeni nesil kablosuz sistemler için yenilikçi bir teknik ve gelişen bir araştırma alanıdır. CR’da lisanslı bandlara erişmek için ikincil kullanıcılar (SU) tarafından araya yerleştirme, altına serme ve üstüne serme teknikleri kullanılabilir. Araya yerleştirme tekniğinde, SU’lar birincil kullanıcılara (PU) girişim yaratmadan spektrum boşluklarını kullanmak için PU’ların varlığını ya da yokluğunu sezerler. Altına serme tekniğinde, eğer PU’lardaki girişim önceden belirlenmiş bir girişim seviyesinin altındaysa, SU’lara lisanslı spektrumu kullanma hakkı verilir. Üstüne serme tekniğinde ise, lisanssız kullanıcılar genellikle lisanslı spektrumu paylaşmak için spektrum sahiplerinin yararına işbirliği yaparak bir bedel öderler. Literatürde karma ve toplamsal kodlama teknikleri gibi farklı spektrum paylaşım türleri önerilmiştir. Toplamsal kodlamada SU, PU’nun ve kendi işaretini birleştirir, sonra birincil alıcıya (PR) ve ikincil alıcıya (SR) yayın yapar. Ancak bu teknik her iki kullanıcının alıcılarında önemli girişime neden olur. Sistemin, spektrumdan yarar sağlamak ve PU ile işbirliği yapmak için farklı teknikleri bir araya getirdiği karma yöntemlerden de yararlanabilir.

İletilen işarete kanalların sönmeme etkisini azaltabilen, modülasyon çeşitlemesi olarak da bilinen bir çeşitleme tekniği işaret uzayı çeşitlemesidir (SSD). SSD fazladan band genişliği ya da güç kullanmadan sönmeme kanallarda başarıyı artırır. SSD işleminde veri iletiminin öncesinde modülasyonlu işaret kümeleri belli bir açı ile döndürülür ve döndürülen işaretler arasındaki minimum çarpımsal uzaklık maksimize edilir. Döndürülmüş işaret kümesine koordinat serpiştirmeli dik tasarım (CIOD) uygulandıktan sonra düzensiz bir modülasyonlu işaret kümesi elde edilir. Normalde işbirlikli haberleşmede verinin alıcıya iletilmesi birden fazla zaman aralığı aldığı için tüm sistemin band verimliliği düşer. Ancak, SSD ve CIOD tekniklerini sistem

yapısında kullanmak sistemin karmaşıklığını artırmadan işbirlikli sistemlerde band verimliliğini kolaylıkla artırabilir.

Bu tezde, üstüne serme yöntemiyle çalışan bilişsel radyo için iki farklı spektrum paylaşım protokolü önerilmiştir.

İlk protokolde, birincil sistem her biri bir antenle donatılmış bir birincil verici (PT) ve bir birincil alıcı (PR) ile ikincil sistem ise her biri bir antenle donatılmış bir ikincil verici (ST) ve bir ikincil alıcı (SR) dan oluşmaktadır. Birincil sistem ile işbirliği çerçevesinde, SU'nun PU ya ait spektrum bandını kullanmasına izin verilmektedir. Bu çalışmada hem spektral verimliliği ve çeşitlemeyi artırmak hem de iki kullanıcının karşılıklı girişimini ortadan kaldırmak amacıyla üç zaman aralığında iki kullanıcının iletimini sağlayan CIOD uzay zaman kodlaması kullanan bir iletim protokolu önerilmektedir. İlk zaman aralığında, PT kendi işaretini PR ve ST'ye iletir ve ST iletilen işareti çözmeye çalışır. ST, PU nun işaretini doğru çözerse, serpiştirilmiş birincil işaret koordinat çiftini PR'ye ikinci zaman aralığında iletilmektedir ve PR, PT ve ST'den aldığı işaretler yardımıyla işareti çözmeye çalışır. Ancak, ST'nin PT'den aldığı işareti doğru çözemediği durumda, PR sadece ilk zaman aralığında PT den gelen işarete dayanarak iletilen işareti çözmeye çalışır. Son olarak, ST üçüncü zaman aralığında kendi (ikincil) işaretini SR'ye iletir. Önerilen protokolde ikincil kullanıcıya ayrı bir zaman aralığı ayrılması iki kullanıcı arasındaki girişimi kaldırırken iki birincil işaretin CIOD yardımıyla iki zaman aralığında iletilmesi üç kanal kullanımı başına iki birincil işaretin iletilmesini sağlamakta, böylece iki kanal kullanımı başına bir birincil işaretin iletildiği referans sistemlere göre kanalın daha verimli kullanılmasını sağlamaktadır. PT ile ST arasında bir kritik uzaklık tanımlanmakta, ST, PT ye bu uzaklıktan daha yakın olduğu sürece PU nun servis kesilme olasılığı spektrum paylaşımı olmadığı durumdakine eşit veya daha düşük olmaktadır. Rayleigh sönümlenmeli kanalda, PU ve SU nun servis kesilme olasılıkları için kapalı biçimde kuramsal ifadeler türetilmekte, hedeflenen farklı hızlar için protokolün başarımı değerlendirilmektedir. Kuramsal sonuçların bilgisayar benzetimleriyle bütünüyle uyum içerisinde olduğu görülmektedir. Önerilen protokol için hem PU nun hem de SU nun başarımında ST de toplamsal kodlamanın kullanıldığı literatürde verilen referans protokole göre önemli kazançlar elde edilmektedir. Diğer yandan birincil kullanıcının bit hata olasılığı için kuramsal bir üst sınır elde edilmekte, sonuçlar bilgisayar benzetimleriyle desteklenmektedir. Beklendiği gibi bilgisayar benzetim sonuçları artan işaret-gürültü oranı ile kuramsal üst sınıra yaklaşmaktadır. Son olarak, ikincil kullanıcının BER başarımı klasik doğrudan iletme eşdeğerdir. 4QAM ve 16QAM modülasyonları ve ST ile SR arasındaki uzaklığın farklı değerleri için elde edilen BER başarımları önerilen protokolün toplamsal kodlamalı referans protokole üstünlüğünü ortaya koymaktadır.

İkincil protokolde birincil kullanıcı, birer antenli PT ve PR den oluşurken ikincil kullanıcı için ST iki antenli olup SR bir antenlidir. ST bir önceki protokolden farklı olarak en büyük oran birleştirme (MRC) ve Alamouti uzay-zaman kodlama tekniklerinden yararlanmaktadır. Protokol yine üstüne serme tekniğine dayalı olup spektral verimliliği artırma, çeşitleme sağlama ve alıcılarda girişimi önleme amacıyla CIOD ve Alamouti uzay zaman kodlama teknikleri bir arada kullanılmaktadır. Protokol PU nun iki, SU nun bir işaretini üç zaman aralığında iletmektedir. Birinci zaman aralığında PT iki birincil işaretin yalnız gerçel ve sanal kısımlarını PR ve ST ye iletmekte, ST iki anteni yardımıyla MRC uygulayarak bu iki birincil işareti yalnız

gerçel ve sanal bileşenlerinden çözmekte, ikinci zaman aralığında ilişkin sanal ve gerçel bileşenleri bir araya getirerek birinci anteninden PR ye iletmektedir. Kendi ikincil işaretini ise aynı anda ikinci anteninden SR ye iletmektedir. Üçüncü zaman aralığında ise ikinci zaman aralığında ilettiği işaretlere Alamouti uzay zaman blok kodlaması uygulayarak her iki anteninde iletmektedir. ST, PT den gelen işareti çözemezse ikinci ve üçüncü zaman aralıklarında Alamouti koduna uygun biçimde kendi işaretini iletmektedir. Protokol hem PR hem de SR de Alamouti kodlamasının getirdiği tek simge çözüme özelliğiyle girişimi ortadan kaldırmakta ayrıca her iki kullanıcı için uzay çeşitlemesi sağlamaktadır. Tezde birincil kullanıcının bit hata olasılığı için kuramsal bir üst sınır türetilmekte, üst sınırın geçerliliği bilgisayar benzetim sonuçlarıyla desteklenmektedir. PT, ST ve PR arasındaki farklı uzaklık değerleri için sonuçlar irdelenmekte, protokolün sağladığı BER başarımlarını kazancı referans protokolle karşılaştırılarak ortaya konmaktadır. Diğer yandan, ikincil kullanıcının BER başarımlarını klasik Alamouti kodununkine eşdeğer olmakta, ST ile SR arasındaki uzaklığın çeşitli değerleri ve 16QAM modülasyonu için irdelenmekte, doğrudan iletim durumu ve toplamsal kodlamasının kullanıldığı referans protokolle karşılaştırılarak üstünlüğü ortaya konmaktadır.

1. INTRODUCTION

In recent years, the increasing wireless applications are faced with the spectrum accommodation problem as in spectrum allocation chart [1], most of the spectrum is under use. There is also a common misconception that the current spectrum is becoming deficient. However, this deficiency is not because of its physical lack, but of the poor management of spectrum distribution. Furthermore, spectrum measurements show that large amount of the spectrum is not continuously used [2].

CR [2–7] has emerged in the last decade as a great deal to solve the accommodation problem of spectrum utilization and to increase the spectrum efficiency by allowing lower priority unlicensed users to use the licensed spectrum of PUs with higher priority. To access to the licensed band, three major approaches are introduced in the literature. Interweave, underlay and overlay patterns can be used by the secondary users (cognitive users). In the interweave protocol, SU senses the presence or absence of PU to use vacant spectrum without causing interference at PU. In the underlay protocol, SU is allowed to use the spectrum if the interference at PU is below a predefined interference level. In the overlay protocol, PU shares its spectrum with SU and in return it benefits from cooperation and therefore better error performance. Different alternative methods are proposed for the application of these three patterns. A number of different models for spectrum sharing in cognitive radio have emerged in the literature, and in most of them superposition coding [3] and hybrid approaches are used [5, 6]. Hybrid approaches combine two of the interweave, overlay and underlay patterns.

1.1 Literature Review

Several alternative methods are proposed for the overlay protocol. In protocols applying superposition coding, ST allocates some of its power to transmit primary signal and the remind power to send its own signal. This type of power allocation for sending symbols simultaneously in the same time slot causes severe interference

at both receivers and limits especially the performance of secondary system. In cooperative cognitive radio protocol given in [3], also referred to compare our results, a distance limit from PT to ST is introduced and as long as ST is located within this distance limit from PT, it can act as a cognitive radio to cooperate with PU and can transmit its own signal by using the superposition coding technique. This protocol works in two time slots, where at the first time slot PT transmits the primary signal and at the second time slot ST broadcasts the superimposed primary and secondary signals, if it is able to successfully decode the primary signal which is transmitted by PT. In that case, the primary system has only need to be aware of Decode-and-Forward (DF) relaying mode operation and does not have to be aware of whether the relay is a passive node or a secondary system transmitter. The problem with this method is that it cannot work at high rates. As an example, for a rate of 4 bits/sec/Hz for 16-QAM which is a small rate in today's wireless demand, secondary system allocates more than 99% of its power to transmit primary user's signal. As a result, less than 1% is remained for the secondary user's signal. In this case, the secondary system plays mostly the role of passive relay node for the primary system without sufficiently benefiting from the link and most of the time will be in outage. Many researchers have proposed cognitive radio systems combining two of interweave, overlay and underlay protocols. In [5], a novel hybrid spectrum sharing protocol for SU based on primary system Quality of Service (QoS) has been proposed. In this protocol, if the required QoS for PU is satisfied, PU shares its licensed band with SU and SU benefits from the spectrum by operating on underlay mode with an allowable interference threshold. On the other hand, an overlay protocol must be applied at SU to help PU to obtain the required QoS. As a result, SU operates on both overlay and underlay mode. In [6], the cognitive system can switch from the interweave mode to the underlay mode to maximize the throughput of SU while satisfying the aimed target rate of PU. In [8], a protocol which avoids the mutual interference in both PU and SU system is proposed. In [9], a three phase cooperative spectrum sharing technique in cognitive radio is presented. ST and PR receives the transmitted signal from PT, then ST decodes and retransmits the signal to PR in the second phase. At the last phase, ST sends its own data to SR. Cooperative relaying in multi-user cognitive radios for spectrum sensing has been presented in [10]. In [11], a power control strategy is proposed to maximize SU's achievable rate without any degradation in PU's outage probability.

In cooperative communication, user's data is not only transmitted from the source but also regenerated and retransmitted from the relay in the next time slot. As a result, the overall spectral efficiency of the system is decreased by half in comparison with the non-cooperation mode (direct transmission). Therefore, in this thesis, we use the SSD and CIOD concepts to increase the system spectral efficiency. In SSD, symbols are rotated by an optimized angle in a way to maximize the minimum product distance of the rotated constellation [12,13], where a cooperative communication based on the SSD concept is presented. In [14], some parts of the rotated symbols are transmitted from the source and the other parts are regenerated and sent by a relay. [15] proposes a system with a single relay using SSD concept to enhance the overall system spectral efficiency compared to direct communication and also provides diversity gain by exposing the real and imaginary parts of the symbol to different channel fading coefficients. Performance analysis of the CIOD and decoding procedure are given in [16, 17].

1.2 Contribution of the Thesis

In Section.4, a new overlay spectrum sharing protocol based on SSD, is proposed for cognitive radio networks. The considered network comprises of one licensed PT/PR pair and one ST/SR pair assisting for cooperation before transmitting its own signal on the licensed primary user's spectrum. The overall transmission is completed in three signaling intervals to avoid any mutual interference between users and the SSD is provided by CIOD which increases the transmission rate of the PU's. The outage probabilities of both primary and secondary users are analytically derived and supported via computer simulations. The results show that significant performance improvement is provided by the proposed protocol compared to the non-cooperation case and the reference scheme [3] based on the transmission of superimposed primary and secondary signals which causes severe interference at both users. Moreover, an upper bound on the BEP of the primary system is analytically derived and supported via computer simulation results.

In Section.5, a spectrum sharing protocol that combines CIOD and Alamouti's STBC is proposed for CR networks. PT and PR are equipped both by one antenna while ST and SR are equipped by two and one antennas, respectively. CIOD applied by means

of PT and ST, provides signal-space diversity at PR and STBC, especially Alamouti coding applied at two antennas of ST avoids interference at both PR and SR while providing spatial diversity for both receivers. An upper bound on the BEP of primary system is analytically derived for Rayleigh fading channels and supported via computer simulations. The results show that the new protocol significantly improves the primary system bit error performance compared to the conventional non-cooperative case and the reference cooperative scheme based on the transmission of superimposed primary and secondary signals from ST which causes severe interference at both users; while allowing the secondary system's periodic access with an improved performance level.

2. WIRELESS COMMUNICATION CHANNELS AND MIMO SYSTEMS

Transmitted data from one point to another is passed through a medium referred as channel which could be wired like a fiber or a wireless link. Wireless channels differ from wired ones due to their unreliable behavior. Wireless channel's state may change within a short time span. These state changes in channel depending on the distance between two antennas, the path taken by the signal and the environment around the path. Furthermore, different propagation environments have been identified such as urban, suburban, indoor and underwater. Due to the rapid change of wireless channel state and even the speed of the mobile antennas, performance in wireless communication is limited. This change in channel state makes the communication over wireless a difficult task.

2.1 Wireless Channel Models

Wireless channel models can be classified into large-scale and small-scale fading as shown in Fig.(2.1) [18]. The three components of the wireless channels are pathloss, shadowing and multipath which should be considered when designing and evaluating the wireless system performance. Moreover, pathloss depends only on the distance from transmitter to receiver and as a result it has a deterministic effect since in most cases distance does not significantly changes. However, shadowing and multipath are not deterministic and are random processes which are based on the environmental conditions such as urban or suburban areas and obstacles like buildings. The result of the multipath is fading which causes significant attenuation changes in the signals. The total attenuation can be written as [19]

$$a(t) = a_P(t).a_S(t).a_F(t) \quad (2.1)$$

where $a_P(t)$, $a_S(t)$ and $a_F(t)$ denote pathloss, shadowing and multipath attenuation on signal, respectively. The effects of these three components on the transmitted signal is shown in Fig.(2.2).

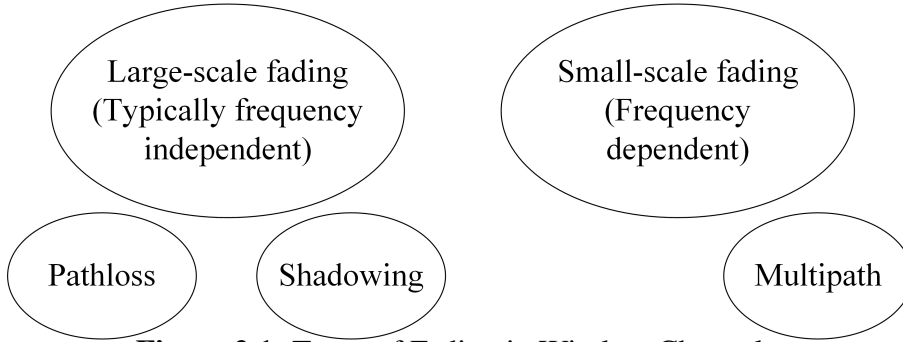


Figure 2.1: Types of Fading in Wireless Channels.

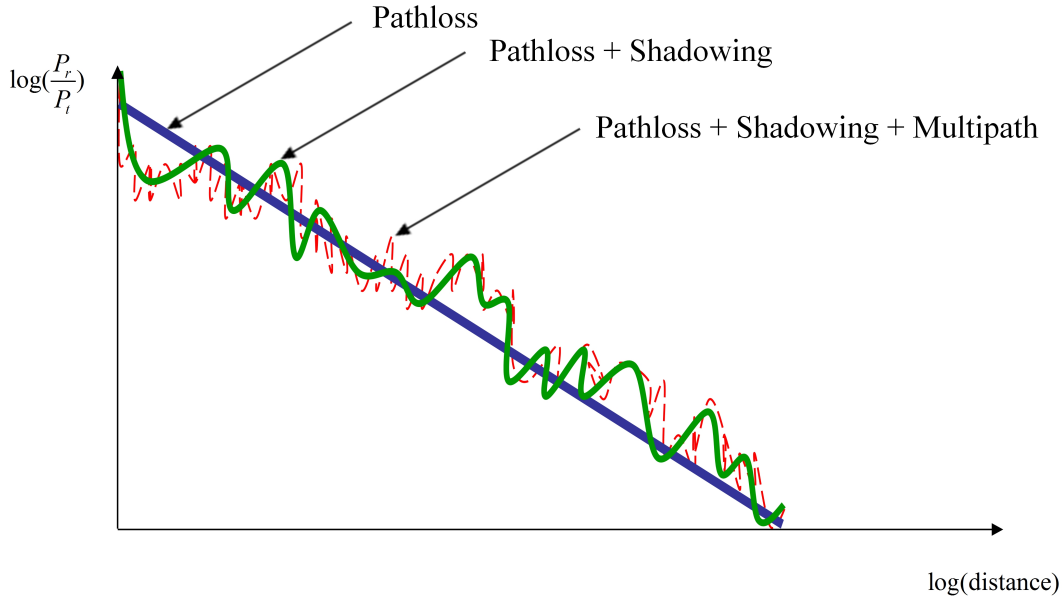


Figure 2.2: Pathloss, Shadowing and Multipath Effects on Distance and Power.

2.1.1 Pathloss

In the propagation of radio wave in free space with line of sight, the transmitted signal spread spherically around the transmitter antenna and attenuates. The power decreases inversely proportional to the square of the distance; however, by considering the terrestrial effect this decrease in the power is given by the pathloss exponent taking values from 2 to 4. In general, the common empirical formula for pathloss can be calculated as [19]

$$P_r = P_t P_0 \left(\frac{d_0}{d} \right)^\alpha \quad (2.2)$$

where P_t is the transmitted power, P_0 is the power at distance d_0 and α is the pathloss exponent as well as d is the distance. However, considering the actual environment to be complex some empirical pathloss models are given as Hata Model, Cost 231 (Extension to Hata Model), Cost 231-Walfish-Ikegami Model, Erceg Model, Stanford University Interim (SUI) Channel Model and ITU Pathloss Models [19].

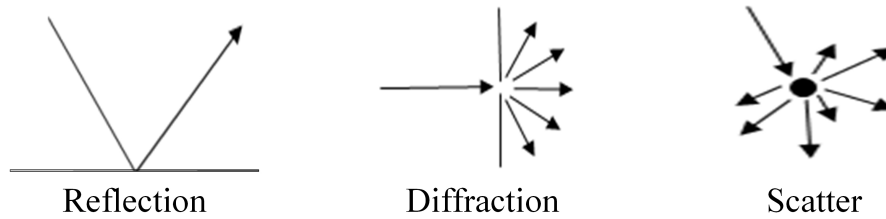


Figure 2.3: Shadowing Effects on Transmitted Electromagnetic Waves.

2.1.2 Shadowing

Some part of the transmitted signal may be lost through reflection, diffraction and scattering along the transmission period as shown in Fig.(2.3). For shadowing the distribution would be log-normal.

2.1.3 Multipath

In the real world the objects that are placed around the wireless signal path reflect the signal. These reflected signals may take different paths and are received at the destination with different phases and amplitudes. Therefore, a slight change in the position of the transmitter and/or receiver antenna has different phase and amplitude effects. Because different paths have different lengths a single transmitted signal will result in multiple copies of the signal with different phase, amplitude and delays that is drawn in Fig.(2.4).

Some of the fading distribution models are Rayleigh and Rician as well as Nakagami fading. Rayleigh fading is considered when there is no line of sight between transmitter and receiver, while Rician Fading is used when there is a line of sight. Rayleigh fading could be useful model in metropolitan cities where there is no line of sight. Note that Rayleigh fading is a small-scale effect. In Rician fading one of the path that is in line of sight is stronger than the other paths. Nakagami fading often gives best fit to indoor-mobile and outdoor-mobile multipath propagation.

Fading could be classified as slow, fast, flat and frequency selective fading as shown in Fig(2.5) where coherence time is a statistical measure of time interval over which the channel can be considered “time invariant” and coherence bandwidth is a statistical measure of range of frequency over which the channel can be considered flat. Doppler spread is a shift in frequency due to the motion.

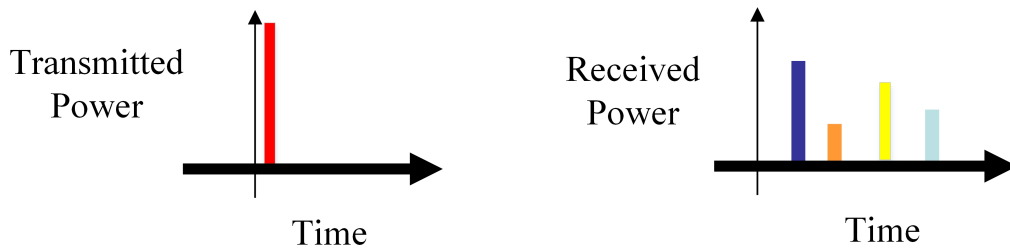


Figure 2.4: Multipath Power and Time Effect on Signal.

In flat fading, the bandwidth of the signal is smaller than the coherence bandwidth of the channel. As a result, the signal frequency components would have the same magnitude of fading; however, in frequency-selective fading the bandwidth of the signal is larger than the coherence bandwidth of the channel and therefore frequency components of the signal experience different fading effects.

In slow fading, signal amplitude and phase changes are considered to be constant over a period of time. Slow fading occurs when the coherence time of the channel is large relative to the signal duration. In fast fading, coherence time of the channel is small relative to the signal duration where it is assumed that the phase and amplitude of the signal change significantly over the time.

However, we can decrease the effect of fading on the system performance by using diversity techniques which transmit the data from different channels to experience different and independent fading effects based on the fact that the probability of a deep fade in all channels is small. Diversity can be provided in time, frequency or/and space. Common methods to mitigate fading are Multiple Input Multiple Output (MIMO), Orthogonal Frequency-Division Multiplexing (OFDM), Rake receivers, Space Time Coding (STC) and diversity at transmitter and/or receiver.

2.2 MIMO System Models

In a wireless network the communication can occur via Single Input Single Output (SISO) channel which has no spatial diversity, Single Input Multiple Output (SIMO) channel achieve receive diversity, whereas transmit diversity is obtained with Multiple Input Single Output (MISO) channel and finally MIMO channel provides both transmit and receive diversities. Spatial diversity can be attained by using multiple antennas at the transmitter and/or the receiver. As a result, MIMO technology has involved much

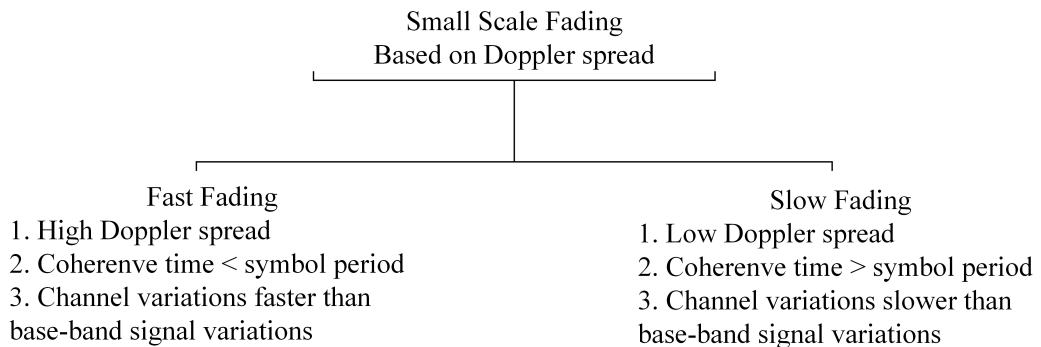
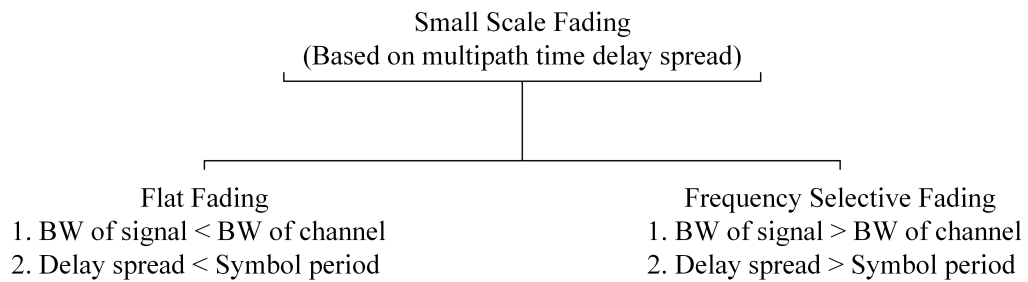


Figure 2.5: Types of Small-Scale Fading.

consideration in wireless communications, because it introduces major improvement in data throughput and link range without an additional increase in bandwidth or transmit power.

MIMO technology can be classified in two main categories, spatial multiplexing and diversity coding shown in Fig.(2.6). First, spatial multiplexing is a method that increases channel capacity at high SNR. In spatial multiplexing, a high-rate signal is divided into multiple lower-rate streams and each stream is transmitted from a different transmit antenna in the same frequency channel, Fig.(2.6). Note that, spatial multiplexing can be used without knowledge of Channel State Information (CSI) at the transmitter.

Second, in the absence of the channel knowledge at the transmitter, diversity coding techniques can be used. In diversity methods, the signal is transmitted from each of the transmit antennas with full or near orthogonal coding. Diversity coding exploits the concept of independent fading in the multiple antenna links to increase the system performance as shown in Fig.(2.6). Also, diversity coding and spatial multiplexing techniques can be used together when some channel knowledge is available at the transmitter.

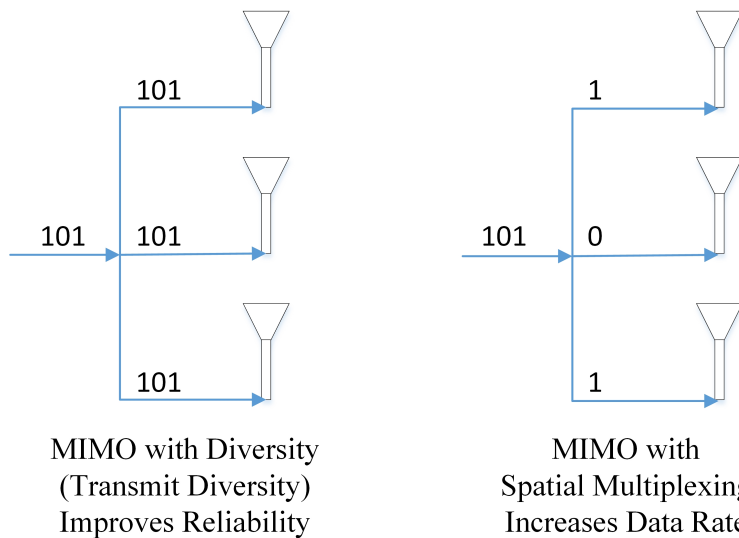


Figure 2.6: MIMO with Transmit Diversity and Spatial Multiplexing.

2.2.1 Space time coding

STC is a method used to increase the BER performance in wireless communication systems by the means of multiple transmit antennas. STC idea is based on transmitting multiple and redundant copies of data information to the receiver in the hope that at least some of them may survive the physical path between transmitter and receiver in a good enough state to allow reliable decoding.

STC were first introduced in [20] as a novel means to provide transmit diversity for the wireless system. In the previous methods, the destructive effects of multipath fading in multiple antenna wireless systems was reduced by other diversity techniques, such as temporal diversity, frequency diversity and receive antenna diversity, with receive antenna diversity being the most widely applied technique. Nevertheless, it is hard to implement antenna diversity at the remote receiver because of the need for them to remain relatively simple, inexpensive and small. As a result, for commercial reasons, multiple antennas are preferred at the base stations, and transmit diversity schemes are growing increasingly as they provide high data rate transmission and/or improved performance over wireless fading channels in both the up link and down link.

There are two main types of STCs, named as STBC and Space Time Trellis Codes (STTC). STBCs transmit a block of input symbols, based on the matrix whose columns and rows represent antennas and time intervals, respectively. STBC's main function is to provide full diversity with a very simple decoding scheme. Furthermore, STBCs do not generally provide coding gain, unless concatenated with an outer code. On

the other hand, in STTCs one input symbol at a time is transmitted which introduce a sequence of vector symbols where length represents antennas. Moreover, STTC provides coding gain beside the diversity gain. Their key advantage over STBCs is the delivery of coding gain. However, the major drawback of STTC is their high complexity in encoders and decoders and they are hard to design [21].

2.2.1.1 Space time trellis codes

STTCs are a type of space–time code used in multiple- antenna wireless communications. This scheme transmits multiple, redundant copies of a trellis (or convolutional) code distributed over time and a number of antennas. These multiple copies of the data are used by the receiver to attempt to reconstruct the actual transmitted data.

STTCs are able to provide both coding gain and diversity gain and provide a better reliability for the system. However, being based on trellis codes, they are more complex than STBCs to encode and decode; they rely on a Viterbi decoder at the receiver while STBCs need only linear processing. STTCs were originally proposed by Tarokh et al. [20,22] as an extension of trellis coding to space-time signal structures.

2.2.1.2 Space time block codes

STBC is a technique used in wireless communications to transmit multiple copies of a data stream across a number of antennas and to use different received versions of the data to improve the system performance. This redundancy results in a higher chance of being able to correctly decode the received signal.

Alamouti STBC Alamouti in [23] proposed a simple transmit diversity technique that improves the wireless system signal quality. Alamouti code is a simple STBC technique to gain diversity by using two transmit antennas Fig(2.7). It is actually the only STBC that could achieve full diversity gain without losing in data rate. Coding matrix of this STBC is given as:

$$C = \begin{pmatrix} c_1 & c_2 \\ -c_2^* & c_1^* \end{pmatrix} \quad (2.3)$$

where columns in matrix indicate antennas and rows present the time slots. In the first time slot, symbols c_1 and c_2 are simultaneously transmitted from antenna one and two,

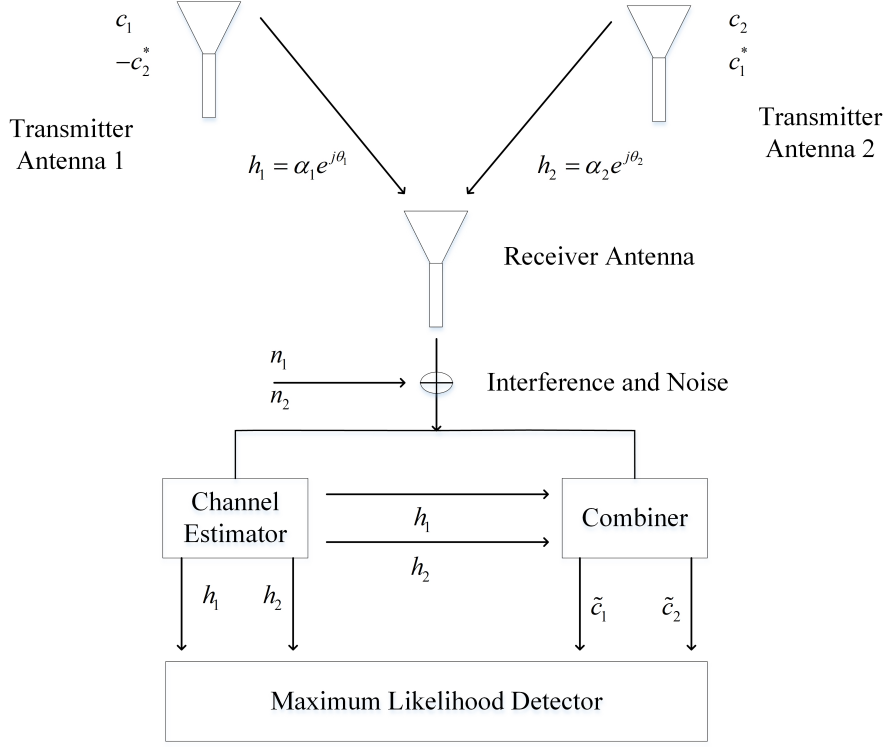


Figure 2.7: Alamouti Scheme.

respectively. In the second time slot, symbol $-c_2^*$ and c_2^* are simultaneously sent from first and second antennas, respectively. If we assume that fading is constant across two consecutive symbol transmission intervals, we can write

$$h_1(t) = h_1(t + T) = h_1 = \alpha_1 \exp j\theta_1, \quad (2.4)$$

$$h_2(t) = h_2(t + T) = h_2 = \alpha_2 \exp j\theta_2 \quad (2.5)$$

where T is the symbol period and h_1 and h_2 are the channel fading coefficients from antenna 1 and 2 to destination assumed constant during the two time slots, respectively.

The received signals are

$$r_1 = r(t) = h_1 c_1 + h_2 c_2 + n_1, \quad (2.6)$$

$$r_2 = r(t + T) = -h_1 c_2^* + h_2 c_1^* + n_2 \quad (2.7)$$

where r_1 and r_2 are the received signals at time t and $t + T$. The combiner combines the received signals as follows:

$$\tilde{c}_1 = h_1^* r_1 + h_2 r_2^* = (\alpha_1^2 + \alpha_2^2) c_1 + h_1^* n_1 + h_2 n_2^*, \quad (2.8)$$

$$\tilde{c}_2 = h_2^* r_1^* - h_1 r_2^* = (\alpha_1^2 + \alpha_2^2) c_2 - h_1 n_2^* + h_2^* n_1, \quad (2.9)$$

and sends them to the Maximum Likelihood (ML) detector, which minimizes the following decision metric

$$|r_1 - h_1 c_1 - h_2 c_2|^2 + |r_2 + h_1 c_2^* - h_2 c_1^*|^2, \quad (2.10)$$

over all possible values of c_1 and c_2 . Expanding (2.10) and deleting terms that are independent of the codewords, the above minimization reduces to separately minimizing

$$|r_1 h_1^* + r_2^* h_2 - c_1|^2 + (\alpha_1^2 + \alpha_2^2 - 1)|c_1|^2,$$

for detecting c_1 and

$$|r_1 h_2^* + r_2^* h_2 - c_2|^2 + (\alpha_1^2 + \alpha_2^2 - 1)|c_2|^2$$

for detecting c_2 . Equivalently, using the equality $d^2(x, y) = (x - y)(x^* - y^*) = |x - y|^2$, the decision rule for each combined signal $\tilde{c}_j, j = 1, 2$ becomes: Pick c_i if and only if

$$(\alpha_1^2 + \alpha_2^2 - 1)|c_i|^2 + d^2(\tilde{c}_j, c_i) \leq (\alpha_1^2 + \alpha_2^2 - 1)|c_k|^2 + d^2(\tilde{c}_j, c_k), \forall k \neq i.$$

For PSK signals (equal energy constellation), this simplifies to, choose c_i if and only if

$$d^2(\tilde{c}_j, c_i) \leq d^2(\tilde{c}_j, c_k), \forall k \neq i.$$

Some advantages of the Alamouti scheme are low complexity decoder, no need for a complete redesign of the existing systems and no feed back from receiver to transmitter as well as same BER performance like MRC if the power is doubled from that used in MRC.

Comparing STBC and STTC performance From the point of view explained in the previous sections the following issues should be understood. STBCs are created by the orthogonal designs, which achieves full diversity, and low complexity decoding in the receiver, but they do not provide coding gain. On the other hand, STTCs includes both diversity and coding gain; however, they have higher complexity in the decoding processing.

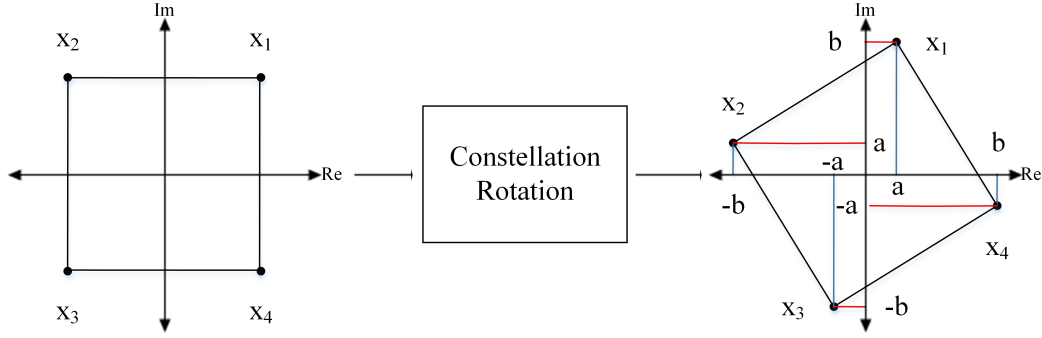


Figure 2.8: Example of Modulation Diversity.

2.3 Signal Space Diversity

SSD, also referred to in the literature as modulation diversity [13] or coordinate interleaving [12], can increase the system performance over fading channels without need to use extra bandwidth or extra power. Two-dimensional signal constellations are used in the SSD concept and then components (real and imaginary parts) of each signal constellation point are sent over independent fading channels. The independence of the fading channels can easily be accomplished by interleaving.

In SSD, signal constellation is rotated by any angle in which each of the real and imaginary components of transmitted signal carries enough information to uniquely represent the original signal. Suppose, χ represents a constellation generated by applying a transformation Θ to a classic two-dimensional constellation as

$$\Theta = \begin{bmatrix} \cos(\theta) & -\sin(\theta) \\ \sin(\theta) & \cos(\theta) \end{bmatrix}. \quad (2.11)$$

To easily understand this concept, let $x = (x_1, x_2)$ be a pair of signal points chosen from the original constellation, $x_1, x_2 \in \chi$, that corresponds to the source message. The current symbols that will be transmitted from the source is formed by interleaving the quadrature components of x_1 and x_2 as follows

$$s = \Re\{x_1\} + j\Im\{x_2\},$$

where $\Re(\cdot)$ and $\Im(\cdot)$ are the real and imaginary part of the symbol, respectively, and $j = \sqrt{-1}$. The rotated symbol s belongs to an expanded constellation Λ defined as

$$\Lambda = \Re\{\chi\} \times \Im\{\chi\},$$

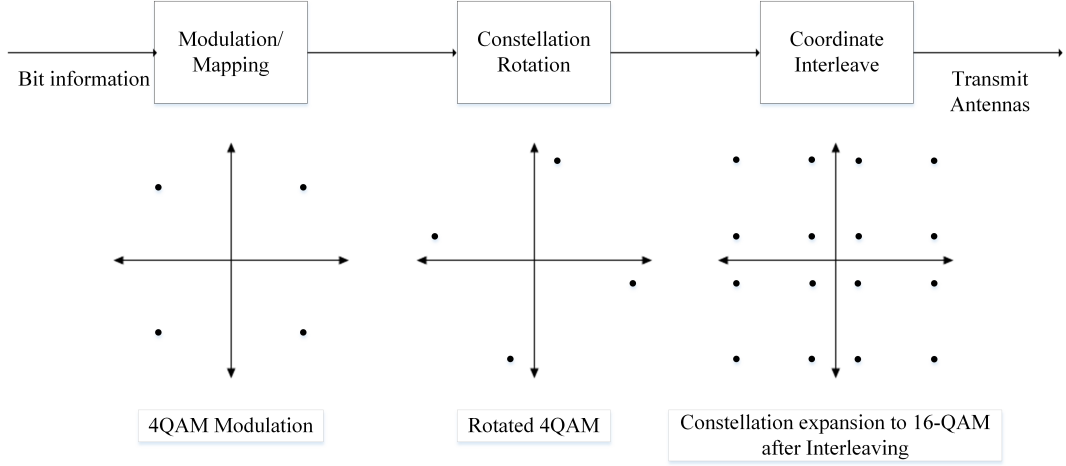


Figure 2.9: Block Diagram of CIOD.

where \times denotes the Cartesian product of two sets. It is important to note that each member of Λ consists of two components each identifies a unique member of χ . Hence, decoding a member of Λ leads to decoding two members of χ .

As an example, Fig.(2.8) illustrates the SSD concept on a 4-Phase-Shift Keying (4-PSK) modulation. 4-PSK constellation points are rotated by Θ which is calculated in (2.11). The new constellation points for x_1 , x_2 , x_3 and x_4 are $(a + jb)$, $(-b + ja)$, $(-a - jb)$ and $(b - ja)$, respectively. It can be shown that after rotation each symbol is uniquely represented by its real or imaginary part. The increase in the dimensionality of the signal set produces significant performance improvement in a fading channel, over the corresponding non-rotated signal set, when the real and imaginary parts of each signal are transmitted over independent fading channels by coordinate interleaving.

2.3.1 Coordinate interleaved orthogonal design

CIOD provides a full diversity full code rate for two, three and four transmit antennas. In this modified version of STBC scheme, the real and imaginary parts of the rotated constellation components are interleaved to mitigate fading in wireless channels. From Fig.(2.9), it can be seen that the information bits are conveyed to the modulation section (here as an example 4-QAM modulation is assumed) and the mapped symbols are rotated by the optimum angle $\theta = 31.7175^\circ$ where the rotation angle θ is chosen to maximize the minimum product distance of the rotated constellation [24] which maximize the error performance. In the next process, symbols are coordinate interleaved and then transmitted by the antennas.

As an example to understand the CIOD concept, let x_i be the complex indeterminate, where $x_i = x_i^R + jx_i^I$, ($i = 1, 2, 3, 4$), x_i^R and x_i^I are the real and imaginary parts of x_i . The coordinate interleaved designs of x_i for different number of transmit antennas are given as follows

$$\begin{aligned}
X(1) &= \begin{pmatrix} x_1^R + x_2^I & 0 \\ 0 & x_1^I + x_2^R \end{pmatrix}, \\
X(2) &= \begin{pmatrix} x_1^R + Jx_3^I & x_2^R + Jx_4^I & 0 & 0 \\ -x_2^R + Jx_4^I & x_1^R - Jx_3^I & 0 & 0 \\ 0 & 0 & x_3^R + Jx_1^I & x_4^R + Jx_2^I \\ 0 & 0 & -x_4^R + Jx_2^I & x_3^R - Jx_1^I \end{pmatrix}, \\
X(3) &= \begin{pmatrix} x_1^R + Jx_3^I & x_2^R + Jx_4^I & 0 \\ -x_2^R + Jx_4^I & x_1^R - Jx_3^I & 0 \\ 0 & 0 & x_3^R + Jx_1^I \\ 0 & 0 & -x_4^R + Jx_2^I \end{pmatrix}
\end{aligned}$$

where $X(1)$, $X(2)$ and $X(3)$ are the signal transmission matrices whose columns and rows represent antennas and time slots, respectively. Note that $X(1)$ and $X(2)$ are CIOD and $X(3)$ is a generalized CIOD [17].

2.4 Cooperative Communication in Wireless Networks

In the previous section, it was shown that the transmit diversity using MIMO systems has been widely acknowledged concept that have been used in cellular base stations. However, it may not be appropriate for other applications due to the cost, size or other limitations. Handsets size or the nodes in wireless sensor networks are examples for this case where MIMO system could not be installed due to the size and power limitations.

In this section, cooperative communication will be discussed. In cooperative communication, single antenna mobiles try to get some of the advantages of the MIMO systems and provide diversity by sharing other user's antenna or using passive relays to make a virtual MIMO system. As a result, cooperative communication provides transmit diversity which mitigates the deteriorious effects of fading and increases coverage, reliability and throughput of wireless systems. This technique has found applications in the conventional wireless systems. By the concept of cooperative communication, the data will be sent over more than one statistically independent fading channels, which generates spatial diversity. The price of using cooperative communication would be rate loss in the cooperating mobile, overall interference in

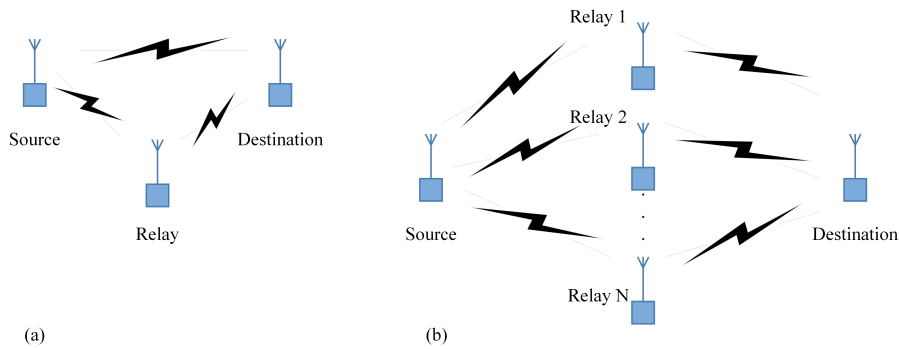


Figure 2.10: Wireless Relay Channels.

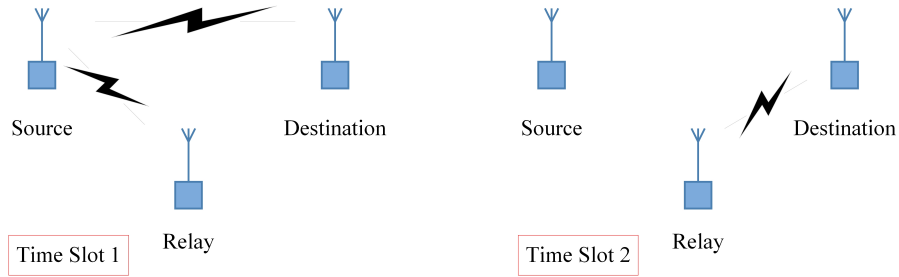


Figure 2.11: Relay Transmission.

the network, hand off. Another way of cooperation is multi-hopping technique where a source tries to communicate with the destination with the help of dedicated relays to combat signal attenuation, but it does not provide diversity advantages.

2.4.1 Cooperation with relay systems

The important issue in cooperative communication is sharing the resource among the nodes. The typical channel model in a cooperative communication is made of three terminal nodes, as shown in Fig.(2.10,a), where S, D and R represent source, destination and relay, respectively. The relay actually helps the source to send its information to the destination without being information source. Moreover, multiple relay models can also be used in the communication systems as seen in Fig.(2.10,b). Different relaying strategies at relay are presented in [25] such as Amplify-and-Forward (AF) and DF which will be discussed in the next sections. Considering Fig.(2.10,a), where the source transmits its data with the help of relay, time-division approach can be represented as in Fig.(2.11). In the first time slot, transmitted signal from the source is received by relay and destination. In the second time slot, relay can send the information to the destination based on the relaying protocol. However, the main drawback of this cooperation is the 50% decrease in the spectral efficiency due to two transmission phases [26].

2.4.1.1 Decode and forward relaying

In this scheme, relay tries to estimate the data information x_p which is already sent from the source to the relay and destination nodes in the first time slot. The received signals at relay and destination are given as

$$y_R = h_{sr}x_p + n_{sr}, \quad (2.12)$$

$$y_{D1} = h_{sd}x_p + n_{sd} \quad (2.13)$$

where h_{sr} and h_{sd} denote channel fading coefficients of source-relay and source-destination channels, respectively. In (2.12) and (2.13), n_{sr} and n_{sd} represent Additive White Gaussian Noise (AWGN) terms at the receivers. In the second time slot, relay sends the estimated version of the symbol x_p as \hat{x}_p to the destination which is received as

$$y_{D2} = h_{rd}\hat{x}_p + n_{rd} \quad (2.14)$$

where h_{rd} is the channel fading coefficient of relay-destination channel and n_{rd} is the AWGN term. The destination processes the received signals to determine the transmitted signal x_p by applying MRC technique. Unlike the AF scheme, fixed DF relaying technique reduces the additive noise effect. However, relay may forward the erroneously detected symbols to the destination. As a result, it is crucial that both relay and destination decode the transmitted data without error. The outage probability ($Pr[I_{DF} < R]$) for the high SNR values has been calculated in [25] as

$$Pr[I_{DF} < R] \sim \frac{1}{\sigma_{sd}^2} \frac{2^{2R} - 1}{\gamma} \quad (2.15)$$

where, $\gamma = P/\sigma^2$ denotes SNR, R is the target rate and σ_{sd}^2 is the variance of channel coefficient between S and D, respectively. I_{DF} is the maximum average mutual information between S and D as the minimum of the two maximum rates given as

$$I_{DF} = \frac{1}{2} \min\{\log(1 + \gamma|h_{sd}|^2), \log(1 + \gamma|h_{sr}|^2 + \gamma|h_{rd}|^2)\}. \quad (2.16)$$

It can be seen from (2.15) that for high SNR, fixed DF does not provide diversity gain (γ^{-1}).

2.4.1.2 Amplify and forward relaying

In AF technique, the relay amplifies the received signal from the source and then retransmits it to the destination in the second time slot. The received signal at R and D during the first time slot is given as

$$y_R = h_{sr}x_p + n_{sr}, \quad (2.17)$$

$$y_{D1} = h_{sd}x_p + n_{sd}, \quad (2.18)$$

respectively. In the second time slot, the received signal at D is

$$y_{D2} = h_{rd} \cdot \beta \cdot y_R + n_{rd}, \quad (2.19)$$

where β is the relay transmit average power constraint coefficient and is given as

$$\beta \leq \sqrt{\frac{P_r}{P_1 |h_{sr}|^2 + \sigma^2}} \quad (2.20)$$

where P_r is the relay power. Finally, D tries to decode the received signals y_{D1} and y_{D2} by simply combining them. Maximum achieved mutual information can be calculated as

$$I_{AF} = \frac{1}{2} \log \left[1 + \gamma |h_{sd}|^2 + \frac{\gamma |h_{rd} \beta h_{sr}|^2}{1 + |h_{rd} \beta|^2} \right]. \quad (2.21)$$

Finally, approximate outage probability at high SNR can be written as [25]

$$Pr [I_{AF} < R] \sim \frac{\sigma_{sr}^2 + \sigma_{rd}^2}{2\sigma_{sd}^2(\sigma_{sr}^2\sigma_{rd}^2)} \left(\frac{2^{2R} - 1}{\gamma} \right)^2 \quad (2.22)$$

where the factor γ^{-2} indicates the diversity gain of 2 in the fixed AF protocol. In (2.22), σ_{sr}^2 and σ_{rd}^2 are the variances of channel fading coefficients between S and R and R and D, respectively.

2.4.2 Coded cooperation between users

This technique integrates cooperation into channel coding [27, 28]. In coded cooperation two different portions of each user's codeword is sent over two independent fading channels. Moreover, the incremental redundancy is sent by each user to its partner. Only under the condition that the incremental redundancy could not be sent, the users try to act as in noncooperation mode. The important factor

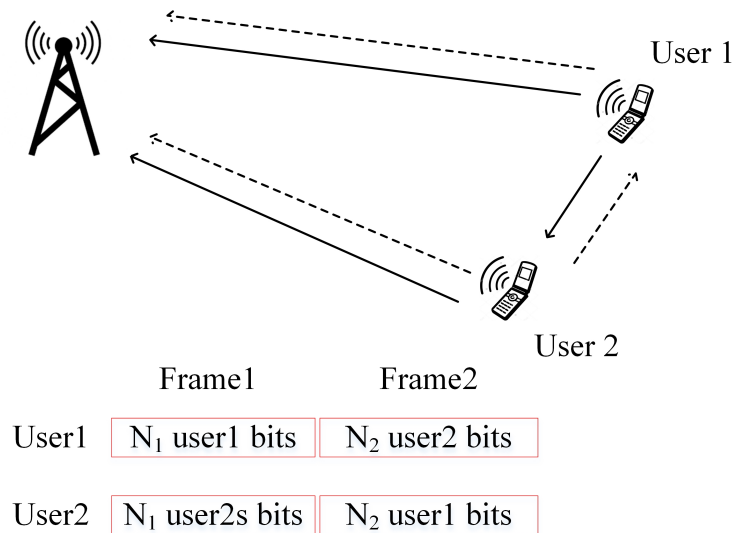


Figure 2.12: Coded Cooperation.

in efficiency by this method is managing automatically through code design with no feedback among users.

User's source data are divided into blocks that are already added with cyclic redundancy check code. Considering that the original code has $N_1 + N_2$ bits for each user the transmission schedule period is divided into two time slots that here is assumed as frames where N_1 and N_2 are bit lengths, respectively. For the first frame, N_1 bits are sent by each users while trying to decode the partners data. If it could not decode correctly, the user will transmit its own signal containing N_2 bits. However, if this attempt is successful, in the second frame, each user transmits the second code partition of its partner which contains N_2 bits. In total each user transmits a total of $N = N_1 + N_2$ bits per source block over two time slots. This method is presented in Fig.(2.12), where at the second time slot users act independently with no knowledge of whether their own first frame was correctly decoded. There is four possibility of cooperative modes as both or neither users cooperates or User 1 cooperates and User 2 does not and vice versa [29].

3. COGNITIVE RADIO

As wireless technology and the demand for high data rates continue to grow, it seems that more and more spectrum resources will be needed. The vast majority of the available spectral resources is licensed and allocated to specific services. However, recent studies of spectrum utilization have indicated that a large portion of the spectrum is not used at anytime [1]. Moreover, the spectrum usage varies in time, frequency and geographical locations. By considering the spectrum usage [1], secondary users could use the licensed band to improve the spectrum utilization when the primary system is absent or present. CR first proposed in [30] is a new technology that can improve the radio spectrum usage. CR is an intelligent device that can be set and designed dynamically. Its transceiver is designed to use the best wireless channels in its vicinity. CR automatically detects available channels in wireless spectrum, then accordingly changes its transmission or reception parameters to use the spectrum band. CR is able to fill in spectrum holes and serve its users without causing interference to the primary user, Fig. (3.1). To do so, CR continuously scans the spectrum to detect the primary user existence. By detecting the primary user, secondary user based on the protocol can stop operating in the band to be used by primary user or to minimize the interference threshold. This process is a form of dynamic spectrum management and requires a challenging task as different primary users have different data rates, modulation type and power transmission. As a summary, CR determines which part of the spectrum is accessible (Spectrum Sensing), select the best available channel (Spectrum Management) and coordinates access to the selected channel (Spectrum Sharing) as well as vacates the spectrum in the presence of primary user (Spectrum Mobility). In the following, the cognitive radio classification and spectrum management will be introduced [4, 31, 32].

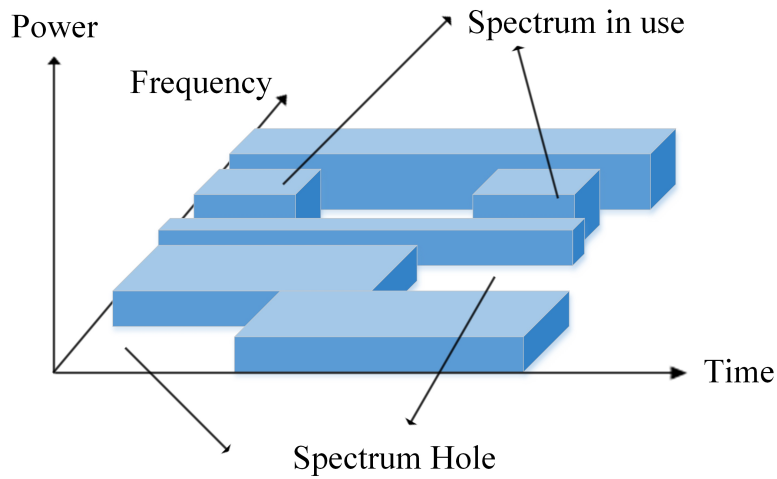


Figure 3.1: Spectrum Hole Concept.

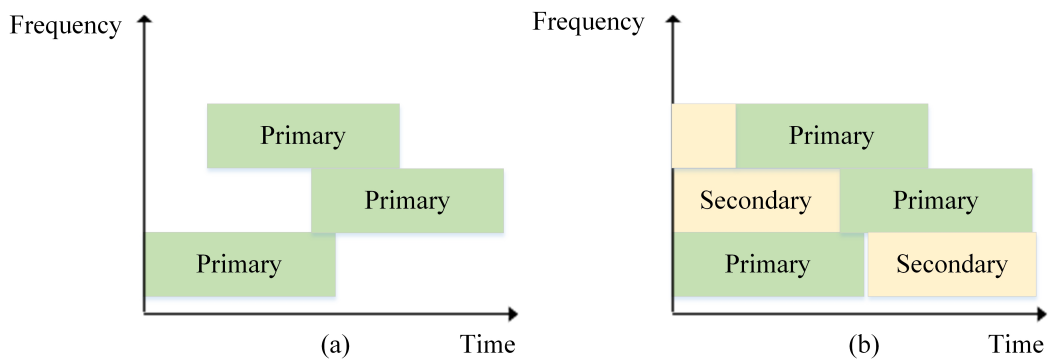


Figure 3.2: Cognitive Radio Spectrum Sharing.

3.1 Spectrum Sensing

Spectrum sensing is one of the most important factors in CR. CR should be able to measure, sense, learn and be aware of its surrounding environment for the availability of the primary user. So, it can use the spectrum holes, (Fig.(3.2)). Nevertheless, this task is somehow difficult for CR. Therefore, there are some methods to be aware of the channels between primary transmitter and receiver which is shown in Fig. (3.3). Active and passive spectrum awareness techniques are the key elements for identifying spectrum access opportunities [33]. Spectrum awareness is classified as active (spectrum sensing) and passive methods (Fig.(3.3)). Active awareness techniques could be performed in non-cooperation and cooperation models whereas in passive awareness spectrum information is received from other than the secondary system such as predefined policy, primary system etc. Active awareness classification is briefly illustrated in the sequel [4].

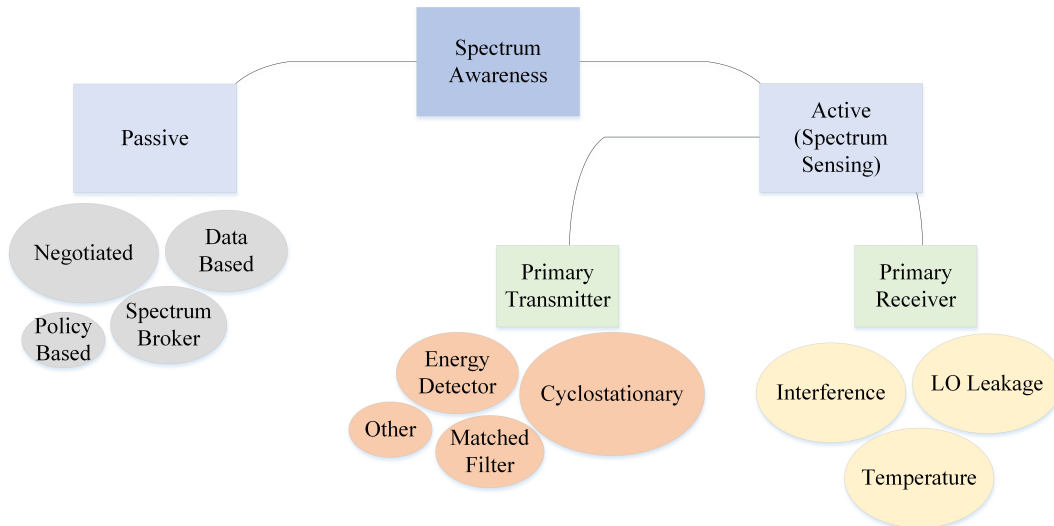


Figure 3.3: Spectrum Awareness.

Active awareness is categorized into primary transmitter and receiver. At the primary transmitter, the approaches are matched filter, energy detection and cyclostationary feature as well as other techniques (like waveform). Another approach (primary receiver) consists of Local Oscillator (LO) package, interference and temperature, (Fig.(3.3)). The common techniques are explained in the following.

Energy detector is a common technique because of its low computational complexity. This technique performs non-coherent detection and does not need any knowledge of the PU's transmitted signal. Moreover, cyclostationary method is based on the inherent redundancy in the transmitted signals of primary user. Finally, matched filter is an optimal method since it maximizes received SNR in comparison to the other methods. In brief, active or passive techniques are just used to obtain information about the spectrum. The above mentioned techniques could be combined to improve the spectrum decision accuracy [4].

3.2 Spectrum Sharing

In this section, the existing spectrum sharing protocols is classified. This classification is based on the access technology of the licensed spectrum, network architecture and access behavior as seen in Fig.(3.4) [34, 35].

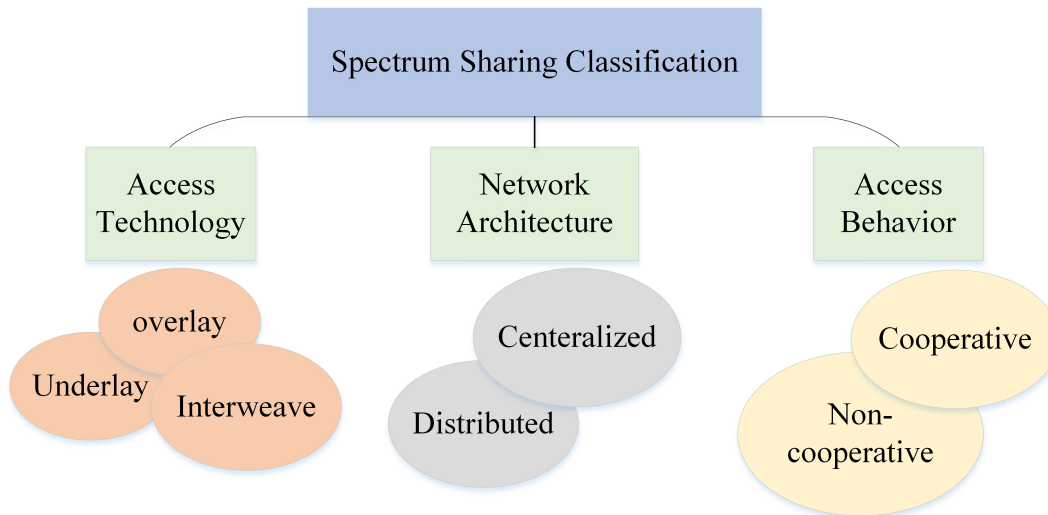


Figure 3.4: Classification of Spectrum Allocation and Sharing Schemes.

3.2.1 Network architecture

Network architecture is categorized as centralized and distributed. In centralized method, a central unit is responsible to control and coordinate the spectrum allocation to manage the secondary users. However, in the distributed technologies each secondary user regulates and controls its spectrum access strategy, based on its observation from its surrounding environment.

3.2.2 Access behavior

Access behavior can be cooperative or non-cooperative. In cooperative method, secondary users cooperate with each other to reach a common goal. For example, SUs of one specific service provider would cooperate by coordinating their spectrum access to improve the system performance. In most cases, this type of method uses centralized technology to easily coordinate allocation and spectrum between different users. On the other hand, secondary users may act like in a non-cooperative mode to send their data and benefit from the spectrum.

3.2.3 Access technology

Depending on the regularity constraints on spectrum usage, access technology can be categorized as interweave, underlay and overlay which will be discussed in the

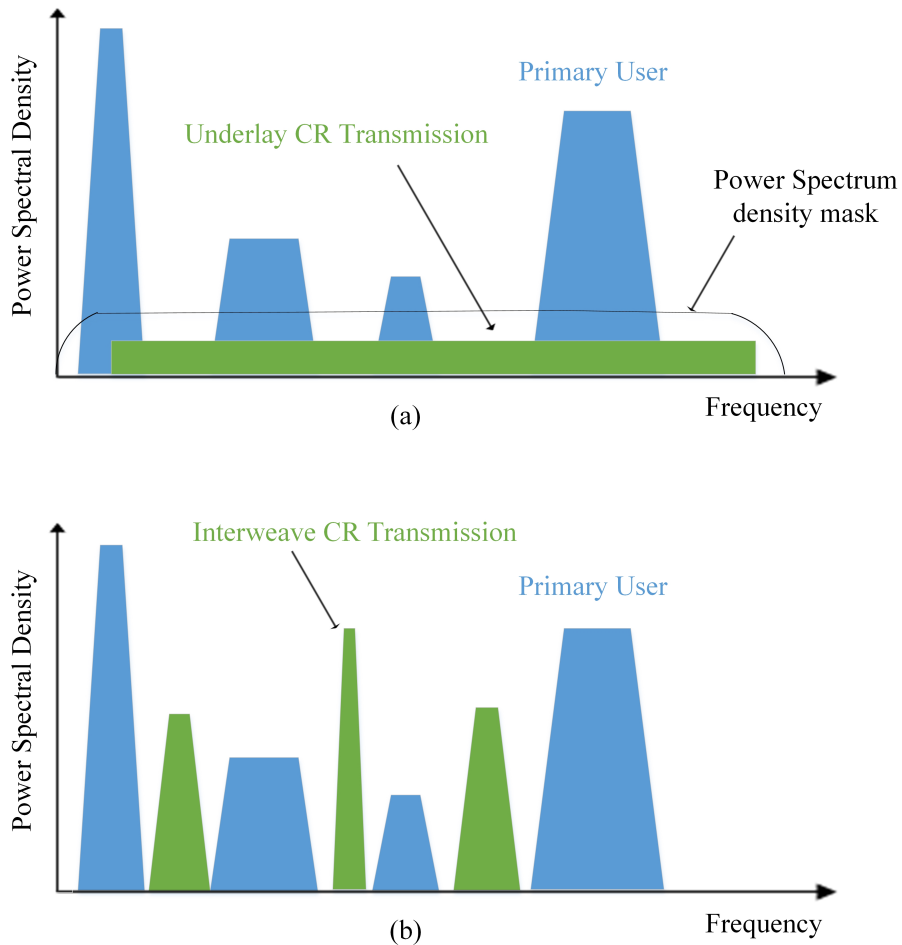


Figure 3.5: Underlay and Interweave Spectrum Sharing Paradigm.

following. For all mentioned methods, in a multiple SUs mode, users should share the available bandwidth among themselves and PUs, based on their protocols [4].

3.2.3.1 Interweave

Interweave method (opportunistic spectrum access) was the original motivational move for the CR idea where studies showed that some frequency bands based on time and space are underutilization. In this method, SUs are allowed to send their data only in the absence of primary users. As a result, harmful interference is totally avoided to PUs, (Fig.(3.5,b)), and SUs in this paradigm must continuously monitor for the presence of the primary users over time, space and frequency and communicate over spectrum holes. However, detection of the spectrum hole is a challenging fact in this technique since PU activity changes over time and depends on the geographical location and miss detection and collision may occur.

3.2.3.2 Underlay

In the underlay protocol, SUs are allowed to transmit their data simultaneously at the existence of PU, by considering the fact that a threshold has been defined to limit the interference at PR. So, SU can send its data without any harmful results for the PU (Fig.(3.5,a)). The threshold shown in Fig.(3.5,a) can be defined as a spectral mask (Power Spectral Density (PSD)) along the frequency band. The challenging task in the underlay systems is determining accurately the exact interference level SU transmitter causes at the primary receiver. This method is mostly used in the licensed band, but it can also provide different services to different users in the unlicensed bands.

3.2.3.3 Overlay

Secondary users in spectrum overlay are allowed to send their data only if they support the performance of PU or at least they don't affect its performance. So, SU must have knowledge of the transmitted data from PU. SU can use this knowledge to improve the performance of PU and SU in different ways or it may use this information to avoid the interference both in the primary and secondary receivers. Furthermore, SU can cooperate with PU to improve its performance. As an example, ST uses superposition technique in which ST assigns some parts of its power to transmit PU's signal and the remainder to its data [3]. However, this method causes interference in both receivers. Moreover, in higher rates SU acts as a relay due to the fact that much of its power is assigned to PU's data. On the other hand, some protocols are proposed in this thesis to avoid the interference, which use the overlay technique to improve PU's and SU's performance. Some challenging task in this paradigm are security and privacy concepts as well as encoding and decoding techniques with reasonable complexity. This technique can be used in the licensed or unlicensed bands. In licensed bands, SUs are allowed to share the band with PUs when SUs do not decrease PUs performance or rather improve it by cooperation. In unlicensed bands both SU's and PU's may have equal priority in using the band.

4. SPECTRUM SHARING IN CR USING SIGNAL SPACE DIVERSITY

In this section, we propose a new spectrum sharing protocol based on SSD [14, 24] for overlay cognitive radio networks. The overall transmission is completed in three signaling intervals to avoid any mutual interference between users and the SSD is provided by CIOD [17] which increases the transmission rate of the primary users compared to the straightforward DF CR protocols given in the literature, while allowing single-symbol decoding at the primary receiver. The theoretical outage probability and the BEP analyses for both primary and secondary users are derived and the results are supported via computer simulations. It is shown that the outage performance is significantly improved by the proposed protocol compared to the non-cooperation case and the reference protocol of [3] based on the transmission of superimposed primary and secondary signals which causes severe interference at both user's receivers. For PU, BER analysis nearly reports no enhancement. Nevertheless, BER performance for SU has noticeable improvement compared to that of the reference [3].

The considered CR network and the proposed spectrum sharing protocol are presented in Section 4.1. The outage analysis for the proposed protocol is given in Section 4.2. Section 4.2.4 and 4.3.3 deals with the outage and bit error probability performance evaluation for the proposed protocol and comparisons, respectively.

4.1 System Model

The considered CR network configuration with three transmission time slots is shown in Fig.4.1 where PT transmits its signal to PR and ST during the first time slot. The proposed overlay protocol applies DF relaying at ST to cooperate and share the spectrum along with PU. If ST correctly decodes the primary signal it acts as a relay during the second signaling interval to cooperate with PT and send its symbol to PR, otherwise PR considers only the signal received from PT during the first time slot.

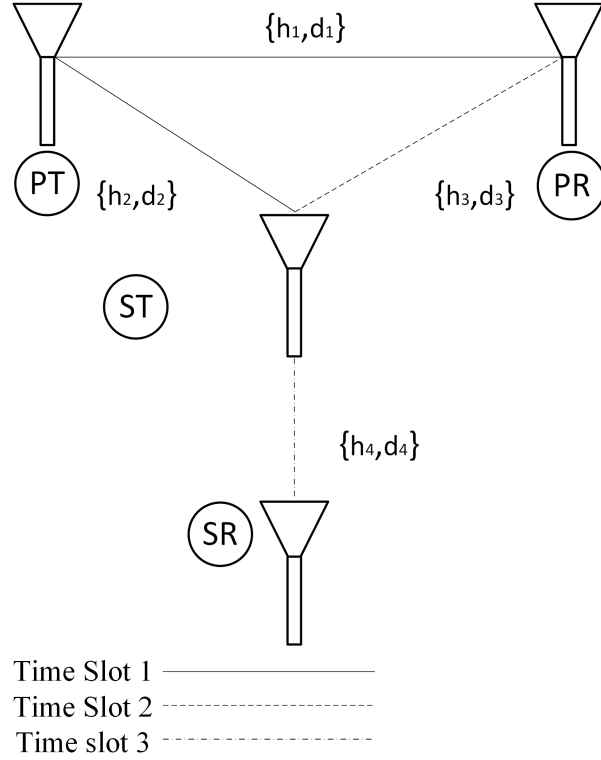


Figure 4.1: Considered CR Network Model with One Antenna at ST.

During the third time slot, ST transmits its own symbol to SR, PT and PR staying silent.

The important attempt in our model is introducing the SSD concept in CR networks. SSD [24] is based on interleaving the real and imaginary parts of two-dimensional signals taken from a rotated constellation to increase the diversity order over fading channels. This is provided in our model by applying STBC as CIOD. Note that the classical Alamouti coding [23] is not applicable in this case, since ST does not know the primary signal in the first time slot. We consider a rotated M-PSK or M-QAM constellation for which each symbol can be uniquely determined only by its real or imaginary part since all symbols have different real and imaginary parts after rotation. As an example, based on [24], the optimum rotation angle which minimizes the Pairwise Error probability (PEP) for QPSK modulation is 31.7 degree. Therefore, in the first time slot PT transmits the interleaved data packet $\mathbf{x}_1^R + j\mathbf{x}_2^I$ to both PR and ST where \mathbf{x}_1^R and \mathbf{x}_2^I are the real and imaginary parts of the first and second primary data packets, respectively. If ST correctly decodes this packet pair $(\mathbf{x}_1, \mathbf{x}_2)$ from only real and imaginary parts of symbols, respectively, it transmits the interleaved data packet $\mathbf{x}_2^R + j\mathbf{x}_1^I$ to PR during the second time slot, where \mathbf{x}_2^R and \mathbf{x}_1^I are the real and imaginary

Table 4.1: Proposed Protocol Transmission Schedule Using CIOD.

	PT	ST
T1	$\mathbf{x}_1^R + j\mathbf{x}_2^I$	–
T2	–	$\mathbf{x}_2^R + j\mathbf{x}_1^I$
T3	–	$\mathbf{s}^R + j\mathbf{s}^I$

parts of the second and first primary packet, respectively. Note that with successful decoding, ST cooperates regardless of the outage or non-outage state of PT→PR link. The combination of these two signals and the maximum likelihood decoding procedure at PR are as given in [17]. Finally, at the third time slot, ST transmits its own data packet $\mathbf{s}^R + j\mathbf{s}^I$ to SR. Note that, the achievable rate for the primary user will be affected by a degradation factor of 2/3 (due to the two transmitted primary packets during three time slots) for the proposed protocol which improves the spectral efficiency compared to the classical cooperative DF relaying with superimposed transmission given in [3] where this factor is equal to 1/2. The transmission schedule is given as in Table.4.1, where the first and second columns denote transmission packets from PT and ST, respectively. Rows correspond to time slots. The received vector at PR and ST during the first time slot is given as

$$\mathbf{y}_{PR1} = h_1 \sqrt{P_p} (\mathbf{x}_1^R + j\mathbf{x}_2^I) + \mathbf{n}_{PR1}, \quad (4.1)$$

$$\mathbf{y}_{ST} = h_2 \sqrt{P_p} (\mathbf{x}_1^R + j\mathbf{x}_2^I) + \mathbf{n}_{ST}, \quad (4.2)$$

respectively. In the second time slot, the received vector at PR is

$$\mathbf{y}_{PR2} = h_3 \sqrt{P_s} (\mathbf{x}_2^R + j\mathbf{x}_1^I) + \mathbf{n}_{PR2}, \quad (4.3)$$

when ST cooperates and in the last time slot, the received vector at SR is

$$\mathbf{y}_{SR} = h_4 \sqrt{P_s} (\mathbf{s}^R + j\mathbf{s}^I) + \mathbf{n}_{SR}. \quad (4.4)$$

In (4.1) - (4.4), \mathbf{n}_{PR1} , \mathbf{n}_{ST} , \mathbf{n}_{PR2} and \mathbf{n}_{SR} are the AWGN vectors whose components are Gaussian distributed r.v.s with mean zero and variance σ^2 . All channels are assumed subject to Rayleigh fading, therefore omitting the indice for simplicity we have $h \sim CN(0, d^{-\beta})$, where h is the symmetric complex Gaussian random variable with mean zero and variance $d^{-\beta}$ and d is the distance between two nodes denoted in Fig.4.1.

$2 \leq \beta \leq 4$ is the path loss exponent. So $|h|^2$ follows the exponential distribution with mean $d^{-\beta}$. We denote the fading channel coefficient and distance pairs as (h_1, d_1) , (h_2, d_2) , (h_3, d_3) and (h_4, d_4) and channel gains as $\Gamma_1 = |h_1|^2$, $\Gamma_2 = |h_2|^2$, $\Gamma_3 = |h_3|^2$ and $\Gamma_4 = |h_4|^2$ for the links PT→PR, PT→ST, ST→PR and ST→SR, respectively. The distance normalization between nodes is done with respect to the distance between PT and PR which is assumed to be equal to 1.

4.2 Outage Analysis

In this section, we derive analytical expressions for the outage probabilities of the primary and secondary systems. We also derive an upper bound for the distance between PT and ST which defines a critical radius from PT so that the outage performance of the primary system is guaranteed to be better or equivalent to that of the non-cooperation case when ST is located within this region.

4.2.1 Primary system outage performance

First, let us consider the direct transmission between PT and PR. The achievable rate in this case can be given as

$$R_1 = \log_2 \left(1 + \frac{P_p}{\sigma^2} \Gamma_1 \right) \quad (4.5)$$

where P_p is the transmit power of PT and σ^2 is the variance of Gaussian noise component at PR which is taken equal at all receivers. The outage probability which is defined as the probability that the achievable rate is less than the target rate μ_p can be calculated as

$$\begin{aligned} P_{out}^{non} &= \Pr \{ R_1 < \mu_p \} = 1 - \Pr \left\{ \log_2 \left(1 + \frac{P_p}{\sigma^2} \Gamma_1 \right) > \mu_p \right\} \\ &= 1 - \Pr \left\{ \Gamma_1 > \frac{\sigma^2}{P_p} \rho_2 \right\} = 1 - \exp \left(-\frac{\sigma^2}{P_p} \rho_2 \right) \end{aligned} \quad (4.6)$$

where $\rho_2 = 2^{\mu_p} - 1$.

The achievable rate between PT and ST when cooperation occurs is given by

$$R_2 = \frac{2}{3} \log_2 \left(1 + \frac{P_p}{\sigma^2} \Gamma_2 \right) \quad (4.7)$$

where the factor $2/3$ indicates that the transmission is split into three time slots and multiplied by 2 which indicates the number of primary data packets transmitted during

three time slots. At the end of the first time slot, ST attempts to decode the data packet $\mathbf{x}_1^R + j\mathbf{x}_2^I$, if it fails, it remains silent during the second time slot and PR attempts to decode the primary packet by considering only the received vector from PT.

The achievable rate between PT and PR, conditioned on the successful decoding at ST, is given by

$$R_1^{MRC} = \frac{2}{3} \log_2 \left(1 + \frac{P_p}{\sigma^2} \Gamma_1 + \frac{P_s}{\sigma^2} \Gamma_3 \right). \quad (4.8)$$

The outage probability of the primary system with target rate μ_P is given by

$$P_{out}^{P-coop} = \Pr\{R_2 > \mu_P\} \Pr\{R_1^{MRC} < \mu_P\} + \Pr\{R_2 < \mu_P\} \Pr\{\frac{2}{3}R_1 < \mu_P\}. \quad (4.9)$$

Since the channel gains are exponentially distributed, the probabilities in (4.8) can be easily calculated. By applying the method given in [36] for the pdf of sum of independent, non-identical exponentially distributed random variables, we obtain,

$$\begin{aligned} \Pr\{R_1^{MRC} < \mu_P\} &= 1 - \Pr\left\{\frac{2}{3} \log_2 \left(1 + \frac{P_p}{\sigma^2} \Gamma_1 + \frac{P_s}{\sigma^2} \Gamma_3 \right) > \mu_P\right\} \\ &= 1 - \Pr\left\{\frac{P_p}{\sigma^2} \Gamma_1 + \frac{P_s}{\sigma^2} \Gamma_3 > \rho_1\right\}. \end{aligned} \quad (4.10)$$

where $\rho_1 = 2^{\frac{3}{2}\mu_P} - 1$. In order to calculate $\Pr\{\frac{P_p}{\sigma^2} \Gamma_1 + \frac{P_s}{\sigma^2} \Gamma_3 > \rho_1\}$ in (4.10), we should find the pdf for $X = \frac{P_p}{\sigma^2} \Gamma_1 + \frac{P_s}{\sigma^2} \Gamma_3$. By using the definitions and equations in [36] the pdf of $\frac{P_p}{\sigma^2} \Gamma_1 + \frac{P_s}{\sigma^2} \Gamma_3$ where Γ_1 and Γ_3 are exponentially distributed is given as

$$f_x(x) = \left(\sum_{n=1}^N E_n \lambda_n e^{-\lambda_n x} + \sum_{k=1}^K A_k \frac{x^{k-1} \lambda_e^k e^{-\lambda_e x}}{\Gamma(k)} \right) U(x) \quad (4.11)$$

where $U(\cdot)$ is the unit-step function and $\Gamma(n) = \int_0^{\infty} t^{n-1} \exp^{-t} dt$, K is the number of r.v.s of the same mean $\frac{1}{\lambda_e}$ among M r.v.s and $N = M - K$ is the remaining r.v.s of different means denoted as $\frac{1}{\lambda_n}$ where $n = 1, 2, \dots, N$. Using (4.11) in our case where Γ_1 and Γ_3 with different mean $\frac{1}{\lambda_1}$ and $\frac{1}{\lambda_2}$ where identically and independent distributed r.v.s with $K = 0$ and $N = 2$. (4.11) can be simplified as

$$f_x(x) = \left(\sum_{n=1}^2 E_n \lambda_n e^{-\lambda_n x} \right) u(x) = E_1 \lambda_1 e^{-\lambda_1 x} + E_2 \lambda_2 e^{-\lambda_2 x} \quad (4.12)$$

where E_n is found by Heaviside's expansion [37] as

$$E_n = \left(\frac{1}{1 - \frac{\lambda_n}{\lambda_e}} \right)^K \prod_{\substack{u=1 \\ u \neq n}}^N \frac{1}{1 - \frac{\lambda_n}{\lambda_u}} \quad (4.13)$$

respectively. By Substituting E_1 and E_2 from (4.13) in (4.12) we obtain

$$f_x(x) = \frac{\lambda_1}{1 - \frac{\lambda_1}{\lambda_2}} e^{-\lambda_1 x} + \frac{\lambda_2}{1 - \frac{\lambda_2}{\lambda_1}} e^{-\lambda_2 x}. \quad (4.14)$$

By applying (4.14) in (4.10) the outage probability for the cooperation case can be calculated as

$$\begin{aligned} \Pr\{R_1^{MRC} < \mu_P\} &= 1 - \Pr\{f_x(x) > \rho_1\} = 1 - \int_{\rho_1}^{\infty} f_x(x) dx \\ &= 1 - \frac{1}{1 - \frac{\lambda_1}{\lambda_2} \rho_1} \int_{\rho_1}^{\infty} \lambda_1 e^{-\lambda_1 x} dx - \frac{1}{1 - \frac{\lambda_2}{\lambda_1} \rho_1} \int_{\rho_1}^{\infty} \lambda_2 e^{-\lambda_2 x} dx \\ &= 1 - \frac{\lambda_2}{\lambda_2 - \lambda_1} e^{-\lambda_1 \rho_1} - \frac{\lambda_1}{\lambda_1 - \lambda_2} e^{-\lambda_2 \rho_1}. \end{aligned} \quad (4.15)$$

By substituting $\lambda_1 = \frac{N_o}{P_p} d_1^\beta$ and $\lambda_2 = \frac{N_o}{P_s} d_3^\beta$ we obtain

$$\Pr\{R_1^{MRC} < \mu_P\} = 1 - \frac{d_3^\beta \frac{N_o}{P_s}}{d_3^\beta \frac{N_o}{P_s} - \frac{N_o}{P_p}} e^{-\frac{N_o}{P_p} \rho_1} - \frac{\frac{N_o}{P_p}}{\frac{N_o}{P_p} - d_3^\beta \frac{N_o}{P_s}} e^{-d_3^\beta \frac{N_o}{P_s} \rho_1}, \quad (4.16)$$

Taking $\Lambda_1 = \frac{\sigma^2}{P_p}$, $\Lambda_2 = \frac{\sigma^2}{P_s}$ the outage probability for the cooperation mode can be obtained as

$$\Pr\{R_1^{MRC} < \mu_P\} = 1 - \left[\frac{\Lambda_1}{\Lambda_1 - \Lambda_2 d_3^\beta} \exp\left(-\rho_1 \Lambda_2 d_3^\beta\right) + \frac{\Lambda_2 d_3^\beta}{\Lambda_2 d_3^\beta - \Lambda_1} \exp\left(-\rho_1 \Lambda_1\right) \right]. \quad (4.17)$$

For the other probabilities in (4.9), we have

$$\begin{aligned} \Pr\left\{\frac{2}{3} R_1 < \mu_p\right\} &= 1 - \Pr\left\{\frac{2}{3} \log_2\left(1 + \frac{P_p}{\sigma^2} \Gamma_1\right) > \mu_p\right\} \\ &= \int_{\frac{\sigma^2}{P_p} \rho_1}^{\infty} \exp(-x) dx = 1 - \exp\left(-\frac{\sigma^2}{P_p} \rho_1\right) \end{aligned} \quad (4.18)$$

and

$$\begin{aligned} \Pr\{R_2 > \mu_p\} &= \Pr\left\{\frac{2}{3} \log_2\left(1 + \frac{P_p}{\sigma^2} \Gamma_2\right) > \mu_p\right\} = \Pr\left\{\Gamma_2 > \frac{\sigma^2}{P_p} \rho_1\right\} \\ &= \int_{\frac{\sigma^2}{P_p} \rho_1}^{\infty} d_2^\beta \exp(-d_2^\beta x) dx = \exp\left(-d_2^\beta \frac{\sigma^2}{P_p} \rho_1\right). \end{aligned} \quad (4.19)$$

Substituting (4.17), (4.18) and (4.19) in (4.9), we have

$$\begin{aligned}
P_{out}^{p-coop} &= \Pr\{R_2 > \mu_P\} \Pr\{R_1^{MRC} < \mu_P\} + \Pr\{R_2 < \mu_P\} \Pr\{\frac{2}{3}R_1 < \mu_P\} \\
&= \exp(-d_2^\beta \Lambda_1 \rho_1) \left(1 - \left[\frac{\Lambda_1}{\Lambda_1 - \Lambda_2 d_3^\beta} \exp\left(-\rho_1 \Lambda_2 d_3^\beta\right)\right.\right. \\
&\quad \left.\left.+ \frac{\Lambda_2 d_3^\beta}{\Lambda_2 d_3^\beta - \Lambda_1} \exp(-\rho_1 \Lambda_1)\right]\right) + (1 - \exp(-d_2^\beta \Lambda_1 \rho_1))(1 - \exp(-\Lambda_1 \rho_1)) \\
&= 1 - [\exp(-d_2^\beta \Lambda_1 \rho_1)] \left[\frac{\Lambda_1}{\Lambda_1 - \Lambda_2 d_3^\beta} \exp\left(-\rho_1 \Lambda_2 d_3^\beta\right) + \frac{\Lambda_2 d_3^\beta}{\Lambda_2 d_3^\beta - \Lambda_1} \exp(-\rho_1 \Lambda_1)\right] \\
&\quad - [1 - \exp(-d_2^\beta \Lambda_1 \rho_1)] [\exp(-\Lambda_1 \rho_1)] \\
&= 1 - \left[\frac{\Lambda_1}{\Lambda_1 - \Lambda_2 d_3^\beta} \exp\left(-\rho_1 (d_2^\beta \Lambda_1 + \Lambda_2 d_3^\beta)\right) + \frac{\Lambda_2 d_3^\beta}{\Lambda_2 d_3^\beta - \Lambda_1} \exp(-\Lambda_1 \rho_1 (1 + d_2^\beta))\right] \\
&\quad - [\exp(-\Lambda_1 \rho_1) - \exp(-\Lambda_1 \rho_1 (1 + d_2^\beta))]. \tag{4.20}
\end{aligned}$$

After some calculation we obtain

$$\begin{aligned}
P_{out}^{p-coop} &= 1 - \left(\frac{\Lambda_1}{\Lambda_1 - \Lambda_2 d_3^\beta}\right) \exp[-\rho_1 (\Lambda_1 d_2^\beta + \Lambda_2 d_3^\beta)] \\
&\quad + \exp[-\Lambda_1 \rho_1 (1 + d_2^\beta)] \left(1 - \frac{\Lambda_2 d_3^\beta}{\Lambda_2 d_3^\beta - \Lambda_1}\right) - \exp(-\rho_1 \Lambda_1). \tag{4.21}
\end{aligned}$$

4.2.2 Acceptable distance from primary transmitter

The proposed spectrum sharing protocol with cooperation is practicable only when it is ensured that the outage probability of the primary system is lower or equal to that of the non-cooperation case, which means that

$$P_{out}^{p-coop} \leq P_{out}^{nc}. \tag{4.22}$$

From (4.6) and (4.21), by considering the constraint of (4.22) we have

$$\begin{aligned}
&1 - \left(\frac{\Lambda_1}{\Lambda_1 - \Lambda_2 d_3^\beta}\right) \exp[-\rho_1 (\Lambda_1 d_2^\beta + \Lambda_2 d_3^\beta)] - \exp(-\rho_1 \Lambda_1) \\
&+ \exp[-\Lambda_1 \rho_1 (1 + d_2^\beta)] \left(1 - \frac{\Lambda_2 d_3^\beta}{\Lambda_2 d_3^\beta - \Lambda_1}\right) < 1 - \exp\left(-\frac{\sigma^2}{P_p} \rho_2\right).
\end{aligned}$$

By simplifying

$$\begin{aligned}
&\left(\frac{\Lambda_1}{\Lambda_1 - \Lambda_2 d_3^\beta}\right) \exp[-\rho_1 (\Lambda_1 d_2^\beta + \Lambda_2 d_3^\beta)] - \exp[-\Lambda_1 \rho_1 (1 + d_2^\beta)] \left(1 - \frac{\Lambda_2 d_3^\beta}{\Lambda_2 d_3^\beta - \Lambda_1}\right) \\
&> \exp(-\Lambda_1 \rho_2) - \exp(-\rho_1 \Lambda_1) \tag{4.23}
\end{aligned}$$

and therefore,

$$\exp(-\rho_1 \Lambda_1 d_2^\beta) (A \exp(-\rho_1 \Lambda_2 d_3^\beta) - B \exp(-\Lambda_1 \rho_1)) > C. \quad (4.24)$$

By taking $\text{Ln}(\cdot) = \log_e(\cdot)$ and after some calculation in (4.24) we have

$$d_2^\beta < \frac{1}{\rho_1 \Lambda_1} \text{Ln} \frac{D}{C}.$$

Finally, the critical region for d_2 is given by

$$d_2 \leq d_2^* = \left(\frac{1}{\rho_1 \Lambda_1} \ln \frac{D}{C} \right)^{1/\beta} \quad (4.25)$$

where $C = \exp(-\Lambda_1 \rho_2) - \exp(-\Lambda_1 \rho_1)$, $D = A \exp(-\Lambda_2 \rho_1 d_3^\beta) - B \exp(-\Lambda_1 \rho_1)$, $A = \frac{\Lambda_1}{\Lambda_1 - \Lambda_2 d_3^\beta}$ and $B = 1 - \frac{d_3^\beta \Lambda_2}{\Lambda_2 d_3^\beta - \Lambda_1}$. Therefore, as long as the distance d_2 between PT and ST satisfies the constraint of (4.25), the secondary spectrum access to the licensed primary spectrum is allowed.

4.2.3 Secondary system outage performance

Since SR receives the data packet $\mathbf{s}_R + j\mathbf{s}_I$ just from ST in the last time slot, the received data vector at SR is given by

$$\mathbf{y}_{ST} = h_4 \sqrt{P_s} (\mathbf{s}_R + j\mathbf{s}_I) + \mathbf{n}_{ST}. \quad (4.26)$$

The achievable rate between ST and SR is

$$R_4 = \frac{1}{3} \log_2 \left(1 + \frac{P_s}{\sigma^2} \Gamma_4 \right) \quad (4.27)$$

where P_s is the transmit power of ST. Note that for the secondary system one data packet per three time slots is transmitted. The outage probability of the secondary system for target rate μ_s is given by

$$\begin{aligned} P_{Out}^{Sec} &= \Pr \{ R_4 < \mu_s \} = 1 - \Pr \left\{ \frac{1}{3} \log_2 \left(1 + \frac{P_s}{\sigma^2} \Gamma_4 \right) > \mu_s \right\} \\ &= 1 - \Pr \left\{ \Gamma_4 > \frac{\sigma^2}{P_s} \rho_3 \right\} = 1 - \exp(-d_4^\beta \frac{\sigma^2}{P_s} \rho_3) \end{aligned} \quad (4.28)$$

where $\rho_3 = 2^{3\mu_s} - 1$.

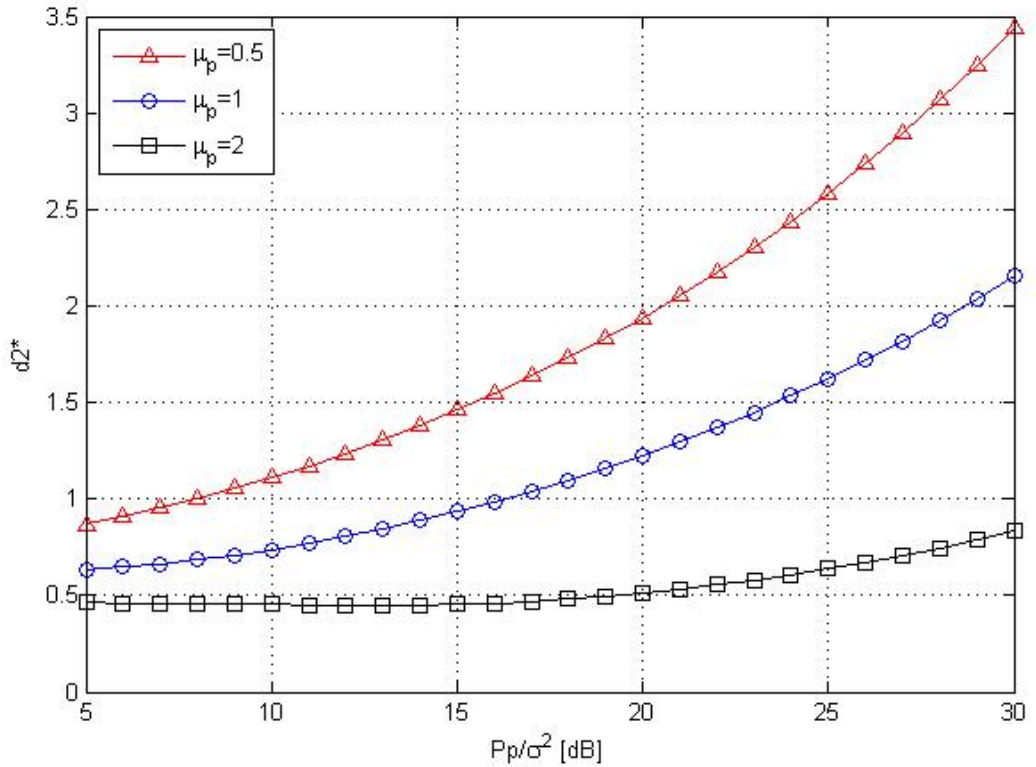


Figure 4.2: Critical Regions for The Proposed Protocol.

4.2.4 Outage performance evaluation

In this section, we evaluate the outage performance of the proposed protocol for both primary and secondary users in the light of analytical results of the previous section and validate them via computer simulation results. All results are compared with the non-cooperation case and the reference CR spectrum sharing protocol given in [3].

First, in Fig.4.2, the critical region of the proposed scheme derived from (4.25) for different rates μ_p is presented, where the path loss coefficient $\beta = 4$, $d_3 = 0.5$ and $P_s/\sigma^2 = 20$ dB. It could be seen from Fig.4.2 that by increasing the target rate μ_p the critical region becomes smaller. The primary system outage probability curves versus P_p/σ^2 are depicted in Fig.4.3 for target rates of $\mu_p = 1$ and 2, when $\beta = 4$, $d_2 = 0.5$ and $d_4 = 0.5$. Here it is assumed that the primary and secondary transmit powers are equal. In this figure, the simulation results denoted by symbols perfectly match with the theoretic outcomes denoted by solid curves.

On the other hand, in realistic view, by skipping the high P_s/σ^2 assumption in [3] made to derive analytically the outage probability, we also effectuated the computer

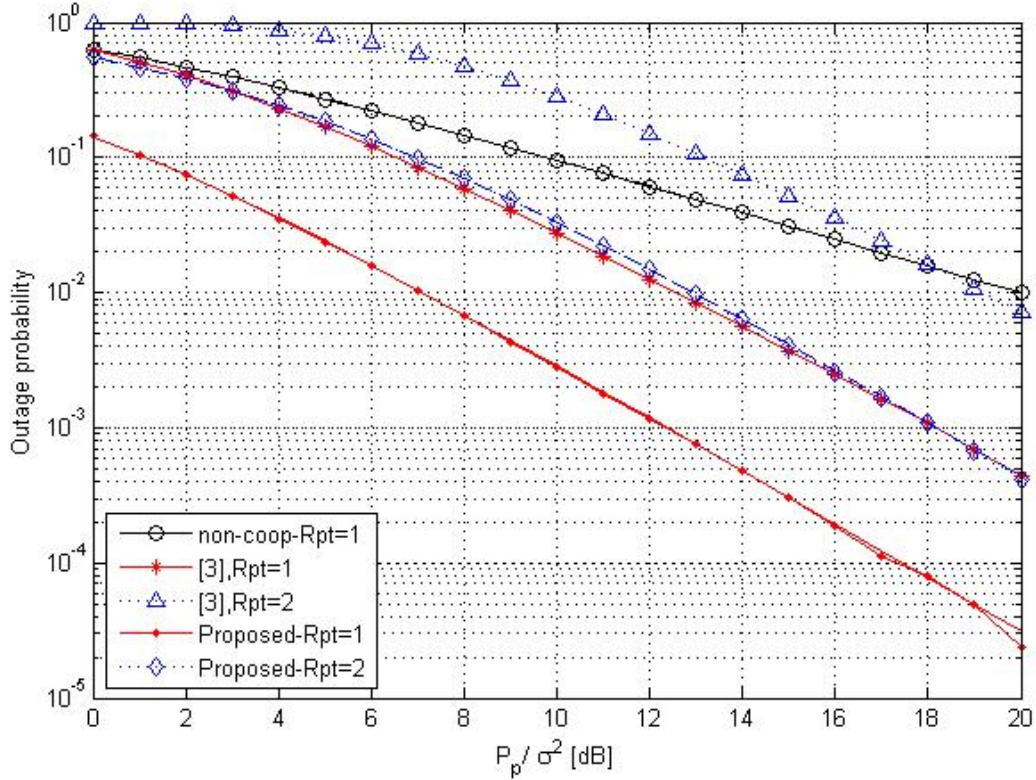


Figure 4.3: Primary System Outage Probability.

simulations for the scheme given in [3] and compared the results with those of the proposed scheme. From Fig.4.3 we can see that for an outage probability of 10^{-2} , our protocol provides an SNR gain of approximately 6 dB for both target rates of $\mu_p = 1$ and 2. In Fig.4.4, the outage probability curves of the secondary system are plotted for target rates $\mu_s = 1$ and 2, $\beta = 4$ and for fixed P_p / σ^2 taken equal to 20 dB. It is observed from these curves that the secondary system achieves reasonable outage probability values while providing performance improvement for the primary system by cooperation. It is obvious that the outage performance of the secondary system is better for smaller values of d_4 . More important is that, compared to the protocol given in [3] the proposed protocol provides SNR gains of 4 dB and 7 dB for $\mu_s = 1$ and 2, respectively. This means that the advantage of the new protocol becomes more obvious with increasing target rates. The worse performance of the scheme of [3] is due to the superimposed primary and secondary signals in the second time slot, where major part of the secondary transmitter power is needed to be allocated to the primary signal. Moreover, in [3] the transmission of the secondary signal from ST is conditioned on the non-outage of the links from PT to ST and SR. However, the link from PT to SR

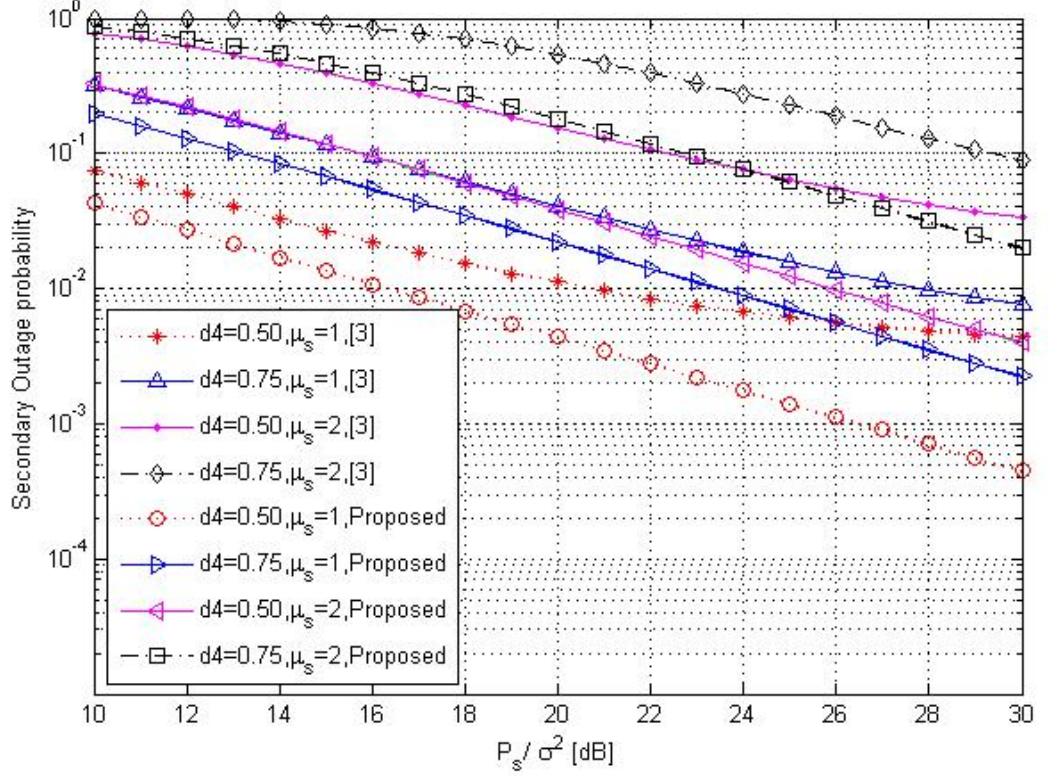


Figure 4.4: Secondary System Outage Probability.

is omitted in our protocol and ST always transmit its own signal during the third time slot irrespective of the $PT \rightarrow ST$ link's instantaneous channel condition.

4.3 Bit Error Probability Analysis

In this section, an analytical upper bound for the BEP of the proposed protocol for primary system is obtained. Moreover, for secondary system BEP is equal to the classical direct transmission scheme BEP and taken directly from [38] for comparison purposes.

4.3.1 Primary system BEP performance

The overall BEP for the primary system in the context of the proposed scheme is obtained as

$$P_{PR}^b = P_{PT \rightarrow PR}^b P_{PT \rightarrow ST}^s + (1 - P_{PT \rightarrow ST}^s) P_{coop}^b \quad (4.29)$$

where $P_{PT \rightarrow PR}^b$ and $P_{PT \rightarrow ST}^s$ denote the BEP and symbol error probability (SEP) of the links $PT \rightarrow PR$ and $PT \rightarrow ST$, respectively. SEP for the link $PT \rightarrow ST$ is assumed in (4.29)

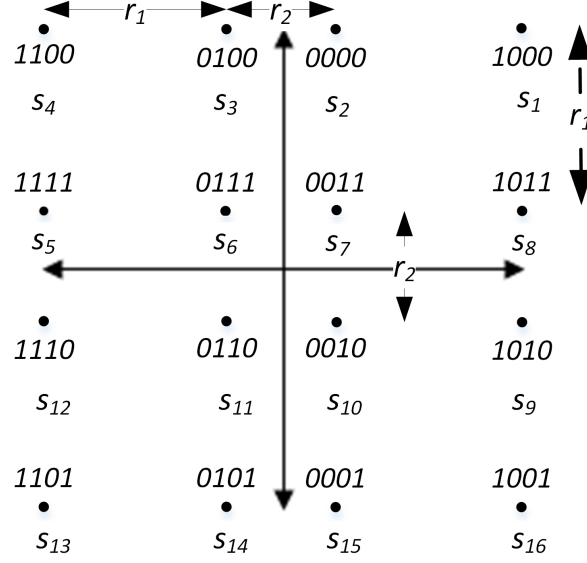


Figure 4.5: Irregular 16-QAM Signal Constellation and Its Bit Mapping.

since ST cooperates only when it correctly decodes the primary symbol. P_{coop}^b is the BEP at PR when ST cooperates with the primary system.

4.3.1.1 Calculation of $P_{PT \rightarrow ST}^s$

In the proposed scheme, primary symbol is transmitted from ST only if it decodes this symbol correctly. Therefore, we consider the SEP for the R-4QAM constellation in the link $PT \rightarrow ST$ and calculate $P_{PT \rightarrow ST}^s$. After some calculation by considering the decision areas [38] for the constellation of Fig.4.5, Conditional SEP (CSEP) could be expressed for SISO system as is calculated in Appendix.(0.3):

$$P(e|\gamma) = 2Q(\sqrt{2g_1\gamma}) - Q^2(\sqrt{2g_1\gamma}) + Q(\sqrt{2g_2\gamma}) - \frac{1}{4}Q^2(\sqrt{2g_2\gamma}) - Q(\sqrt{2g_1\gamma})Q(\sqrt{2g_2\gamma}) \quad (4.30)$$

where the SNR γ is the exponentially distributed r.v., $g_1 = (0.3716)^2$ and $g_2 = (0.23)^2$. The term $Q(\sqrt{2g_1\gamma})Q(\sqrt{2g_2\gamma})$ in (4.30) could be ignored with respect to the other terms. $P_{PT \rightarrow ST}^s$ can be obtained by averaging CSEP of (4.30) over the pdf of SNR γ for Rayleigh fading channel as

$$P_{PT \rightarrow ST}^s = \int_0^{\infty} P(e|\gamma)P(\gamma)d\gamma. \quad (4.31)$$

Based on [39]¹, average SEP for the link $PT \rightarrow ST$ over Rayleigh fading channel under one antenna reception can be obtained numerically from (4.31).

¹The term $(2k - 1)$ in the denominator of (18) in [39] should be corrected as $(2k + 1)$.

4.3.1.2 Calculation of $P_{PT \rightarrow PR}^b$

$P_{PT \rightarrow PR}^b$ is the BEP at the PR on the link PT→PR when ST could not successfully decode the primary signal and as a result PR tries to decode the transmitted signal directly from the signal received from PT. Based on the bit mapping rule irregular 16QAM constellation given in Fig.4.5 where $r_1 = 0.7432\sqrt{E_s}$ and $r_2 = 0.46\sqrt{E_s}$, upper bound on $P_{PT \rightarrow PR}^b$ is calculated from BER union bound for $M - RQAM$ which is given in Appendix.(0.2).

4.3.1.3 Calculation of P_{coop}^b

In the first and second time slots, the received signals at PR are given as,

$$y_{PR1} = h_1(x_1^R + jx_2^I) + n_1, \quad (4.32)$$

$$y_{PR2} = h_3(x_2^R + jx_1^I) + n_3 \quad (4.33)$$

where h_1 and h_3 denote the fading coefficients of links from PT→PR and ST→PR and n_1 and n_3 stand for the AWGN samples at PR, at the first and second time slots, respectively. By calculation and normalization at PR from (4.32) and (4.33) we have,

$$\begin{bmatrix} h_1^* y_{PR1} \\ h_3^* y_{PR2} \end{bmatrix} = \begin{bmatrix} |h_1|^2 & 0 \\ 0 & |h_3|^2 \end{bmatrix} \begin{bmatrix} x_1^R + jx_2^I \\ x_2^R + jx_1^I \end{bmatrix} + \begin{bmatrix} h_1^* n_1 \\ h_3^* n_3 \end{bmatrix} \quad (4.34)$$

where for simplicity we obtain,

$$\begin{aligned} \tilde{y}_{PR1} &= h_1^* y_{PR1} = |h_1|^2(x_1^R + jx_2^I) + \Re\{h_1^* n_1\} + j\Im\{h_1^* n_1\} \\ &= |h_1|^2 x_1^R + |h_1|^2 jx_2^I + \Re\{h_1^* n_1\} + j\Im\{h_1^* n_1\} \end{aligned} \quad (4.35)$$

$$\begin{aligned} \tilde{y}_{PR2} &= h_3^* y_{PR2} = |h_3|^2(x_2^R + jx_1^I) + \Re\{h_3^* n_3\} + j\Im\{h_3^* n_3\} \\ &= |h_3|^2 x_2^R + |h_3|^2 jx_1^I + \Re\{h_3^* n_3\} + j\Im\{h_3^* n_3\}. \end{aligned} \quad (4.36)$$

Considering (4.35) and (4.36), symbols x_1 and x_2 can be acquired by applying combining and deinterleaving operations at PR in the light of [17] as

$$\begin{aligned} \hat{y}_{PR1} &= \Re\{\tilde{y}_{PR1}\} + j\Im\{\tilde{y}_{PR2}\} \\ &= |h_1|^2 x_1^R + \Re\{h_1^* n_1\} + j|h_3|^2 jx_1^I + j\Im\{h_3^* n_3\} \\ &= |h_1|^2 x_1^R + j|h_3|^2 x_1^I + N_1, \end{aligned} \quad (4.37)$$

and

$$\begin{aligned}
\hat{y}_{PR2} &= \Re\{\tilde{y}_{PR2}\} + j\Im\{\tilde{y}_{PR1}\} \\
&= |h_3|^2 x_2^R + \Re\{h_3^* n_3\} + j|h_1|^2 x_2^I + j\Im\{h_1^* n_1\}, \\
&= |h_3|^2 x_2^R + j|h_1|^2 x_2^I + N_2,
\end{aligned} \tag{4.38}$$

respectively. In (4.37) and (4.38) by considering the probability density function (pdf) of r.v $n_1 \sim CN(0, 2\sigma^2)$ and $n_3 \sim CN(0, 2\sigma^2)$, their variances of noise terms can be expressed as ²

$$\text{Var}(\Re\{h_1^* n_1\}) = \text{Var}(h_1^R n_1^R + h_1^I n_1^I) = |h_1^R|^2 \sigma^2 + |h_1^I|^2 \sigma^2 = |h_1|^2 \sigma^2, \tag{4.39}$$

$$\text{Var}(\Im\{h_3^* n_3\}) = \text{Var}(h_3^R n_3^I - h_3^I n_3^R) = |h_3^R|^2 \sigma^2 + |h_3^I|^2 \sigma^2 = |h_3|^2 \sigma^2, \tag{4.40}$$

$$\text{Var}(\Re\{h_3^* n_3\}) = \text{Var}(h_3^R n_3^R + h_3^I n_3^I) = |h_3^R|^2 \sigma^2 + |h_3^I|^2 \sigma^2 = |h_3|^2 \sigma^2, \tag{4.41}$$

$$\text{Var}(\Im\{h_1^* n_1\}) = \text{Var}(h_1^R n_1^I - h_1^I n_1^R) = |h_1^R|^2 \sigma^2 + |h_1^I|^2 \sigma^2 = |h_1|^2 \sigma^2, \tag{4.42}$$

respectively. The total variance for N_1 and N_2 would be

$$\text{Var}(N_1) = (|h_1|^2 + |h_3|^2) \sigma^2, \tag{4.43}$$

and

$$\text{Var}(N_2) = (|h_3|^2 + |h_1|^2) \sigma^2, \tag{4.44}$$

respectively. Simplified versions of (4.37) and (4.38) can be calculated as

$$\hat{y}_{PR1} = ax_1^R + jbx_1^I + u_1, \tag{4.45}$$

$$\hat{y}_{PR2} = bx_2^R + jax_2^I + u_2 \tag{4.46}$$

where $a = |h_1|^2$, $b = |h_3|^2$, $u_1^R = \Re\{h_1^* n_1\}$, $u_1^I = \Im\{n_3 h_3^*\}$, $u_2^R = \Re\{n_3 h_3^*\}$ and $u_2^I = \Im\{h_1^* n_1\}$. Variances of the AWGN samples u_1^R , u_1^I , u_2^R and u_2^I are as follows:

$$\text{Var}(u_1^R) = \text{Var}(u_2^I) = a\sigma^2, \text{Var}(u_1^I) = \text{Var}(u_2^R) = b\sigma^2.$$

ML decision rule from [17] for x_1 and x_2 based on Appendix.(0.4) are

$$\hat{x}_1 = \underset{x_1^R, x_1^I}{\text{argmin}} (b|\hat{y}_{PR1}^R - ax_1^R|^2 + a|\hat{y}_{PR1}^I - bx_1^I|^2) \tag{4.47}$$

² $\text{Var}(aX + bY) = a^2 \text{var}(X) + b^2 \text{var}(Y)$ and $\text{Var}(aX - bY) = a^2 \text{var}(X) + b^2 \text{var}(Y)$.

and

$$\hat{x}_2 = \underset{x_2^R, x_2^I}{\operatorname{argmin}} (a|\hat{y}_{PR2}^R - bx_2^R|^2 + b|\hat{y}_{PR2}^I - ax_2^I|^2), \quad (4.48)$$

respectively. Therefore, CPEP for x_1 and x_2 are given by Appendix.(0.5) as

$$\begin{aligned} P(x_1 \rightarrow \hat{x}_1 | \{h_1, h_3\}) &= P[b|\hat{y}_{PR1}^R - a\hat{x}_1^R|^2 + a|\hat{y}_{PR1}^I - b\hat{x}_1^I|^2 \\ &< b|\hat{y}_{PR1}^R - ax_1^R|^2 + a|\hat{y}_{PR1}^I - bx_1^I|^2] \\ &= P[(2\Delta_R u_1^R + 2\Delta_I u_1^I) < (-a\Delta_R^2 - b\Delta_I^2)] \end{aligned} \quad (4.49)$$

and

$$\begin{aligned} P(x_2 \rightarrow \hat{x}_2 | \{h_1, h_3\}) &= P[a|\hat{y}_{PR2}^R - b\hat{x}_2^R|^2 + b|\hat{y}_{PR2}^I - a\hat{x}_2^I|^2 \\ &< a|\hat{y}_{PR2}^R - bx_2^R|^2 + b|\hat{y}_{PR2}^I - ax_2^I|^2] \\ &= P[(2\Delta_R u_2^R + 2\Delta_I u_2^I) < (-b\Delta_R^2 - a\Delta_I^2)], \end{aligned} \quad (4.50)$$

respectively, where $\Delta_R = |x_i^R - \hat{x}_i^R|$ and $\Delta_I = |x_i^I - \hat{x}_i^I|$. The terms $2\Delta_R u_1^R + 2\Delta_I u_1^I$ and $2\Delta_R u_2^R + 2\Delta_I u_2^I$ in (4.49) and (4.50) are both Gaussian r.v. with zero mean and variances $4\sigma^2(a\Delta_R^2 + b\Delta_I^2)$ and $4\sigma^2(b\Delta_R^2 + a\Delta_I^2)$, respectively.

CPEP for x_1 and x_2 could be calculated as following. By simplifying³ (4.49), CPEP for x_1 is given as,

$$P(x_1 \rightarrow \hat{x}_1 | \{h_1, h_3\}) = P[A > a\Delta_R^2 + b\Delta_I^2 | \{h_1, h_3\}] \quad (4.51)$$

where $A = 2\Delta_R u_1^R + 2\Delta_I u_1^I$ and $A \sim N(0, 4\sigma^2(a\Delta_R^2 + b\Delta_I^2)) = N(0, \gamma^2)$. After some calculation

$$P[A > a\Delta_R^2 + b\Delta_I^2 | \{h_1, h_3\}] = \int_{a\Delta_R^2 + b\Delta_I^2}^{\infty} \frac{1}{\sqrt{2\pi\gamma^2}} \exp\left(-\frac{A^2}{2\gamma^2}\right) dA. \quad (4.52)$$

Assuming $\frac{A}{\gamma} = Z$, $\frac{A^2}{\gamma^2} = Z^2$ and $dA = \gamma dZ$ we obtain

$$P[A > a\Delta_R^2 + b\Delta_I^2 | \{h_1, h_3\}] = \int_{\tau}^{\infty} \frac{1}{\sqrt{2\pi}} \exp\left(-\frac{Z^2}{2}\right) dZ = Q(\tau) \quad (4.53)$$

where $\tau = \sqrt{(a\Delta_R^2 + b\Delta_I^2)/4\sigma^2}$. By some simplification in (4.50), we acquire the CPEP for x_2 as,

$$P(x_2 \rightarrow \hat{x}_2 | \{h_1, h_3\}) = P[A > b\Delta_R^2 + a\Delta_I^2 | \{h_1, h_3\}] \quad (4.54)$$

³By symmetry in Gaussian random variable, we have $P(A < -C) = P(A > C)$.

where $A = 2\Delta_R u_R^2 + 2\Delta_I u_I^2$ and $A \sim N(0, 4\sigma^2(b\Delta_R^2 + a\Delta_I^2)) = N(0, \gamma^2)$. After some calculation

$$P[A > b\Delta_R^2 + a\Delta_I^2 | \{h_1, h_3\}] = \int_{b\Delta_R^2 + a\Delta_I^2}^{\infty} \frac{1}{\sqrt{2\pi\gamma^2}} \exp\left(-\frac{A^2}{2\gamma^2}\right) dA. \quad (4.55)$$

Assuming $\frac{A}{\gamma} = Z$, $\frac{A^2}{\gamma^2} = Z^2$ and $dA = \gamma dZ$ we have

$$P[A > b\Delta_R^2 + a\Delta_I^2 | \{h_1, h_3\}] = \int_{\xi}^{\infty} \frac{1}{\sqrt{2\pi}} \exp\left(-\frac{Z^2}{2}\right) dZ = Q(\xi). \quad (4.56)$$

where $\xi = \sqrt{(b\Delta_R^2 + a\Delta_I^2)/4\sigma^2}$. Omitting indices of the fading coefficients for simplicity, the pdf of Rayleigh distributed r.v. h is $f(h) = (2h/\Omega)\exp(-h^2/\Omega)$ where $\Omega = E[|h|^2] = d^{-\beta}$ is the expected channel fading power. Note that $\alpha_1^2 = |h_1|^2$ and $\alpha_3^2 = |h_3|^2$. The PEP of x_1 can be calculated from (4.53) by averaging over fading coefficients as

$$\begin{aligned} P(x_1 \rightarrow \hat{x}_1) &= \int_0^{\infty} \int_0^{\infty} \int_{\Psi}^{\infty} \frac{1}{\sqrt{2\pi}} \exp\left(-\frac{Z^2}{2}\right) dZ \frac{2\alpha_1}{d_1^{-\beta}} \exp\left(-\frac{\alpha_1^2}{d_1^{-\beta}}\right) d\alpha_1 \\ &\quad \times \frac{2\alpha_3}{d_3^{-\beta}} \exp\left(-\frac{\alpha_3^2}{d_3^{-\beta}}\right) d\alpha_3 \end{aligned} \quad (4.57)$$

where $\Psi = \sqrt{(\alpha_1^2\Delta_R^2 + \alpha_3^2\Delta_I^2)/4\sigma^2}$. By simplifying

$$\begin{aligned} P(x_1 \rightarrow \hat{x}_1) &= \int_0^{\infty} \int_0^{\infty} \int_{\Psi}^{\infty} \frac{4}{\sqrt{2\pi}d_1^{-\beta}d_3^{-\beta}} \exp\left(-\frac{Z^2}{2}\right) \alpha_1 \alpha_3 \\ &\quad \times \exp\left(-\left(\frac{\alpha_1^2}{d_1^{-\beta}} + \frac{\alpha_3^2}{d_3^{-\beta}}\right)\right) dZ d\alpha_1 d\alpha_3. \end{aligned} \quad (4.58)$$

Assuming

$$W_1^2 = \frac{\alpha_1^2}{d_1^{-\beta}}, \quad \alpha_1^2 = \frac{W_1^2}{d_1^{\beta}}, \quad \alpha_1 = \frac{W_1}{\sqrt{d_1^{\beta}}}$$

and

$$W_3^2 = \frac{\alpha_3^2}{d_3^{-\beta}}, \quad \alpha_3^2 = \frac{W_3^2}{d_3^{\beta}}, \quad \alpha_3 = \frac{W_3}{\sqrt{d_3^{\beta}}}$$

and substituting in (4.58) we have

$$P(x_1 \rightarrow \hat{x}_1) = \int_0^\infty \int_0^\infty \int_\kappa^\infty \frac{4}{\sqrt{2\pi}d_1^{-\beta}d_3^{-\beta}} \exp\left(-\frac{Z^2}{2}\right) \frac{W_1}{\sqrt{d_1^\beta}} \frac{W_3}{\sqrt{d_3^\beta}} \\ \times \exp(-(W_1^2 + W_3^2)) dZ \frac{dW_1}{\sqrt{d_1^\beta}} \frac{dW_3}{\sqrt{d_3^\beta}} \quad (4.59)$$

$$= \int_0^\infty \int_0^\infty \int_\kappa^\infty \frac{4}{\sqrt{2\pi}} \exp\left(-\frac{Z^2}{2}\right) W_1 W_3 \exp(-(W_1^2 + W_3^2)) dZ dW_1 dW_3 \quad (4.60)$$

where $\kappa = \sqrt{(\frac{W_1^2}{d_1^\beta} \Delta_R^2 + \frac{W_3^2}{d_3^\beta} \Delta_I^2) / 4\sigma^2}$. We replace $W_1 = \rho \cos \phi$, $W_3 = \rho \sin \phi$, $dW_1 dW_3 = \rho d\rho d\phi$, $Z = \rho v$ and $dZ = \rho dv$ in (4.60) and acquire,

$$P(x_1 \rightarrow \hat{x}_1) = \int_0^{\frac{\pi}{2}} \int_0^\infty \int_y^\infty \frac{4}{\sqrt{2\pi}} \exp\left(-\frac{\rho^2 v^2}{2}\right) \rho dv (\rho \cos \phi) (\rho \sin \phi) \exp(-(\rho^2)) \rho d\rho d\phi \\ = \int_0^{\frac{\pi}{2}} \int_0^\infty \int_y^\infty \frac{4}{\sqrt{2\pi}} \rho^4 \cos \phi \sin \phi \exp\left(-\frac{\rho^2(v^2 + 2)}{2}\right) dv d\rho d\phi \\ = \int_0^{\frac{\pi}{2}} \int_y^\infty \frac{4}{\sqrt{2\pi}} \cos \phi \sin \phi \int_0^\infty \rho^4 \exp\left(-\frac{\rho^2(2 + v^2)}{2}\right) d\rho dv d\phi \quad (4.61)$$

where $x = \sqrt{(\frac{\rho^2 \cos^2 \phi}{d_1^\beta} \Delta_R^2 + \frac{\rho^2 \sin^2 \phi}{d_3^\beta} \Delta_I^2) / 4\sigma^2} = \rho \sqrt{(\frac{\cos^2 \phi}{d_1^\beta} \Delta_R^2 + \frac{\sin^2 \phi}{d_3^\beta} \Delta_I^2) / 4\sigma^2}$ and $y = x/\rho$. By simplifying⁴ $\frac{4}{\sqrt{2\pi}} \int_0^\infty \rho^4 \exp(-\rho^2 B) d\rho$ in (4.61) where $B = \frac{(2+v^2)}{2}$ we obtain,

$$\frac{4}{\sqrt{2\pi}} \int_0^\infty \rho^4 \exp(-\rho^2 B) d\rho = \frac{4}{\sqrt{2\pi}} \frac{3}{4B^2} \int_0^\infty e^{-\rho^2 B} d\rho. \quad (4.62)$$

By some calculation⁵ and substituting in the (4.62) we can have,

$$\frac{4}{\sqrt{2\pi}} \frac{3}{4B^2} \int_0^\infty e^{-\rho^2 B} d\rho = \frac{4}{\sqrt{2\pi}} \frac{3}{4B^2} \frac{\sqrt{\pi}}{2\sqrt{B}}. \quad (4.63)$$

Finally, Eq.(4.62) can be expressed as

$$\frac{4}{\sqrt{2\pi}} \int_0^\infty \rho^4 \exp\left(-\frac{\rho^2(2 + v^2)}{2}\right) d\rho = \frac{6}{(2 + v^2)^{5/2}}. \quad (4.64)$$

⁴Taking Hopital 2 times and using $U.V - \int V dU$ in integrals.

⁵ $erf(x) = \frac{2}{\sqrt{\pi}} \int_0^x e^{-t^2} dt$, $erf(\sqrt{A}.x) = \frac{2\sqrt{A}}{\sqrt{\pi}} \int_0^x e^{-At^2} dt$.

Calculation of integral in (4.62) could also be obtained by [40]⁶. Substituting the result (4.64) in (4.61) we obtain

$$P(x_1 \rightarrow \hat{x}_1) = \int_0^{\frac{\pi}{2}} \int_y^{\infty} \frac{6}{(2+v^2)^{5/2}} \cos \phi \sin \phi d v d \phi. \quad (4.65)$$

Replacing $V = \sin^2 \phi$, $1 - V = \cos^2 \phi$ and $dV = 2 \sin \phi \cos \phi d \phi$, we obtain

$$P(x_1 \rightarrow \hat{x}_1) = \frac{1}{2} \int_0^1 \int_q^{\infty} \frac{6}{(2+v^2)^{5/2}} d v d V, \quad (4.66)$$

where $q = \sqrt{(\frac{1-V}{d_1^\beta} \Delta_R^2 + \frac{V}{d_3^\beta} \Delta_I^2) / 4\sigma^2}$. Substituting

$$\int_q^{\infty} \frac{6}{(2+v^2)^{5/2}} d v = 1 - \frac{q(3+q^2)}{(2+q^2)^{3/2}}. \quad (4.67)$$

in (4.66) we obtain,

$$P(x_1 \rightarrow \hat{x}_1) = \frac{1}{2} \int_0^1 1 - \frac{q(3+q^2)}{(2+q^2)^{3/2}} d V. \quad (4.68)$$

Finally, the PEP obtained by using Mathematica software can be expressed as

$$\begin{aligned} P(x_1 \rightarrow \hat{x}_1) &= \frac{1}{2} \left[1 + d_1^\beta d_3^\beta \left(\frac{\Delta_R^2 \sqrt{d_1^{-\beta} \Delta_R^2} \sqrt{4N_o + d_1^{-\beta} \Delta_R^2}}{(-d_3^\beta \Delta_R^2 + d_1^\beta \Delta_I^2)(\Delta_R^2 + 4d_1^\beta N_o)} \right. \right. \\ &\quad \left. \left. + \frac{\Delta_I^2 \sqrt{d_3^{-\beta} \Delta_I^2} \sqrt{4N_o + d_3^{-\beta} \Delta_I^2}}{(d_3^\beta \Delta_I^2 - d_1^\beta \Delta_I^2)(\Delta_I^2 + 4d_3^\beta N_o)} \right) \right] \\ &= \frac{1}{2} \left[1 + \frac{d_1^\beta d_3^\beta}{(d_1^\beta \Delta_I^2 - d_3^\beta \Delta_R^2)} \left(\frac{\Delta_R^2 \sqrt{d_1^{-\beta} \Delta_R^2} \sqrt{4N_o + d_1^{-\beta} \Delta_R^2}}{(\Delta_R^2 + 4d_1^\beta N_o)} \right. \right. \\ &\quad \left. \left. - \frac{\Delta_I^2 \sqrt{d_3^{-\beta} \Delta_I^2} \sqrt{4N_o + d_3^{-\beta} \Delta_I^2}}{(\Delta_I^2 + 4d_3^\beta N_o)} \right) \right]. \quad (4.69) \end{aligned}$$

Now, we apply Taylor series⁷ to (4.69) via Mathematica software with respect to N_o at high SNR to find a simplified expression of the PEP. After some calculation and simplification PEP can be expressed as

$$P(x_1 \rightarrow \hat{x}_1) = \frac{3N_o^2}{\Delta_R^2 \Delta_I^2} d_1^\beta d_3^\beta + O(N_o^3). \quad (4.70)$$

⁶ $\int_0^{\infty} x^{2n} \exp(-ax^2) dx = \frac{2n!}{n!2^{n+1}} \sqrt{\frac{\pi}{a^{2n+1}}}$ where in our case $n = 2$ and $a = \frac{2+u^2}{2}$.

⁷ $f(x) = f(0) + N_o f'(0) + \frac{N_o^2 f''(0)}{2} + O(N_o^3)$

where $O(N_o^3)$ shows the terms of N_o with orders equal or higher than three. Another attempt to calculate the PEP from (4.68) is by assuming that $R = \frac{\Delta_R^2}{d_1^\beta}$, $I = \frac{\Delta_I^2}{d_3^\beta}$, $W = (1-V)R + VI$, $q = \sqrt{\frac{W}{2N_o}}$ and $dW = dV(I-R)$. Therefore, (4.68) can be expressed as

$$P(x_1 \rightarrow \hat{x}_1) = \frac{1}{2} \int_R^I \left(1 - \frac{q(3+q^2)}{(2+q^2)^{5/2}}\right) \frac{dW}{I-R} = \frac{1}{2(I-R)} \int_R^I \left(1 - \frac{q(3+q^2)}{(2+q^2)^{5/2}}\right) dW. \quad (4.71)$$

By simplifying the integral part in (4.71) we obtain,

$$\int_R^I \left(1 - \frac{q(3+q^2)}{(2+q^2)^{5/2}}\right) dW = W \left(1 - \frac{\sqrt{W}}{\sqrt{4N_o+W}}\right) \Big|_R^I. \quad (4.72)$$

Finally, PEP is obtained as

$$\begin{aligned} P(x_1 \rightarrow \hat{x}_1) &= \frac{1}{2(I-R)} \left(I \left(1 - \frac{\sqrt{I}}{\sqrt{4N_o+I}}\right) - R \left(1 - \frac{\sqrt{R}}{\sqrt{4N_o+R}}\right) \right) \\ &= \frac{1}{2(I-R)} \left(I - R - \frac{I\sqrt{I}}{\sqrt{4N_o+I}} + \frac{R\sqrt{R}}{\sqrt{4N_o+R}} \right) \\ &= \frac{1}{2} \left(1 - \frac{1}{(I-R)} \left(\frac{I\sqrt{I}}{\sqrt{4N_o+I}} - \frac{R\sqrt{R}}{\sqrt{4N_o+R}} \right) \right). \end{aligned} \quad (4.73)$$

Now applying Taylor series in (4.73), the PEP can be rewritten as

$$P(x_1 \rightarrow \hat{x}_1) = \frac{3N_o^2}{RI} + O(N_o^3) \quad (4.74)$$

where $R = \frac{\Delta_R^2}{d_1^\beta}$ and $I = \frac{\Delta_I^2}{d_3^\beta}$. Replacing R and I in (4.74), it can be easily seen that the two results in (4.74) and (4.70) are the same given as

$$P(x_1 \rightarrow \hat{x}_1) = \frac{3N_o^2}{\Delta_R^2 \Delta_I^2} d_1^\beta d_3^\beta + O(N_o^3). \quad (4.75)$$

Here, assuming equally likely symbols and using the upper bound on SEP, average SEP for x_1 can be written as

$$P_s \leq \frac{1}{M} \sum_{i=1}^M \sum_{\substack{j=1 \\ i \neq j}}^M P(x_i \rightarrow x_j) = P(x_1 \rightarrow x_2) + P(x_1 \rightarrow x_3) + P(x_1 \rightarrow x_4) \quad (4.76)$$

where in our case (4RQAM) $M=4$. Reminding that $\Delta_R = |x_i^R - \hat{x}_i^R|$, $\Delta_I = |x_i^I - \hat{x}_i^I|$ and taking $\alpha_{R4QAM} = \{0.23 + i0.9732, -0.23 - i0.9732, 0.9732 - i0.23, -0.9732 + i0.23\}$ and substituting in (4.76) we have

$$\begin{aligned} P(x_1 \rightarrow x_2) &= \frac{3N_o^2}{\left|0.23\sqrt{E_s} + 0.9732\sqrt{E_s}\right|^2 \left|-0.23\sqrt{E_s} + 0.9732\sqrt{E_s}\right|^2} d_1^\beta d_3^\beta \\ &= 1.25 \left(3 \left(\frac{N_o}{E_s}\right)^2 d_1^\beta d_3^\beta\right), \end{aligned} \quad (4.77)$$

$$\begin{aligned}
P(x_1 \rightarrow x_3) &= \frac{3N_o^2}{|0.23\sqrt{E_s} + 0.23\sqrt{E_s}|^2 |0.9732\sqrt{E_s} + 0.9732\sqrt{E_s}|^2} d_1^\beta d_3^\beta \\
&= 1.247 \left(3 \left(\frac{N_o}{E_s}\right)^2 d_1^\beta d_3^\beta\right), \tag{4.78}
\end{aligned}$$

$$\begin{aligned}
P(x_1 \rightarrow x_4) &= \frac{3N_o^2}{|0.23\sqrt{E_s} - 0.9732\sqrt{E_s}|^2 |0.23\sqrt{E_s} + 0.9732\sqrt{E_s}|^2} d_1^\beta d_3^\beta \\
&= 1.25 \left(3 \left(\frac{N_o}{E_s}\right)^2 d_1^\beta d_3^\beta\right), \tag{4.79}
\end{aligned}$$

respectively. Substituting (4.77), (4.78) and (4.79) in (4.76) we obtain an upper bound for SEP given as:

$$\begin{aligned}
P_s &\leq 3 \left(\frac{N_o}{E_s}\right)^2 d_1^\beta d_3^\beta (1.25 + 1.247 + 1.25) \\
P_s &\leq 3 \left(\frac{N_o}{E_s}\right)^2 d_1^\beta d_3^\beta (3.747). \tag{4.80}
\end{aligned}$$

Calculating upper bound BEP in Appendix.(0.2) where $M=4$ and $k=2$ as well as considering the bit mapping for 4-RQAM given in the previous section, average BEP for x_1 can be written as

$$P_b^{coop} \leq \frac{1}{4} (6P(x_1 \rightarrow x_4) + 2P(x_1 \rightarrow x_3)) \tag{4.81}$$

Finally, substituting (4.81), (4.31) and (A.3) in (4.29), the overall upper bound on the BEP of primary system can be obtained. In total, the energy to transmit 2 symbols (4 bits) of 4-RQAM in 2 time intervals is equal to $P_p + P_s$, where $P_p = P_s$, P_p and P_s being the transmit powers of PT and ST, respectively.

4.3.2 Secondary system BEP performance

In the third time slot, SU symbol is transmitted. In this time slot, direct transmission is applied at SR. In total, we consume P_s energy to transmit one secondary symbol. Exact BER derivation for 16-QAM is given in [38] and directly used for comparison purposes in the next section.

4.3.3 BER performance evaluation

In this section, simulation results are provided to support theoretical derivations both for PU and SU where we plot Bit Error Rate (BER) curves of the proposed protocol

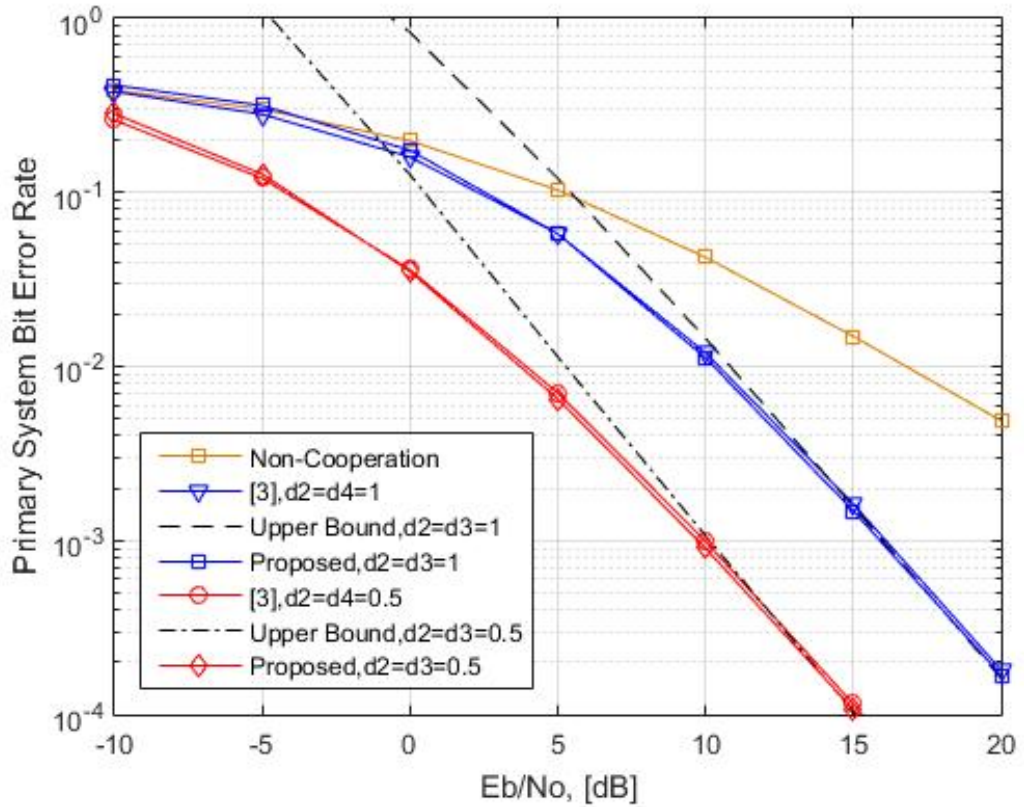


Figure 4.6: Primary System Bit Error Rate for Irregular 16-QAM ($d_2 = d_4 = 1$ and $d_2 = d_4 = 0.5$).

over Rayleigh fading channel versus SNR. We generate at least 2×10^6 bits to calculate BER for each SNR values in MATLAB program to make the simulation trustworthy.

In Fig.4.6 and Fig.4.7, BER curves for non-cooperation case and the protocol given in [3] for PU is also depicted for the sake of comparison. All distances are assumed to be the same for the proposed protocol and for that of [3]. In both mentioned figures simulation and theoretical upper bound results are represented by solid and dashed lines, respectively. It is calculated that for $R = 4$ where 16-QAM modulation (4 bits per one symbol) is used, ST at [3] allocates 99.86% of its power to PU data transmission. Therefore, in [3] for one symbol (4 bits) a total power of $P_p + P_s$ is spent in two time slots to transmit the PU's data where $P_p = P_s$, respectively. Fig.4.6 and Fig.4.7 are depicted for various values of distances between PT, PR and ST which in all cases significant improvement in BER performance is provided by our protocol compared to straightforward case. The derived upper is in perfect match with simulation results at high SNR values.

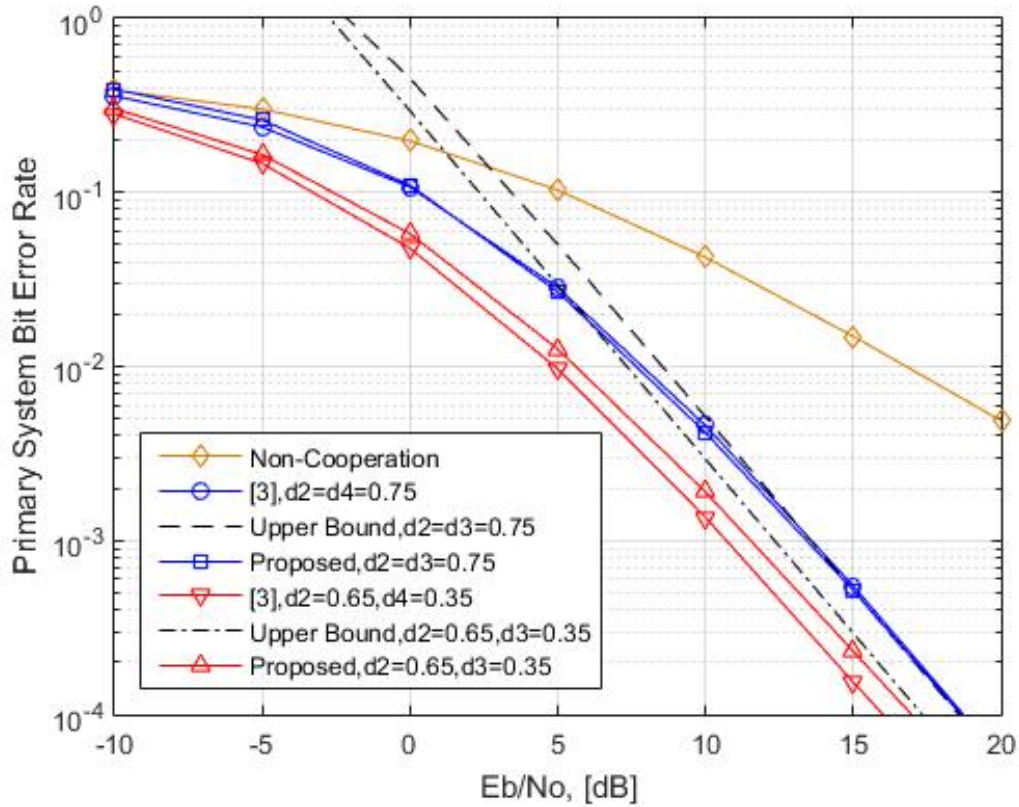


Figure 4.7: Primary System Bit Error Rate for Irregular 16-QAM ($d_2 = d_4 = 0.75$ and $d_2 = 0.65, d_4 = 0.35$).

As an example in Fig.4.6, the achieved gain at a BER value of 10^{-2} is nearly 7 and 14 dB for $d_2 = d_4 = 1$ and $d_2 = d_4 = 0.5$, respectively. In Fig.4.7 for a BER value of 10^{-2} , SNR gains of nearly 10 and 13 dB are provided compared to the non-cooperation case with $d_2 = d_3 = 0.75$ and $d_2 = 0.65, d_3 = 0.35$, respectively.

Due to the fact that, by using SSD and CIOD concept, we obtain an irregular 16-QAM constellation Fig.4.5 whose symbols are closer to each other in the constellation rather than the classical 16-QAM constellation. As a results, it causes more error compared to the traditional 16-QAM modulation when we consider the SER performance at the PT→ST link. Therefore, approximately no SNR gain is reported for our protocol in Fig.4.6 and Fig.4.7 when we compare with that of [3]. However, in [3] secondary system is in outage when it operates in 16-QAM modulation due to the power allocation at ST while for our protocol significant improvement in the BER of SU is provided. In other words, our protocol provides the same BER for PU in comparison to the reference protocol [3], on the other hand, for our protocol SU have reasonable BER performance compared to that of [3].

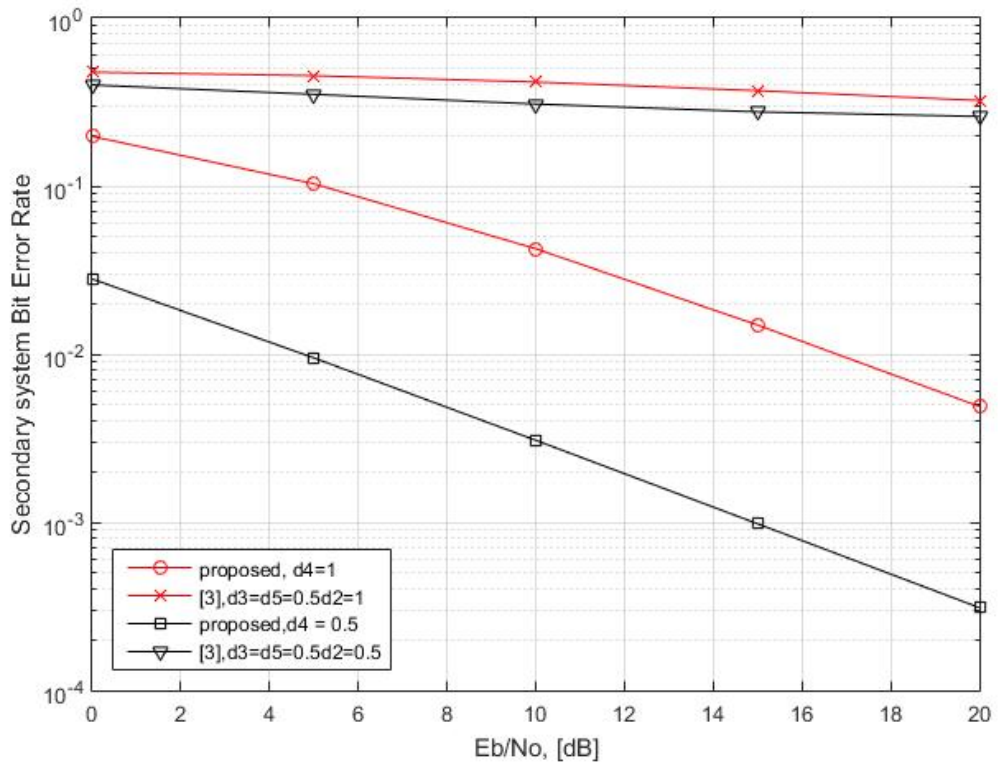


Figure 4.8: Secondary System Bit Error Rate for Classical 16-QAM ($d_4 = 1$ and $d_4 = 0.5$).

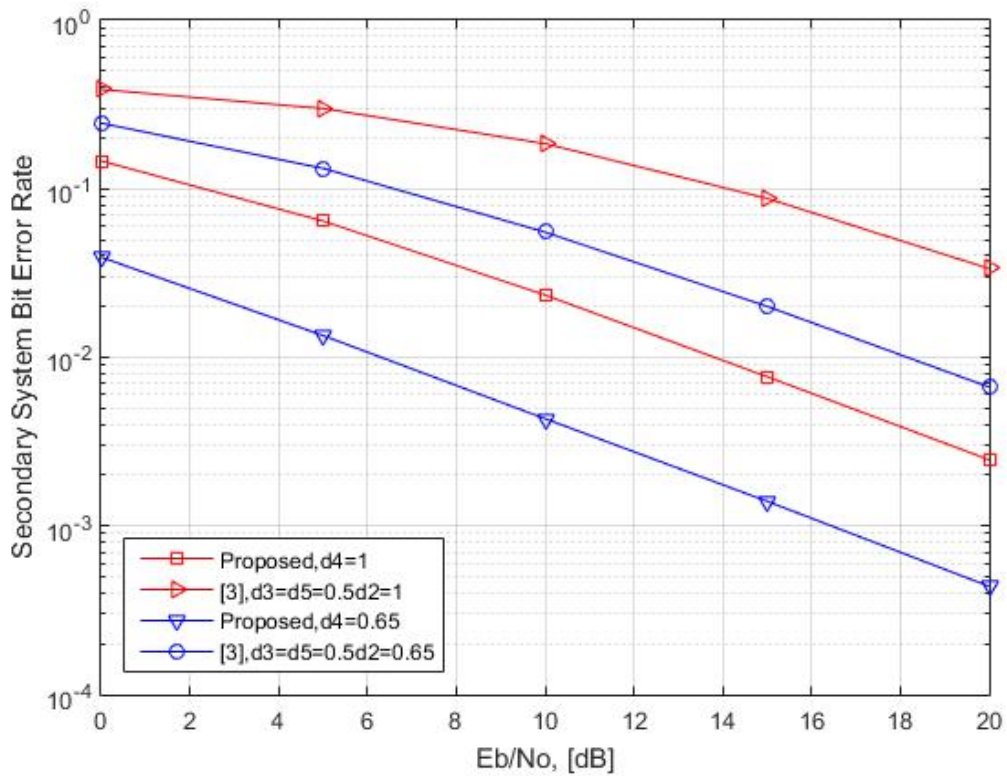


Figure 4.9: Secondary System Bit Error Rate for Classical 4-QAM ($d_4 = 1$ and $d_4 = 0.5$).

In Fig.4.8 and Fig.4.9 BER performance of SU for classical 16-QAM and 4-QAM modulation is depicted for different distance values between ST and SR where in both cases we assume $d_4 = 1$ and $d_4 = 0.5$. Both Fig.4.8 and Fig.4.9 show significant improvement in BER performance of SU. In Fig.4.8, the proposed protocol is compared for the classical 16-QAM with the reference scheme given in [3] which uses superposition coding at ST and consumes 99.68 of its power for transmitting PU's data and the remainder for its own symbol transmission at the second time slot. In Fig.4.9, same comparisons are performed for 4-QAM. In [3], it is calculated that 0.93 of SU's power is allocated for PU's data transmission. From Fig.4.9, we conclude that significant improvement in BER is provided by the proposed protocol compared to that of [3].

5. SPECTRUM SHARING IN CR BASED ON COMBINED CIOD AND STBC

In this chapter, we introduce a new spectrum sharing protocol which combines CIOD [17] and Alamouti's STBC [23] for cognitive radio networks. CIOD provides signal-space diversity at PR and increases the transmission rate of PU compared to the straightforward DF cognitive radio protocols given in the literature. Alamouti's STBC allows interference-free reception at PR and SR due to its single symbol decoding property and provides additional diversity. We obtain an upper bound expression for the primary system's BEP in Rayleigh fading channels when a rotated 4-QAM (R-4QAM) signal constellation is considered, by applying the pdf based PEP derivations. The theoretical results supported via computer simulations show that the BEP performance of the primary system is significantly improved by the proposed protocol compared to the non-cooperative case and the cooperative spectrum sharing protocol given in [3]. Moreover, continuous transmission of the secondary system by Alamouti coding is guaranteed by the new protocol, since ST transmits secondary signal during the second and third time slots even the reception of primary signal is failed in the first time slot. On the other hand, the transmission rate for the primary system is increased to 2 symbols per three channel uses compared to [3] where this rate is one symbol per two channel uses.

This chapter is divided into sections as follows. In Section 5.1, the system model and the new protocol are described. BEP analysis is explained in Section 5.2 and finally Section 5.3 is destined to the performance evaluation.

5.1 System Model and Protocol Description

In this section, we present the considered system configuration depicted in Fig.5.1 and the proposed spectrum sharing protocol for cognitive radio networks. The primary system comprises one transmitter (PT) and one receiver (PR) both equipped by one antenna. ST has two antennas and SR has one antenna. The overall transmission is

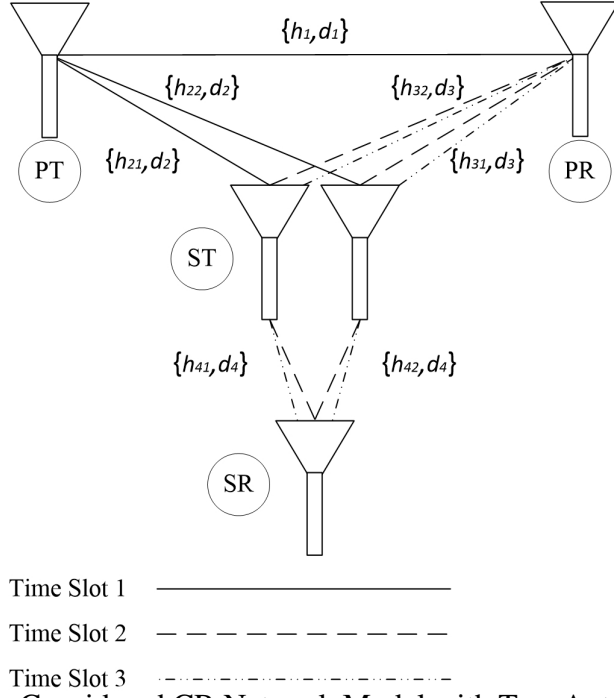


Figure 5.1: Considered CR Network Model with Two Antennas at ST.

completed in three time slots. During the first time slot, PT transmits to both PR and ST and during the second and third time slots, ST transmits to both PR and SR.

All channels are assumed to be exposed to Rayleigh fading with coefficient $h_i \sim CN(0, d_i^{-\beta})$ where h_i is the symmetric complex Gaussian random variable (r.v.). Here, d_i stands for the link distance which is depicted in Fig.5.1 for $i = 1, 2, 3, 4$ and β is the path loss exponent. All fading channel coefficients are assumed independent, identical distributed and constant over the transmission interval of three time slots and vary independently from one interval to another. All noise components are zero-mean AWGN r.v. with variance $\sigma^2 = N_0/2$ per dimension. The distances are normalized with respect to the distance of PT \rightarrow PR link (d_1) which is assumed equal to 1. $|h|^2$ denotes the channel gain which is exponentially distributed with mean $d_i^{-\beta}$, $(\cdot)^*$ and $(\cdot)^T$ stand for conjugate and transpose operations, $(\cdot)^R$ and $(\cdot)^I$ denote the real and imaginary parts of the complex symbols, respectively.

The fundamental attempt in our model is combining CIOD and STBC concepts for cognitive radio networks to provide diversity at both receivers PR and SR to improve their performance and, to improve the performance of the PT \rightarrow ST link by applying MRC to the signals received by two antennas of ST. CIOD is based on interleaving the real and imaginary parts of two-dimensional symbols taken from a rotated signal constellation to increase the diversity order over fading channels. This kind of diversity

Table 5.1: Proposed Protocol Transmission Schedule Using both CIOD and STBC.

	PT	ST1	ST2
T1	$x_1^R + jx_2^I$	–	–
T2	–	$x_2^R + jx_1^I$	$s^R + js^I$
T3	–	$-(s^R + js^I)^*$	$(x_2^R + jx_1^I)^*$

is named as signal-space diversity [24]. For a rotated 4-QAM Fig.2.8 signal set, each symbol could be retrieved from only their real or imaginary parts. Note that, after rotation and component interleaving 4QAM signal constellation is expanded to a nonuniform 16QAM constellation, (Fig.2.9). Also, note that classical Alamouti coding [23] is not applicable in the first time slot of the proposed protocol, since the primary symbols are unknown at ST, during the first time slot.

The proposed spectrum sharing protocol is as follows. In the first time slot, PT transmits the interleaved symbol $x_1^R + jx_2^I$ to both PR and ST where x_1^R and x_2^I are the real and imaginary parts of the first and second primary symbols, respectively. If ST correctly decodes the signal pair (x_1, x_2) from only their real and imaginary parts, respectively, it applies Alamouti's STBC during the second and third time slots to the signal $x_2^R + jx_1^I$ to be transmitted to PR and its own signal $s = s^R + js^I$ to be transmitted to SR. The transmission schedule can be expressed as given in Table.5.1 whose rows correspond to the time slots and columns to PT's antenna, ST's first and second antennas. In the first time slot, the received signal at PR and at the first and second antennas of ST are given as,

$$y_{PR1} = h_1(x_1^R + jx_2^I) + n_1, \quad (5.1)$$

$$y_{ST1} = h_{21}(x_1^R + jx_2^I) + n_{21}, \quad (5.2)$$

$$y_{ST2} = h_{22}(x_1^R + jx_2^I) + n_{22} \quad (5.3)$$

where h_1, h_{21}, h_{22} denote the fading coefficients of links from PT to PR, to the first and second antennas of ST, and n_1, n_{21}, n_{22} stand for the AWGN samples at PR, at the first and second antennas of ST, respectively. Note that ST applies MRC to decide the primary signal. The received signal vector $\mathbf{y} = (y_{PR2}, y_{PR3})^T$ at PR during the second and third time slots can be written as

$$\mathbf{y} = \mathbf{A}\mathbf{h} + \mathbf{n} \quad (5.4)$$

where $\mathbf{h} = (h_{31}, h_{32})^T$ is the fading coefficients vector for the link $ST \rightarrow PR$, $\mathbf{n} = (n_{31}, n_{32})^T$ is the AWGN sample vector at PR at the second and third time slots and

$$\mathbf{A} = \begin{pmatrix} x_2^R + jx_1^I & s^R + js^I \\ -(s^R + js^I)^* & (x_2^R + jx_1^I)^* \end{pmatrix}$$

is the Alamouti STBC matrix. Applying the decoding steps given in [23], PR can extract the combined signal for the primary signal $x_2^R + jx_1^I$ from (5.4) without making decision on symbol $x_2^R + jx_1^I$ as

$$\tilde{y}_{PR} = (|h_{31}|^2 + |h_{32}|^2)(x_2^R + jx_1^I) + n_{31}h_{31}^* + n_{32}^*h_{32}. \quad (5.5)$$

Finally, PR decides to the symbol pair (x_1, x_2) from

$$(\hat{x}_1, \hat{x}_2) = \underset{x_1, x_2}{\operatorname{argmin}} \{ |y_{PR1} - |h_1|^2(x_1^R + jx_2^I)|^2 + |\tilde{y}_{PR} - (|h_{31}|^2 + |h_{32}|^2)(x_2^R + jx_1^I)|^2 \}. \quad (5.6)$$

If ST fails to decode the signal pair (x_1, x_2) , it transmits only its own signal during the second and third time slots which provides diversity at SR. In the second and third time slots, the received signals at SR are given as

$$y_{SR1} = (x_2^R + jx_1^I)h_{41} + (s^R + js^I)h_{42} + n_{SR1}, \quad (5.7)$$

$$y_{SR2} = -(s^R + js^I)^*h_{41} + (x_2^R + jx_1^I)^*h_{42} + n_{SR2}, \quad (5.8)$$

where h_{41} and h_{42} represent channel fading coefficients of links from ST to SR and n_{SR1} and n_{SR2} are the AWGN samples at SR in second and third time slots, respectively. Applying the Alamouti decoding technique [23], secondary data can be extracted from the received signal.

5.2 Bit Error Probability Analysis

In this section, we derive an analytical upper bound for the BEP of primary system in the context of the proposed spectrum sharing protocol. BEP for the secondary system is equal to the classical Alamouti's scheme BEP and taken directly from [41] for comparison purposes.

5.2.1 Primary system BEP performance

For the primary system, the overall BEP can be expressed as,

$$P_{PR}^b = P_{PT \rightarrow PR}^b P_{PT \rightarrow ST}^s + (1 - P_{PT \rightarrow ST}^s) P_{coop}^b \quad (5.9)$$

where $P_{PT \rightarrow PR}^b$ and $P_{PT \rightarrow ST}^s$ denote the BEP and SEP of the links $PT \rightarrow PR$ and $PT \rightarrow ST$, respectively. Note that since ST cooperates only when it correctly decodes the primary symbol, SEP for the link $PT \rightarrow ST$ is considered in (5.9). P_{coop}^b is the BEP at PR when ST cooperates with the primary system.

5.2.1.1 Calculation of $P_{PT \rightarrow ST}^s$

In the proposed protocol, ST sends the primary symbol only if it decodes this symbol correctly. As a result, for the link $PT \rightarrow ST$ we consider the SEP analysis for the R-4QAM constellation and calculate $P_{PT \rightarrow ST}^s$. After some calculation by considering decision areas [38] for the constellation of Fig.4.5, CSEP could be expressed for SISO system as is calculated in Appendix(0.3):

$$P(e|\gamma) = 2Q(\sqrt{2g_1\gamma}) - Q^2(\sqrt{2g_1\gamma}) + Q(\sqrt{2g_2\gamma}) - \frac{1}{4}Q^2(\sqrt{2g_2\gamma}) - Q(\sqrt{2g_1\gamma})Q(\sqrt{2g_2\gamma}) \quad (5.10)$$

where the SNR γ is an exponentially distributed r.v., $g_1 = (0.3716)^2$ and $g_2 = (0.23)^2$. The term $Q(\sqrt{2g_1\gamma})Q(\sqrt{2g_2\gamma})$ in (5.10) could be ignored with respect to the other terms. For MRC with L independent and identically distributed Rayleigh fading channel, the pdf of SNR γ can be expressed as [38]

$$P_{MRCI}(\gamma) = \frac{\gamma^{L-1}}{(L-1)!\bar{\gamma}_c^L} \exp\left(-\frac{\gamma}{\bar{\gamma}_c}\right) \quad (5.11)$$

where, $L = 2$ in our case and $\bar{\gamma}_c$ is the average SNR per channel defined as

$$\bar{\gamma}_c = \frac{E_s}{N_0} E[h_{21}^2] = \frac{E_s}{N_0} E[h_{22}^2] \quad (5.12)$$

and E_s is the average energy per symbol. $P_{PT \rightarrow ST}^s$ can be derived by averaging CSEP of (5.10) over the pdf of SNR γ given in (5.11) for Rayleigh fading channel as

$$P_{PT \rightarrow ST}^s = \int_0^{\infty} P(e|\gamma) P_{MRCI}(\gamma) d\gamma. \quad (5.13)$$

Average SEP given in (5.13) for the link PT→ST under MRC reception can be obtained numerically using the method provided in [39]¹.

5.2.1.2 Calculation of $P_{PT \rightarrow PR}^b$

Second attempt is to calculate the BEP on the link PT→PR denoted by $P_{PT \rightarrow PR}^b$. This is the BEP at PR when ST could not successfully decode the primary signal and PR tries to decode it directly from the signal received from PT. Based on the bit mapping rule for the irregular 16QAM constellation given in Fig.4.5 where $r_1 = 0.7432\sqrt{E_s}$ and $r_2 = 0.46\sqrt{E_s}$, upper bound on $P_{PT \rightarrow PR}^b$ is obtained from BER union bound in Appendix.(0.2) as

$$\begin{aligned}
P_{PT \rightarrow PR}^b \leq & \frac{1}{16}(12P(s_1 \rightarrow s_2) + 16P(s_1 \rightarrow s_3) + 4P(s_1 \rightarrow s_4) + 10P(s_1 \rightarrow s_5) \\
& + 12P(s_1 \rightarrow s_6) + 6P(s_1 \rightarrow s_7) + 6P(s_1 \rightarrow s_{11}) + 7P(s_1 \rightarrow s_{12}) + 2P(s_1 \rightarrow s_{13}) \\
& + 3P(s_1 \rightarrow s_{14}) + 10P(s_7 \rightarrow s_3) + 4P(s_7 \rightarrow s_6) + 2P(s_7 \rightarrow s_{11}) + 3P(s_7 \rightarrow s_{12}) \\
& + 8P(s_2 \rightarrow s_5) + 6P(s_2 \rightarrow s_8) + 7P(s_7 \rightarrow s_{14}) + 6P(s_7 \rightarrow s_{12}) + 4P(s_2 \rightarrow s_{14}))
\end{aligned} \tag{5.14}$$

where for simplicity omitting indices we have the generic PEP as, $P(s \rightarrow \hat{s}) = \frac{1}{2}(1 - \sqrt{(a^2c)/(1+a^2c)})$, with $a^2 = |s - \hat{s}|^2/2N_0$ and $c = \bar{\gamma}_c/2$.

5.2.1.3 Calculation of P_{coop}^b

Considering (5.1) and (5.5), in the light of [17], the received signals at PR are combined and de-interleaved to extract the symbol x_1 and x_2 as

$$\begin{aligned}
\hat{y}_{PR1} &= \Re\{\tilde{y}_{PT_PR}\} + j\Im\{\tilde{y}_{ST_PR}\} \\
&= |h_1|^2 x_1^R + \Re\{h_1^* n_1\} + j(|h_{31}|^2 + |h_{32}|^2)x_1^I + j\Im\{n_{31}h_{31}^* + n_{32}^*h_{32}\} \\
&= |h_1|^2 x_1^R + j(|h_{31}|^2 + |h_{32}|^2)x_1^I + N_1.
\end{aligned} \tag{5.15}$$

and

$$\begin{aligned}
\hat{y}_{PR2} &= \Re\{\tilde{y}_{ST_PR}\} + j\Im\{\tilde{y}_{PT_PR}\} \\
&= (|h_{31}|^2 + |h_{32}|^2)x_2^R + \Re\{n_{31}h_{31}^* + n_{32}^*h_{32}\} + j|h_1|^2 x_2^I + j\Im\{h_1^* n_1\} \\
&= (|h_{31}|^2 + |h_{32}|^2)x_2^R + j|h_1|^2 x_2^I + N_2,
\end{aligned} \tag{5.16}$$

¹The term $(2k - 1)$ in the denominator of (18) in [39] should be corrected as $(2k + 1)$.

respectively. In (5.15) by assuming the pdf of r.v $n_1 \sim CN(0, 2\sigma^2)$, $n_{31} \sim CN(0, 2\sigma^2)$ and $n_{32} \sim CN(0, 2\sigma^2)$, their variances can be expressed as ²

$$\text{Var}(\Re\{h_1^* n_1\}) = \text{Var}(h_1^R n_1^R + h_1^I n_1^I) = |h_1^R|^2 \sigma^2 + |h_1^I|^2 \sigma^2 = |h_1|^2 \sigma^2, \quad (5.17)$$

$$\text{Var}(\Im\{h_{31}^* n_{31}\}) = \text{Var}(h_{31}^R n_{31}^I - h_{31}^I n_{31}^R) = |h_{31}^R|^2 \sigma^2 + |h_{31}^I|^2 \sigma^2 = |h_{31}|^2 \sigma^2, \quad (5.18)$$

$$\text{Var}(\Im\{n_{32}^* h_{32}\}) = \text{Var}(n_{32}^R h_{32}^I - n_{32}^I h_{32}^R) = |h_{32}^I|^2 \sigma^2 + |h_{32}^R|^2 \sigma^2 = |h_{32}|^2 \sigma^2, \quad (5.19)$$

respectively. The total variance for N_1 would be

$$\text{Var}(N_1) = (|h_1|^2 + |h_{31}|^2 + |h_{32}|^2) \sigma^2. \quad (5.20)$$

In (5.16), considering the pdf of $n_1 \sim CN(0, 2\sigma^2)$, $n_{31} \sim CN(0, 2\sigma^2)$ and $n_{32} \sim CN(0, 2\sigma^2)$, their variances can be calculated as

$$\text{Var}(\Re\{h_{31}^* n_{31}\}) = \text{Var}(h_{31}^R n_{31}^R + h_{31}^I n_{31}^I) = |h_{31}^R|^2 \sigma^2 + |h_{31}^I|^2 \sigma^2 = |h_{31}|^2 \sigma^2, \quad (5.21)$$

$$\text{Var}(\Re\{n_{32}^* h_{32}\}) = \text{Var}(h_{32}^R n_{32}^R + h_{32}^I n_{32}^I) = |h_{32}^R|^2 \sigma^2 + |h_{32}^I|^2 \sigma^2 = |h_{32}|^2 \sigma^2, \quad (5.22)$$

$$\text{Var}(\Im\{h_1^* n_1\}) = \text{Var}(h_1^R n_1^I - h_1^I n_1^R) = |h_1^R|^2 \sigma^2 + |h_1^I|^2 \sigma^2 = |h_1|^2 \sigma^2, \quad (5.23)$$

respectively. The total variance for N_2 in (5.16) would be

$$\text{Var}(N_2) = (|h_{31}|^2 + |h_{32}|^2 + |h_1|^2) \sigma^2. \quad (5.24)$$

Simplified versions of (5.15) and (5.16) can be expressed as

$$\hat{y}_{PR1} = ax_1^R + jbx_1^I + u_1, \quad (5.25)$$

$$\hat{y}_{PR2} = bx_2^R + jax_2^I + u_2 \quad (5.26)$$

where $a = |h_1|^2$, $b = |h_{31}|^2 + |h_{32}|^2$, $u_1^R = \Re\{h_1^* n_1\}$, $u_1^I = \Im\{n_{31} h_{31}^* + n_{32}^* h_{32}\}$, $u_2^R = \Re\{n_{31} h_{31}^* + n_{32}^* h_{32}\}$ and $u_2^I = \Im\{h_1^* n_1\}$. Variances of the AWGN samples u_1^R , u_1^I , u_2^R and u_2^I are as follows:

$$\text{Var}(u_1^R) = \text{Var}(u_2^I) = a\sigma^2, \text{Var}(u_1^I) = \text{Var}(u_2^R) = b\sigma^2.$$

ML decision rule from [17] for x_1 and x_2 based on Appendix.(0.4) are

$$\hat{x}_1 = \underset{x_1^R, x_1^I}{\text{argmin}} (b|\hat{y}_{PR1}^R - ax_1^R|^2 + a|\hat{y}_{PR1}^I - bx_1^I|^2), \quad (5.27)$$

² $\text{Var}(aX + bY) = a^2 \text{var}(X) + b^2 \text{var}(Y)$ and $\text{Var}(aX - bY) = a^2 \text{var}(X) + b^2 \text{var}(Y)$

$$\hat{x}_2 = \underset{x_2^R, x_2^I}{\operatorname{argmin}} (a|\hat{y}_{PR2}^R - bx_2^R|^2 + b|\hat{y}_{PR2}^I - ax_2^I|^2), \quad (5.28)$$

respectively. Therefore, CPEP for x_1 and x_2 are given by Appendix(0.5) as:

$$\begin{aligned} P(x_1 \rightarrow \hat{x}_1 | \{h_1, h_{31}, h_{32}\}) &= P[b|\hat{y}_{PR1}^R - a\hat{x}_1^R|^2 + a|\hat{y}_{PR1}^I - b\hat{x}_1^I|^2 \\ &< b|\hat{y}_{PR1}^R - ax_1^R|^2 + a|\hat{y}_{PR1}^I - bx_1^I|^2] \\ &= P[(2\Delta_R u_1^R + 2\Delta_I u_1^I) < (-a\Delta_R^2 - b\Delta_I^2)], \end{aligned} \quad (5.29)$$

$$\begin{aligned} P(x_2 \rightarrow \hat{x}_2 | \{h_1, h_{31}, h_{32}\}) &= P[a|\hat{y}_{PR2}^R - b\hat{x}_2^R|^2 + b|\hat{y}_{PR2}^I - a\hat{x}_2^I|^2 \\ &< a|\hat{y}_{PR2}^R - bx_2^R|^2 + b|\hat{y}_{PR2}^I - ax_2^I|^2] \\ &= P[(2\Delta_R u_2^R + 2\Delta_I u_2^I) < (-b\Delta_R^2 - a\Delta_I^2)], \end{aligned} \quad (5.30)$$

respectively, where $\Delta_R = |x_i^R - \hat{x}_i^R|$ and $\Delta_I = |x_i^I - \hat{x}_i^I|$. The terms $2\Delta_R u_1^R + 2\Delta_I u_1^I$ and $2\Delta_R u_2^R + 2\Delta_I u_2^I$ in (5.29) and (5.30) are both Gaussian r.v. with zero mean and variances $4\sigma^2(a\Delta_R^2 + b\Delta_I^2)$ and $4\sigma^2(b\Delta_R^2 + a\Delta_I^2)$, respectively.

CPEP for x_1 and x_2 could be calculated as in the following. By simplifying³ in (5.29) CPEP for x_1 is obtained as,

$$P(x_1 \rightarrow \hat{x}_1 | \{h_1, h_{31}, h_{32}\}) = P[A > a\Delta_R^2 + b\Delta_I^2 | \{h_1, h_{31}, h_{32}\}] \quad (5.31)$$

where $A = 2\Delta_R u_1^R + 2\Delta_I u_1^I$ and $A \sim N(0, 4\sigma^2(a\Delta_R^2 + b\Delta_I^2)) = N(0, \gamma^2)$. After some calculation

$$P[A > a\Delta_R^2 + b\Delta_I^2 | \{h_1, h_{31}, h_{32}\}] = \int_{a\Delta_R^2 + b\Delta_I^2}^{\infty} \frac{1}{\sqrt{2\pi\gamma^2}} \exp\left(-\frac{A^2}{2\gamma^2}\right) dA. \quad (5.32)$$

Taking $\frac{A}{\gamma} = Z$, $\frac{A^2}{\gamma^2} = Z^2$ and $dA = \gamma dZ$ we have

$$P[A > a\Delta_R^2 + b\Delta_I^2 | \{h_1, h_{31}, h_{32}\}] = \int_{\tau}^{\infty} \frac{1}{\sqrt{2\pi}} \exp\left(-\frac{Z^2}{2}\right) dZ = Q(\tau). \quad (5.33)$$

where $\tau = \sqrt{(a\Delta_R^2 + b\Delta_I^2)/4\sigma^2}$. By simplifying in (5.30) we obtain the CPEP for x_2 as,

$$P(x_2 \rightarrow \hat{x}_2 | \{h_1, h_{31}, h_{32}\}) = P[A > b\Delta_R^2 + a\Delta_I^2 | \{h_1, h_{31}, h_{32}\}] \quad (5.34)$$

³By symmetry in Gaussian r.v.s, we have $P(A < -C) = P(A > C)$.

where $A = 2\Delta_{\text{R}}u_{\text{R}}^2 + 2\Delta_{\text{I}}u_{\text{I}}^2$ and $A \sim N(0, 4\sigma^2(b\Delta_{\text{R}}^2 + a\Delta_{\text{I}}^2)) = N(0, \gamma^2)$. After some calculation

$$P[A > b\Delta_{\text{R}}^2 + a\Delta_{\text{I}}^2 | \{h_1, h_{31}, h_{32}\}] = \int_{b\Delta_{\text{R}}^2 + a\Delta_{\text{I}}^2}^{\infty} \frac{1}{\sqrt{2\pi\gamma^2}} \exp\left(-\frac{A^2}{2\gamma^2}\right) dA. \quad (5.35)$$

Taking $\frac{A}{\gamma} = Z$, $\frac{A^2}{\gamma^2} = Z^2$ and $dA = \gamma dZ$ we have

$$P[A > b\Delta_{\text{R}}^2 + a\Delta_{\text{I}}^2 | \{h_1, h_{31}, h_{32}\}] = \int_{\kappa}^{\infty} \frac{1}{\sqrt{2\pi}} \exp\left(-\frac{Z^2}{2}\right) dZ = Q(\kappa). \quad (5.36)$$

where $\kappa = \sqrt{(b\Delta_{\text{R}}^2 + a\Delta_{\text{I}}^2)/4\sigma^2}$. Omitting indices of the fading coefficients for simplicity, the pdf of Rayleigh distributed r.v. h is $f(h) = (2h/\Omega)\exp(-h^2/\Omega)$ where $\Omega = E[|h|^2] = d^{-\beta}$ is the expected channel fading power and $\alpha_1^2 = |h_1|^2$, $\alpha_{31}^2 = |h_{31}|^2$ and $\alpha_{32}^2 = |h_{32}|^2$. Averaging over fading coefficients the PEP of x_1 can be calculated from (5.33) as in the following

$$\begin{aligned} P(x_1 \rightarrow \hat{x}_1) &= \int_0^{\infty} \int_0^{\infty} \int_0^{\infty} \int_{\varpi}^{\infty} \frac{1}{\sqrt{2\pi}} \exp\left(-\frac{Z^2}{2}\right) dZ \frac{2\alpha_1}{d_1^{-\beta}} \exp\left(-\frac{\alpha_1^2}{d_1^{-\beta}}\right) d\alpha_1 \\ &\quad \times \frac{2\alpha_{31}}{d_{31}^{-\beta}} \exp\left(-\frac{\alpha_{31}^2}{d_{31}^{-\beta}}\right) d\alpha_{31} \frac{2\alpha_{32}}{d_{32}^{-\beta}} \exp\left(-\frac{\alpha_{32}^2}{d_{32}^{-\beta}}\right) d\alpha_{32} \end{aligned} \quad (5.37)$$

where $\varpi = \sqrt{(\alpha_1^2\Delta_{\text{R}}^2 + (\alpha_{31}^2 + \alpha_{32}^2)\Delta_{\text{I}}^2)/4\sigma^2}$. By simplifying

$$\begin{aligned} P(x_1 \rightarrow \hat{x}_1) &= \int_0^{\infty} \int_0^{\infty} \int_0^{\infty} \int_{\varpi}^{\infty} \frac{8}{\sqrt{2\pi}d_1^{-\beta}d_{31}^{-\beta}d_{32}^{-\beta}} \exp\left(-\frac{Z^2}{2}\right) \alpha_1 \alpha_{31} \alpha_{32} \\ &\quad \times \exp\left(-\left(\frac{\alpha_1^2}{d_1^{-\beta}} + \frac{\alpha_{31}^2}{d_{31}^{-\beta}} + \frac{\alpha_{32}^2}{d_{32}^{-\beta}}\right)\right) dZ d\alpha_1 d\alpha_{31} d\alpha_{32}. \end{aligned} \quad (5.38)$$

Taking

$$W_1^2 = \frac{\alpha_1^2}{d_1^{-\beta}}, \quad \alpha_1^2 = \frac{W_1^2}{d_1^{\beta}}, \quad \alpha_1 = \frac{W_1}{\sqrt{d_1^{\beta}}},$$

$$W_{31}^2 = \frac{\alpha_{31}^2}{d_3^{-\beta}}, \quad \alpha_{31}^2 = \frac{W_{31}^2}{d_3^{\beta}}, \quad \alpha_{31} = \frac{W_{31}}{\sqrt{d_3^{\beta}}}$$

and

$$W_{32}^2 = \frac{\alpha_{32}^2}{d_3^{-\beta}}, \quad \alpha_{32}^2 = \frac{W_{32}^2}{d_3^{\beta}}, \quad \alpha_{32} = \frac{W_{32}}{\sqrt{d_3^{\beta}}}$$

and replacing in (5.38) we obtain

$$\begin{aligned}
P(x_1 \rightarrow \hat{x}_1) &= \int_0^\infty \int_0^\infty \int_0^\infty \int_\Psi^\infty \frac{8}{\sqrt{2\pi} d_1^{-\beta} d_{31}^{-\beta} d_{32}^{-\beta}} \exp\left(-\frac{Z^2}{2}\right) \frac{W_1}{\sqrt{d_1^\beta}} \frac{W_{31}}{\sqrt{d_1^\beta}} \frac{W_{32}}{\sqrt{d_1^\beta}} \\
&\quad \times \exp(-(W_1^2 + W_{31}^2 + W_{32}^2)) dZ \frac{dW_1}{\sqrt{d_1^\beta}} \frac{dW_{31}}{\sqrt{d_3^\beta}} \frac{dW_{32}}{\sqrt{d_3^\beta}} \\
&= \int_0^\infty \int_0^\infty \int_0^\infty \int_\Psi^\infty \frac{8}{\sqrt{2\pi}} \exp\left(-\frac{Z^2}{2}\right) W_1 W_{31} W_{32} \\
&\quad \times \exp(-(W_1^2 + W_{31}^2 + W_{32}^2)) dZ dW_1 dW_{31} dW_{32}. \tag{5.39}
\end{aligned}$$

where $\Psi = \sqrt{(\frac{W_1^2}{d_1^\beta} \Delta_R^2 + (\frac{W_{31}^2}{d_3^\beta} + \frac{W_{32}^2}{d_3^\beta}) \Delta_I^2) / 4\sigma^2}$. We substitute $W_{31} = \rho \cos \phi$, $W_{32} = \rho \sin \phi$, $dW_{31} dW_{32} = \rho d\rho d\phi$ and $R = \frac{\Delta_R^2}{d_1^\beta}$ as well as $I = \frac{\Delta_I^2}{d_3^\beta}$ in (5.39) and obtain,

$$\begin{aligned}
P(x_1 \rightarrow \hat{x}_1) &= \int_0^{\frac{\pi}{2}} \int_0^\infty \int_0^\infty \int_\zeta^\infty \frac{8}{\sqrt{2\pi}} \exp\left(-\frac{Z^2}{2}\right) W_1 \rho \cos \phi \rho \sin \phi \\
&\quad \times \exp(-(W_1^2 + \rho^2)) dZ dW_1 \rho d\rho d\phi, \\
&= \int_0^{\frac{\pi}{2}} \int_0^\infty \int_0^\infty \int_\zeta^\infty \frac{8}{\sqrt{2\pi}} \exp\left(-\frac{Z^2}{2}\right) W_1 \rho^3 \frac{1}{2} \sin 2\phi \\
&\quad \times \exp(-(W_1^2 + \rho^2)) dZ dW_1 d\rho d\phi. \tag{5.40}
\end{aligned}$$

where $\zeta = \sqrt{(W_1^2 R + \rho^2 I) / 4\sigma^2}$. By simplifying⁴

$$P(x_1 \rightarrow \hat{x}_1) = \int_0^\infty \int_0^\infty \int_\zeta^\infty \frac{4}{\sqrt{2\pi}} \exp\left(-\frac{Z^2}{2}\right) W_1 \rho^3 \exp(-(W_1^2 + \rho^2)) dZ dW_1 d\rho. \tag{5.41}$$

Taking $W_1 = r \cos \theta$, $\rho = r \sin \theta$, $dW_1 d\rho = r dr d\theta$ and $z = ru$ we obtain,

$$\begin{aligned}
P(x_1 \rightarrow \hat{x}_1) &= \int_0^{\pi/2} \int_0^\infty \int_\eta^\infty \frac{4}{\sqrt{2\pi}} \exp\left(-\frac{r^2 u^2}{2}\right) r \cos \theta r^3 \sin^3 \theta \exp(-(r^2)) r dr d\theta \\
&= \int_0^{\pi/2} \int_0^\infty \int_\eta^\infty \frac{4}{\sqrt{2\pi}} \exp\left(-r^2 \left(\frac{u^2 + 2}{2}\right)\right) r \cos \theta r^3 \sin^3 \theta r dr d\theta \\
&= \int_0^{\pi/2} \int_0^\infty \int_\eta^\infty \frac{4}{\sqrt{2\pi}} \exp\left(-r^2 \left(\frac{u^2 + 2}{2}\right)\right) r^6 \cos \theta \sin^3 \theta du dr d\theta \\
&= \int_0^{\pi/2} \int_\eta^\infty \cos \theta \sin^3 \theta \int_0^\infty \frac{4}{\sqrt{2\pi}} r^6 \exp\left(-r^2 \left(\frac{u^2 + 2}{2}\right)\right) dr du d\theta \tag{5.42}
\end{aligned}$$

⁴ $\int_0^{\pi/2} \sin 2\phi d\phi = 1$.

where $\eta = \sqrt{(R\cos^2\theta + I\sin^2\theta)/4\sigma^2}$. Calculating integral ⁵
 $\frac{4}{\sqrt{2\pi}} \int_0^\infty r^6 \exp(-r^2(\frac{u^2+2}{2}))dr$ in (5.42) and substituting the result in (5.42) we
attain

$$P(x_1 \rightarrow \hat{x}_1) = \int_0^{\pi/2} \int_\eta^\infty \frac{30}{(2+u^2)^{7/2}} \cos\theta \sin^3\theta du d\theta. \quad (5.43)$$

Replacing $v = \sin^2\theta$, $1-v = \cos^2\theta$ and $dv = 2\sin\theta \cos\theta d\theta$, we acquire

$$\begin{aligned} P(x_1 \rightarrow \hat{x}_1) &= \int_0^1 \int_Y^\infty \frac{30}{(2+u^2)^{7/2}} \cos\theta \sin^3\theta du \frac{dv}{2\sin\theta \cos\theta} \\ &= \int_0^1 v \int_Y^\infty \frac{15}{(2+u^2)^{7/2}} du dv \end{aligned} \quad (5.44)$$

where $Y = \sqrt{(R(1-v) + Iv)/4\sigma^2}$. After some integration⁶ we obtain,

$$P(x_1 \rightarrow \hat{x}_1) = \int_0^1 v \left(1 - \frac{x(15 + 2x^2(5+x^2))}{2(2+x^2)^{\frac{5}{2}}}\right) dv \quad (5.45)$$

where $x = Y$. Let $t = R(1-v) + Iv$ and $\sigma^2 = N_o/2$.

$$\begin{aligned} P(x_1 \rightarrow \hat{x}_1) &= \int_R^I \frac{t-R}{I-R} \left(1 - \frac{x(15 + 2x^2(5+x^2))}{2(2+x^2)^{\frac{5}{2}}}\right) \frac{dt}{I-R} \\ &= \frac{1}{(I-R)^2} \int_R^I (t-R) \left(1 - \frac{\sqrt{\frac{t}{2N_o}}(15 + 2\frac{t}{2N_o}(5 + \frac{t}{2N_o}))}{2(2 + \frac{t}{2N_o})^{\frac{5}{2}}}\right) dt \\ &= \frac{1}{(I-R)^2} \int_R^I (t-R) \left(1 - \frac{\sqrt{t}(60N_o^2 + 20tN_o + 2t^2)}{2(4N_o + t)^{\frac{5}{2}}}\right) dt. \end{aligned} \quad (5.46)$$

Finally, the PEP will be

$$\begin{aligned} P(x_1 \rightarrow \hat{x}_1) &= \frac{1}{(I-R)^2} \left(\frac{t^2\sqrt{t}(2R-t)}{2(4N_o+t)^{3/2}} + \frac{N_o t \sqrt{t}(10R-6t)}{2(4N_o+t)^{3/2}} \right. \\ &\quad \left. + \frac{2N_o t(t-2R)}{4N_o+t} + \frac{t^2(t-2R)}{2(4N_o+t)} \right) \Big|_R^I. \end{aligned} \quad (5.47)$$

Now, we apply Taylor series to (5.47) with respect to N_0 at high SNR to find a simplified expression. After some operation, we have

$$P(x_1 \rightarrow \hat{x}_1) = \frac{10N_o^3}{I^2R} + O(N_o^4) \quad (5.48)$$

⁵From integral table we know that $\int_0^\infty x^{2n} \exp(-ax^2) dx = \frac{2n!}{n!2^{2n+1}} \sqrt{\frac{\pi}{a^{2n+1}}}$ where in our case $n = 3$ and $a = \frac{2+u^2}{2}$. Then the result is $\frac{4}{\sqrt{2\pi}} \int_0^\infty r^6 \exp(-r^2(\frac{u^2+2}{2}))dr = \frac{30}{(2+u^2)^{7/2}}$.

⁶ $\int_x^\infty \frac{15}{(2+u^2)^{7/2}} du = 1 - \frac{x(15+2x^2(5+x^2))}{2(2+x^2)^{\frac{5}{2}}}$.

where $O(N_0^4)$ shows the terms of N_0 with orders equal or higher than four. Assuming that the consumed energy for transmitting primary data in the first time slot is E_s and in second and third time slots are $E_s/2$, Δ_R and Δ_I are changed to

$$\Delta_R = |x_1^R - \hat{x}_1^R| \sqrt{E_s} \quad (5.49)$$

and

$$\Delta_I = |x_1^I - \hat{x}_1^I| \sqrt{E_s/2}. \quad (5.50)$$

By replacing (5.49) and (5.50) in (5.48), we have

$$P(x_1 \rightarrow \hat{x}_1) = 40 \left(\frac{N_o}{E_s} \right)^3 \frac{d_1^\beta d_3^{2\beta}}{\Delta_R^2 \Delta_I^4} + O(N_o^4). \quad (5.51)$$

For symbol x_2 , by applying the similar procedure, we obtain,

$$P(x_2 \rightarrow \hat{x}_2) = 40 \left(\frac{N_o}{E_s} \right)^3 \frac{d_1^\beta d_3^{2\beta}}{\Delta_I^2 \Delta_R^4} + O(N_o^4). \quad (5.52)$$

Here, assuming equally likely symbols, using (A.2) with $M = 4$ and $k = 2$, and considering the bit mapping for 4-RQAM given in the previous subsection, average BEP for x_1 can be written as

$$P_{coop}^b = \frac{1}{4} (6P(x_1 \rightarrow x_4) + 2P(x_1 \rightarrow x_3)). \quad (5.53)$$

Finally, substituting (5.53), (5.13) and (5.14) in (5.9), the overall upper bound on the BEP of primary system can be obtained. In total, the energy to transmit 2 symbols (4 bits) of 4-RQAM in 3 time intervals is equal to $P_p + P_s$, where $P_p = P_s$, P_p and P_s being the transmit powers of PT and ST, respectively.

5.2.2 Secondary system BEP performance

Secondary system's transmission takes the last two time slots. In the second and third time slots Alamouti coding is applied which allow single symbol decoding and therefore interference-free decoding at both PR and SR. In total we consume $P_p = P_s$ energy to transmit one secondary symbol. Alamouti coding while providing additional diversity at PR, provides a diversity order of two at SR and as a result, better error performance for the secondary user. Exact BER derivation for 16-QAM is given in [41] and directly used for comparison purposes in the next section.

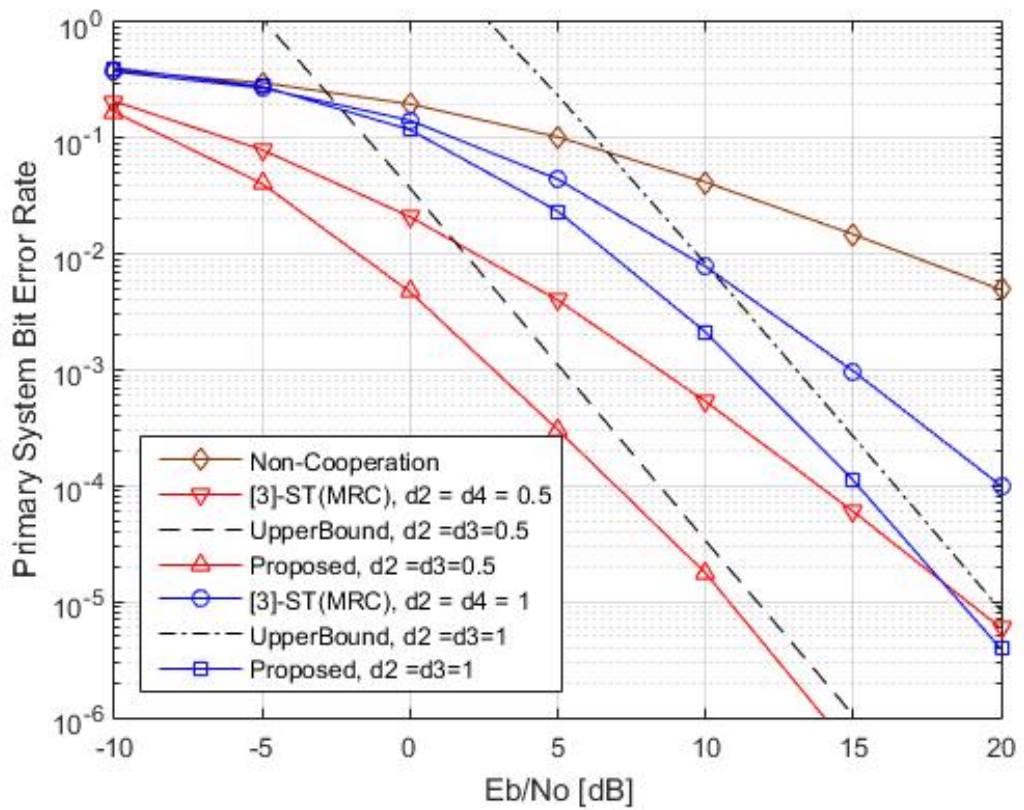


Figure 5.2: Primary System Bit Error Performance for Irregular 16-QAM ($d_2 = d_4 = 1$ and $d_2 = d_4 = 0.5$).

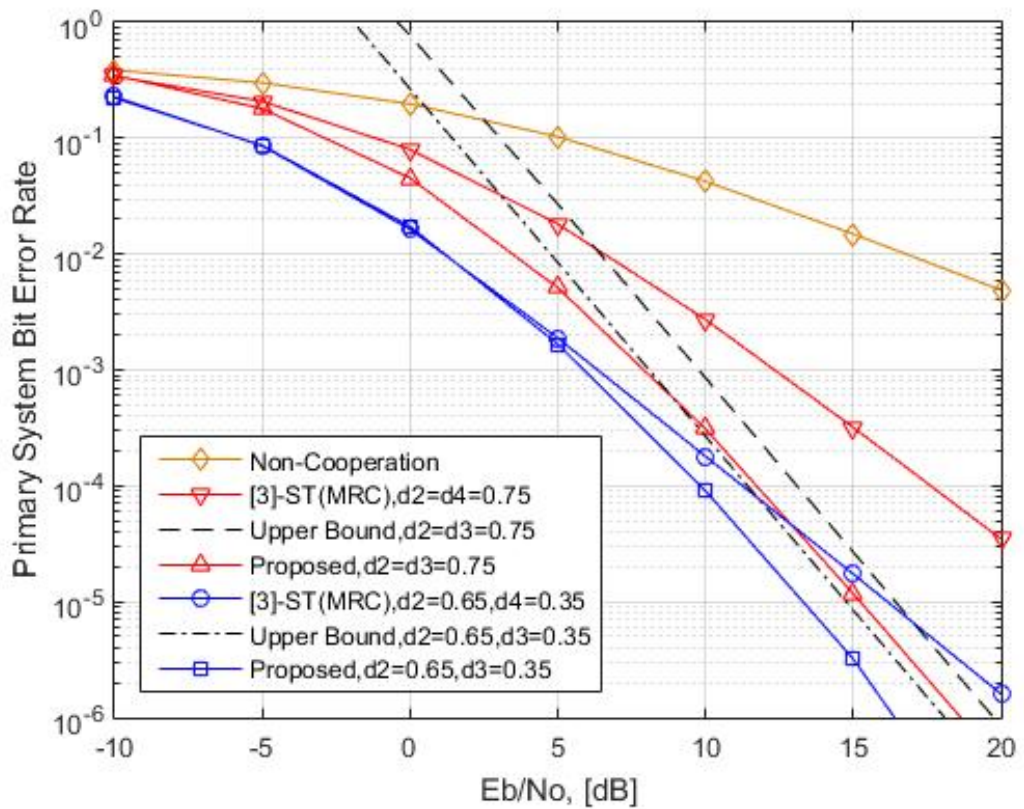


Figure 5.3: Primary System Bit Error Performance for Irregular 16-QAM ($d_2 = d_4 = 0.75$ and $d_2 = 0.65, d_4 = 0.35$).

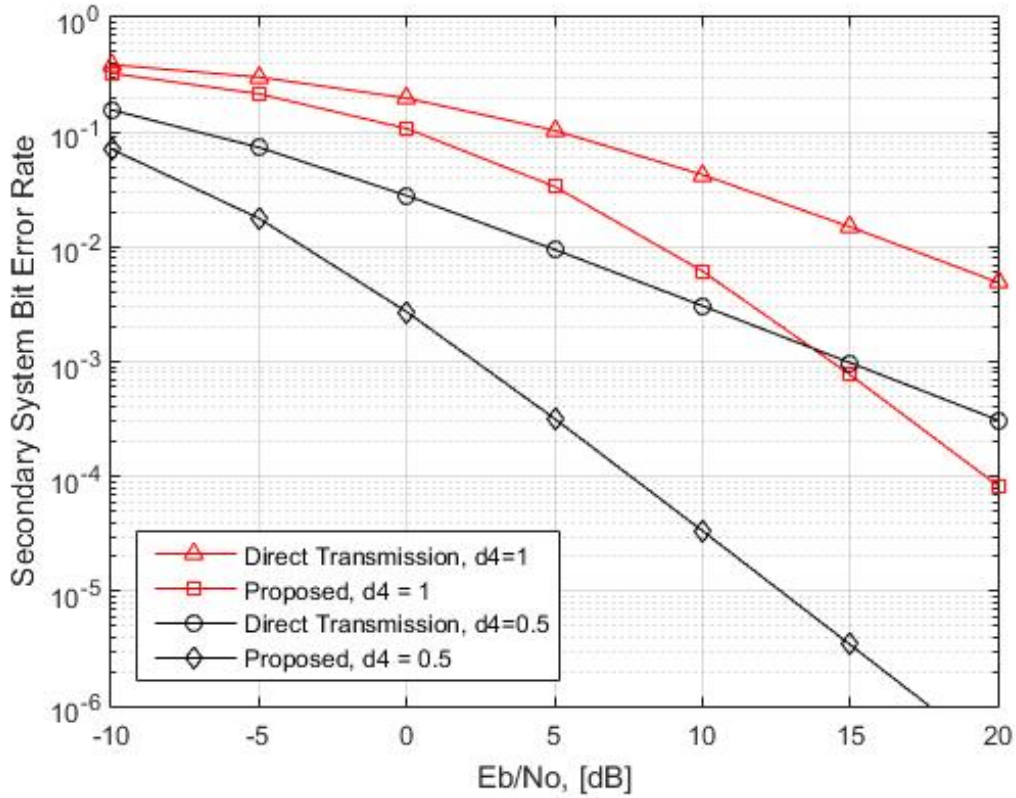


Figure 5.4: Secondary System Bit Error Performance for Classical 16-QAM ($d_4 = 0.5$ and $d_4 = 1$).

5.3 BER performance evaluation

In this section, we evaluate the BER performance of the proposed protocol for both primary and secondary users in the light of the analytical results of the previous section and support them via computer simulation results. In Fig.5.2 and Fig.5.3, we compare our spectrum sharing protocol with non-cooperation case and the protocol given in [3]. All distances are assumed to be the same for the proposed protocol and for that of [3]. Symbols with solid lines in Fig.5.2 and Fig.5.3 show the simulation results and dashed lines are for theoretical upper bound results. For [3], we assume two antennas at ST which applies MRC for reception, to make a fair comparison and consider a rate of $R = 4$ bits per second corresponding to 16-QAM modulation, like in our case. It can be calculated that in [3] by using superposition coding at ST, for 16-QAM, secondary transmitter allocates 99.86% of its power to transmit primary signal. As a result, in [3] approximately a total power of $P_p + P_s$ is used to transmit one primary symbol (4 bits), where $P_p = P_s$. Fig.5.2 shows that significant improvement in BER is provided by our protocol compared to that of [3] and the non-cooperation case. Simulation curves for the proposed protocol match very well with the theoretical upper bound curves in high

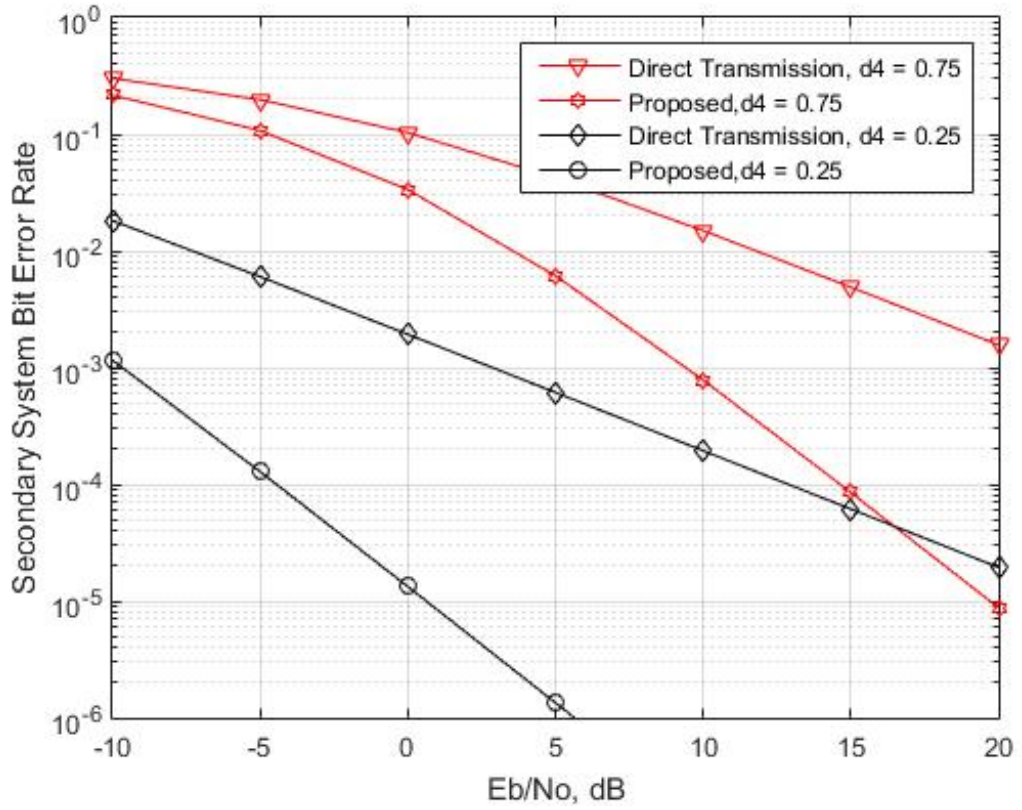


Figure 5.5: Secondary System Bit Error Performance for Classical 16-QAM ($d_4 = 0.25$ and $d_4 = 0.75$).

SNR values. As an example, in Fig.5.2 for a BER of 10^{-2} , SNR gains of nearly 18 dB and 10 dB are provided compared to non-cooperation case with $d_2 = d_3 = 0.5$ and $d_2 = d_3 = 1$, respectively. For a BER of 10^{-4} , 8 dB and 5 dB SNR are saved by our protocol compared to that given in [3] for $d_2 = d_t = 0.5$ and $d_2 = d_t = 1$, where $t = 3$ and $t = 4$ for the proposed protocol and for that of [3], respectively.

In Fig.5.3, for BER value of 10^{-2} , nearly 13 and 16 dB improvement in SNR are provided in comparison to the straightforward transmission when it is assumed that $d_2 = d_3 = 0.75$ and $d_2 = 0.65, d_3 = 0.35$, respectively. Moreover, approximately 5 and 3 dB gains in SNR compared to the reference protocol for a BER value of 10^{-3} and 10^{-5} , respectively. It is assumed that $d_2 = d_3 = 0.75$ and $d_2 = 0.65, d_3 = 0.35$ for the proposed protocol and $d_2 = d_4 = 0.75$ and $d_2 = 0.65, d_4 = 0.35$ for that of [3].

In Fig.5.4 and Fig.5.5 BER performance of secondary system for the proposed protocol is compared with direct transmission case for different distance values between ST and SR. Note that for a rate of $R = 4$ bits per symbol the secondary system will be in outage for the protocol of [3], because of the 99.86% power allocated to the primary signal at

ST. In Fig.5.4, nearly, 12 dB and 7dB SNR gains are provided at a BER of 10^{-3} with $d_4 = 0.5$ and at a BER rate of 10^{-2} with $d_4 = 1$, respectively. In Fig.5.5, for $d_4 = 0.25$ the saved SNR at a BER rate of 10^{-4} is approximately 17 dB and for $d_4 = 0.75$ at a BER rate of 10^{-3} is nearly 12 dB, compared to the direct transmission case. These gains are the result of space-time diversity provided by the Alamouti's STBC.

6. CONCLUSIONS

In this thesis, first, a new protocol for spectrum sharing in overlay cognitive radio networks having one antenna at ST has been proposed which provides signal space diversity and simple single-symbol decoding at the primary receiver during cooperation, coming from the application of the CIOD code. The protocol guarantees an interference-free transmission for both users and the continuous communication of the secondary users during the third time slot of each transmission. Outage probabilities for both users are analytically derived and supported via computer simulation results. Significant SNR gains are provided over the corresponding reference protocol based on superposition coding, for both users. A critical region is derived for the location of the secondary transmitter with respect to the primary one. Moreover, for primary system an upper bound on BEP is analytically derived and compared with that of the reference scheme given in [3]. Simulation results perfectly match with BEP upper bound at high SNR values. The secondary system BER calculation is based on the direct transmission for 16-QAM constellation.

Secondly, another protocol for cooperative spectrum sharing in overlay cognitive radio networks with two antennas at ST has been proposed. The protocol combines CIOD and Alamouti's STBC in three time slots and exploits signal space diversity at PR when ST cooperates with PT. It provides interference-free transmission for both primary and secondary users and space-time diversity at PR and SR thanks to Alamouti's STBC. Continuous transmission of ST is guaranteed by the protocol during second and third time slots. An upper bound on the BEP of PR is analytically derived for 4QAM and supported via computer simulations. The results show that the new protocol provides significant improvement in the BER performance of primary system compared to the non-cooperative case and the reference cognitive radio protocol given in [3] which is

based on superposition coding. Moreover, the BER performance of secondary system is significantly improved with respect to the direct transmission case.

REFERENCES

- [1] **National Telecommunications and Information Administration (NTIA)**, “**FCC Frequency Allocation Chart**,” 2003. [Online], <http://www.ntia.doc.gov/osmhome/allochrt.pdf>, alınıđı tarih: 11.23.2015.
- [2] **Roberson, D., Hood, C., LoCicero, J.L. and MacDonald, J.** (2006). Spectral Occupancy and Interference Studies in support of Cognitive Radio Technology Deployment, *Networking Technologies for Software Defined Radio Networks, 2006. SDR '06.1st IEEE Workshop on*, pp.26–35.
- [3] **Han, Y., Pandharipande, A. and Ting, S.H.** (2009). Cooperative decode-and-forward relaying for secondary spectrum access, *Wireless Communications, IEEE Transactions on*, **8**(10), 4945–4950.
- [4] **Biglieri, E., Goldsmith, A.J., Greenstein, L.J., Mandayam, N.B. and Poor, H.V.** (2013). *Principles of Cognitive Radio*, Cambridge University Press, New York.
- [5] **Duy, T.T., Thanh, T.L. and Bao, V.N.Q.** (2014). A hybrid spectrum sharing approach in cognitive radio networks, *Computing, Management and Telecommunications (ComManTel), 2014 International Conference on*, pp.19–23.
- [6] **Oh, J. and Choi, W.** (2010). A Hybrid Cognitive Radio System: A Combination of Underlay and Overlay Approaches, *Vehicular Technology Conference Fall (VTC 2010-Fall), 2010 IEEE 72nd*, pp.1–5.
- [7] **Li, Y., Wang, T., Peng, M. and Wang, W.** (2014). On the Outage Probability of Cognitive Two-Way Relaying Based on Superposition Coding, *Vehicular Technology Conference (VTC Spring), 2014 IEEE 79th*, pp.1–5.
- [8] **Tran, T.T. and Kong, H.Y.** (2014). A method to avoid mutual interference in a cooperative spectrum sharing system, *Journal of Communications and Networks*, **16**(2), 110–120.
- [9] **Chen, Z., Zhang, X. and Luan, T.** (2010). Cooperation based spectrum sharing in cognitive radio networks, *Information Computing and Telecommunications (YC-ICT), 2010 IEEE Youth Conference on*, pp.17–20.
- [10] **Ganesan, G. and Li, Y.** (2007). Cooperative Spectrum Sensing in Cognitive Radio, Part I: Two User Networks, *IEEE Transactions on Wireless Communications*, **6**(6), 2204–2213.
- [11] **Chen, Y., Yu, G., Zhang, Z., h. Chen, H. and Qiu, P.** (2008). On cognitive radio networks with opportunistic power control strategies in fading channels, *IEEE Transactions on Wireless Communications*, **7**(7), 2752–2761.

- [12] **Taricco, G. and Viterbo, E.** (1996). Performance of component interleaved signal sets for fading channels, *Electronics Letters*, **32**(13), 1170–1172.
- [13] **Schober, R., Lampe, L.H.J., Gerstacker, W.H. and Pasupathy, S.** (2003). Modulation diversity for frequency-selective fading channels, *IEEE Transactions on Information Theory*, **49**(9), 2268–2276.
- [14] **Mesleh, R., Ikki, S. and Amin, O.** (2014). Enhancing cooperative communication spectral efficiency through signal space diversity, *Wireless Communications and Networking Conference (WCNC), 2014 IEEE*, pp.666–670.
- [15] **Lu, T., Ge, J., Yang, Y. and Gao, Y.** (2012). BEP Analysis for DF Cooperative Systems Combined with Signal Space Diversity, *IEEE Communications Letters*, **16**(4), 486–489.
- [16] **Rao, Y. and Wang, M.** (2007). Performance Analysis of Full-rate STBCs from Coordinate Interleaved Orthogonal Designs, *Communications, 2007. ICC '07. IEEE International Conference on*, pp.4610–4615.
- [17] **Ali Khan, M. and Rajan, B.** (2006). Single-symbol maximum likelihood decodable linear STBCs, *Information Theory, IEEE Transactions on*, **52**(5), 2062–2091.
- [18] **Tse, D. and Viswanath, P.** (2005). *Fundamentals of Wireless Communication*, Cambridge University Press, <http://dx.doi.org/10.1017/CBO9780511807213>, cambridge Books Online.
- [19] **Simon, M.K. and Alouini, M.S.** (2005). *Digital communication over fading channels*, volume 95, John Wiley & Sons.
- [20] **Tarokh, V., Seshadri, N. and Calderbank, A.R.** (1998). Space-time codes for high data rate wireless communication: performance criterion and code construction, *IEEE Transactions on Information Theory*, **44**(2), 744–765.
- [21] **Poo, L.** (2002). Space-time coding for wireless communication: a survey, *Report from Stanford University*.
- [22] **Tarokh, V., Naguib, A., Seshadri, N. and Calderbank, A.R.** (1999). Space-time codes for high data rate wireless communication: performance criteria in the presence of channel estimation errors, mobility, and multiple paths, *IEEE Transactions on Communications*, **47**(2), 199–207.
- [23] **Alamouti, S.** (1998). A simple transmit diversity technique for wireless communications, *Selected Areas in Communications, IEEE Journal on*, **16**(8), 1451–1458.
- [24] **Boutros, J. and Viterbo, E.** (1998). Signal space diversity: a power- and bandwidth-efficient diversity technique for the Rayleigh fading channel, *Information Theory, IEEE Transactions on*, **44**(4), 1453–1467.
- [25] **Laneman, J.N., Tse, D.N.C. and Wornell, G.W.** (2004). Cooperative diversity in wireless networks: Efficient protocols and outage behavior, *IEEE Transactions on Information Theory*, **50**(12), 3062–3080.

- [26] **Upadhyay, P.K. and Prakriya, S.** (2010). *Bidirectional Cooperative Relaying*, INTECH Open Access Publisher.
- [27] **Hunter, T.E. and Nosratinia, A.** (2002). Cooperation diversity through coding, *Information Theory, 2002. Proceedings. 2002 IEEE International Symposium on*, pp.220–.
- [28] **Hunter, T.E. and Nosratinia, A.** (2006). Diversity through coded cooperation, *IEEE Transactions on Wireless Communications*, **5**(2), 283–289.
- [29] **Nosratinia, A., Hunter, T.E. and Hedayat, A.** (2004). Cooperative communication in wireless networks, *Communications Magazine, IEEE*, **42**(10), 74–80.
- [30] **Mitola, J. and Maguire, G.Q.** (1999). Cognitive radio: making software radios more personal, *IEEE Personal Communications*, **6**(4), 13–18.
- [31] **Devroye, N., Vu, M. and Tarokh, V.** (2008). Cognitive radio networks, *Signal Processing Magazine, IEEE*, **25**(6), 12–23.
- [32] **Letaief, K.B. and Zhang, W.** (2009). Cooperative communications for cognitive radio networks, *Proceedings of the IEEE*, **97**(5), 878–893.
- [33] **Tabaković, Ž.** A Survey of Cognitive Radio Systems, *Post and Electronic Communications Agency, Jurišićeva*, **13**.
- [34] **Akyildiz, I.F., Lee, W.Y., Vuran, M.C. and Mohanty, S.** (2008). A survey on spectrum management in cognitive radio networks, *Communications Magazine, IEEE*, **46**(4), 40–48.
- [35] **Wang, B. and Liu, K.** (2011). Advances in cognitive radio networks: A survey, *Selected Topics in Signal Processing, IEEE Journal of*, **5**(1), 5–23.
- [36] **Van Khuong, H. and Kong, H.Y.** (2006). General expression for pdf of a sum of independent exponential random variables, *Communications Letters, IEEE*, **10**(3), 159–161.
- [37] **Kreyszig, E.** (2000). *Advanced Engineering Mathematics: Maple Computer Guide*, John Wiley & Sons, Inc., New York, NY, USA, 8th edition.
- [38] **Proakis, J.G.** (1995). *Digital Communication*, McGraw-Hill, New York.
- [39] **Lu, J., Tjhung, T. and Chai, C.** (1998). Error probability performance of L-branch diversity reception of MQAM in Rayleigh fading, *Communications, IEEE Transactions on*, **46**(2), 179–181.
- [40] **Zwillinger, D.** (2014). *Table of Integrals, Series, and Products*, Elsevier Science, <https://books.google.com.tr/books?id=NjnLAWAAQBAJ>.
- [41] **Raju, M., Annavajjala, R. and Chockalingam, A.** (2006). BER analysis of QAM on fading channels with transmit diversity, *Wireless Communications, IEEE Transactions on*, **5**(3), 481–486.

APPENDICES

APPENDIX 0.1: Rotated 4-QAM and Irregular 16-QAM

APPENDIX 0.2: Calculation of $P_{PT \rightarrow PR}^b$

APPENDIX 0.3: Conditional Symbol Error Probability (CSEP) of Irregular 16-QAM in SISO Channel

APPENDIX 0.4: Maximum Likelihood (ML) Decoding

APPENDIX 0.5: Conditional Pairwise Error Probability (CPEP) Calculation

0.1 Rotated 4-QAM and Irregular 16-QAM

As indicated in [24], to provide signal space diversity 4QAM signal constellation is rotated by the operation

$$\begin{bmatrix} x' \\ y' \end{bmatrix} = \begin{bmatrix} \cos \theta & -\sin \theta \\ \sin \theta & \cos \theta \end{bmatrix} \begin{bmatrix} x \\ y \end{bmatrix}. \quad (\text{A.1})$$

The optimum value of θ which minimizes the average PEP between 4QAM symbols was found in [24] as 31.7 degree. Taking the 4QAM symbols as $(\pm 1/\sqrt{2} \pm j1/\sqrt{2})\sqrt{E_s}$, after a counter clockwise rotation and coordinate interleaving, a nonuniform 16QAM constellation is obtained with symbols $(\pm 0.23 \pm j0.23)\sqrt{E_s}$, $(\pm 0.23 \pm j0.97)\sqrt{E_s}$, $(\pm 0.97 \pm j0.23)\sqrt{E_s}$ and $(\pm 0.97 \pm j0.97)\sqrt{E_s}$, average energy per symbol being unchanged which is equal to 1.

0.2 Calculation of $P_{PT \rightarrow PR}^b$

$P_{PT \rightarrow PR}^b$ is the BEP at PR when ST could not successfully decode the primary signal and PR tries to decode it directly from the signal received from PT which is upper bounded as

$$P_{PT \rightarrow PR}^b \leq \frac{1}{M} \sum_{i=1}^M \sum_{\substack{j=1 \\ i \neq j}}^M P(x_i \rightarrow x_j) \frac{w}{k} \quad (\text{A.2})$$

where $M = 16$, w is the Hamming distance between binary codewords mapped to symbols x_i and x_j , k is the number of bits per symbol and it is assumed that all symbols are equiprobable. In (A.2), $P(x_i \rightarrow x_j)$ denotes the pairwise error probability (PEP) which is the probability of erroneously deciding to symbol x_j when the symbol x_i is transmitted. Considering the bit mapping given in Fig. 4.5 the upper bound on average BEP for irregular 16QAM is calculated from [38] for Rayleigh fading channel as

$$\begin{aligned} P_{PT \rightarrow PR}^b \leq & \frac{1}{16} (12P(s_1 \rightarrow s_2) + 16P(s_1 \rightarrow s_3) + 4P(s_1 \rightarrow s_4) + 10P(s_1 \rightarrow s_5) \\ & + 12P(s_1 \rightarrow s_6) + 6P(s_1 \rightarrow s_7) + 6P(s_1 \rightarrow s_{11}) + 7P(s_1 \rightarrow s_{12}) \\ & + 2P(s_1 \rightarrow s_{13}) + 3P(s_1 \rightarrow s_{14}) + 10P(s_7 \rightarrow s_3) + 4P(s_7 \rightarrow s_6) \\ & + 2P(s_7 \rightarrow s_{11}) + 3P(s_7 \rightarrow s_{12}) + 8P(s_2 \rightarrow s_5) + 6P(s_2 \rightarrow s_8) \\ & + 7P(s_7 \rightarrow s_{14}) + 6P(s_7 \rightarrow s_{12}) + 4P(s_2 \rightarrow s_{14})) \end{aligned} \quad (\text{A.3})$$

where for simplicity omitting indices we have the generic PEP as, $P(s \rightarrow \hat{s}) = \frac{1}{2} (1 - \sqrt{(a^2 c) / (1 + a^2 c)})$, with $a^2 = |s - \hat{s}|^2 / 2N_0$ and $c = \bar{\gamma}_c / 2$. Note that, since the R-4QAM (16QAM) signal constellation given in Fig.4.5 is not uniform in terms of distances between symbols, codewords with one bit difference are mapped to symbols which are close to each other, to have better performance. The mapping rule in Fig.4.5 is a result of the bit mapping for 4QAM as follows: $00 \rightarrow x_1 = (1/\sqrt{2} + j1/\sqrt{2})$, $11 \rightarrow x_2 = (-1/\sqrt{2} + j1/\sqrt{2})$, $01 \rightarrow x_3 = (-1/\sqrt{2} - j1/\sqrt{2})$ and $10 \rightarrow x_4 = (1/\sqrt{2} - j1/\sqrt{2})$ as in Fig.1.

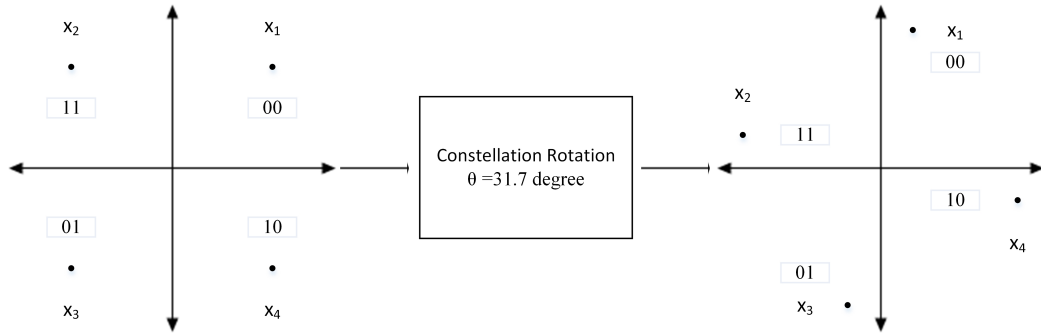


Figure 1: Rotated 4-QAM.

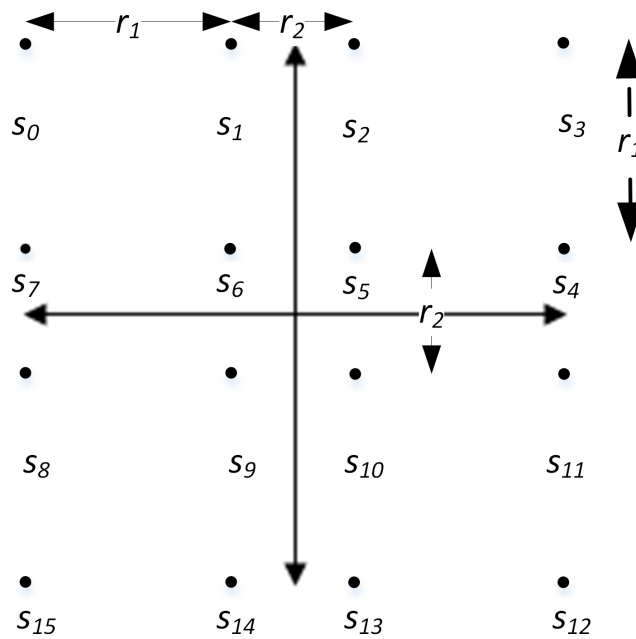


Figure 2: Signal Constellation of Irregular 16-QAM.

0.3 Conditional Symbol Error Probability (CSEP) of Irregular 16-QAM in SISO Channel

In this section, conditional SEP (CSEP) is calculated for SISO system for constellation points in Fig.2 where $r_1 = 0.7432\sqrt{E_s}$ and $r_2 = 0.46\sqrt{E_s}$. Channel is assumed to be exposed to Rayleigh fading with coefficient $h \sim CN(0, d^{-\beta})$ where h is the symmetric complex Gaussian r.v as depicted in Fig.3., d stands for the link distance and β is the path loss exponent. Noise components are zero-mean AWGN samples with variance $\sigma^2 = N_0/2$ per dimension. The received signal at the antenna PR is given as,

$$y = h.s + n \quad (\text{A.4})$$

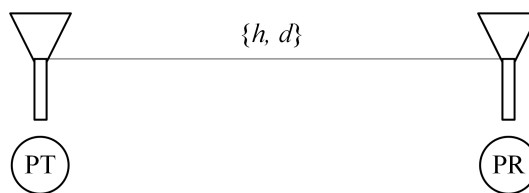


Figure 3: System Configuration for direct transmission.

where h denotes the channel fading coefficient of link from transmitter to receiver antenna, n stands for the AWGN sample at receiver antenna and s is the transmitted signal. By normalizing at receiver and assuming that h is known at the receiver, Eq.(A.4) can be written as

$$r = \frac{y}{h} = s + \frac{n}{h} = s + \hat{n} \quad (\text{A.5})$$

where mean and variance of \hat{n} is $E[\hat{n}] = 0$ and $\text{Var}(\hat{n}) = \frac{\sigma^2}{|h|^2}$ per dimension. The pdf of r per dimension can be written as

$$P_n(r) = \frac{1}{\sqrt{2\pi\sigma^2/|h|^2}} \exp\left(-\frac{(r-s)^2}{2\sigma^2/|h|^2}\right). \quad (\text{A.6})$$

Suppose that the symbol s_5 is sent with constellation point $(0.23, 0.23)\sqrt{E_s}$. So, the pdf of r conditioned on h and s_5 would be $r \sim CN(s_5, \delta^2)$ given as

$$P_n(r|h, s_5) = \frac{1}{\sqrt{2\pi\delta^2}} \exp\left(-\frac{(r-s_5)^2}{2\delta^2}\right). \quad (\text{A.7})$$

where $\delta^2 = \frac{\sigma^2}{|h|^2}$. Conditional probability of correctly decoding symbol s_5 is obtained as

$$P(c|h, s_5) = P(0 < r_R < 0.6016\sqrt{E_s})P(0 < r_I < 0.6016\sqrt{E_s}). \quad (\text{A.8})$$

By calculating the first probability in the right side of Eq.(A.8), we have:

$$\begin{aligned} P(0 < r_R < 0.6016\sqrt{E_s}) &= P(r_R > 0) - P(r_R > 0.6016\sqrt{E_s}) \\ &= Q\left(\frac{(0-s_5)\sqrt{E_s}|h|}{\sigma}\right) - Q\left(\frac{(0.6016\sqrt{E_s}-s_5)|h|}{\sigma}\right) \\ &= 1 - Q\left(\frac{s_5|h|}{\sigma}\right) - Q\left(\frac{(0.6016\sqrt{E_s}-s_5)|h|}{\sigma}\right), \end{aligned} \quad (\text{A.9})$$

and taking the second probability in the right side of Eq.(A.8), we could write:

$$\begin{aligned} P(0 < r_I < 0.6016\sqrt{E_s}) &= P(r_I > 0) - P(r_I > 0.6016\sqrt{E_s}) \\ &= Q\left(\frac{(0-s_5)|h|}{\sigma}\right) - Q\left(\frac{(0.6016\sqrt{E_s}-s_5)|h|}{\sigma}\right) \\ &= 1 - Q\left(\frac{s_5|h|}{\sigma}\right) - Q\left(\frac{(0.6016\sqrt{E_s}-s_5)|h|}{\sigma}\right). \end{aligned} \quad (\text{A.10})$$

By substituting (A.9) and (A.10) in (A.8), conditional probability of correct decoding of symbol s_5 can be expressed as:

$$P(c|h, s_5) = \left[1 - Q\left(0.23\sqrt{\frac{2E_s|h|^2}{N_o}}\right) - Q\left(0.3716\sqrt{\frac{2E_s|h|^2}{N_o}}\right)\right]^2. \quad (\text{A.11})$$

Again, suppose that symbol s_3 is sent over the channel to the receiver with constellation point $(0.9732, 0.9732)\sqrt{E_s}$. The pdf of r conditioned on h and s_3 could be written as $r \sim CN(s_3, \delta^2)$

$$P_n(r|h, s_3) = \frac{1}{\sqrt{2\pi\delta^2}} \exp\left(-\frac{(r-s_3)^2}{2\delta^2}\right). \quad (\text{A.12})$$

Conditional probability of correctly decoding of transmitted symbol s_3 is expressed as

$$P(c|h, s_3) = P(0.6016\sqrt{E_s} < r_R < \infty)P(0.6016\sqrt{E_s} < r_I < \infty). \quad (\text{A.13})$$

The first probability in the right side of Eq.(A.13) is calculated as

$$\begin{aligned} P(0.6016\sqrt{E_s} < r_R < \infty) &= P(r_R > 0.6016\sqrt{E_s}) \\ &= Q\left(\frac{(0.6016\sqrt{E_s} - s_3) |h|}{\sigma}\right) \\ &= 1 - Q\left(\frac{(s_3 - 0.6016\sqrt{E_s}) |h|}{\sigma}\right). \end{aligned} \quad (\text{A.14})$$

Taking the second probability in the right side of Eq.(A.13), we have:

$$\begin{aligned} P(0.6016\sqrt{E_s} < r_I < \infty) &= P(r_I > 0.6016\sqrt{E_s}) \\ &= Q\left(\frac{(0.6016\sqrt{E_s} - s_3) |h|}{\sigma}\right) \\ &= 1 - Q\left(\frac{(s_3 - 0.6016\sqrt{E_s}) |h|}{\sigma}\right). \end{aligned} \quad (\text{A.15})$$

Replacing (A.14) and (A.15) in (A.13), conditional probability of an error free decoding for symbol s_3 can be expressed as:

$$P(c|h, s_3) = [1 - Q(0.3716\sqrt{\frac{2E_s|h|^2}{N_o}})]^2. \quad (\text{A.16})$$

Finally, suppose that the transmitter antenna sends symbol s_4 with constellation point $(0.9732, 0.23)\sqrt{E_s}$ to the receiver, where the pdf of r conditioned on h and s_4 is $r \sim CN(s_4, \delta^2)$

$$P_n(r|h, s_4) = \frac{1}{\sqrt{2\pi}\delta^2} \exp\left(-\frac{(r - s_4)^2}{2\delta^2}\right). \quad (\text{A.17})$$

Conditional Probability of correctly decoding the transmitted symbol s_4 is expressed as

$$P(c|h, s_4) = P(0.6016\sqrt{E_s} < r_R < \infty)P(0 < r_I < 0.6016\sqrt{E_s}). \quad (\text{A.18})$$

Taking first probability in the right side of Eq.(A.18), we have:

$$\begin{aligned} P(0.6016\sqrt{E_s} < r_R < \infty) &= P(r_R > 0.6016\sqrt{E_s}) \\ &= Q\left(\frac{(0.6016\sqrt{E_s} - s_4) |h|}{\sigma}\right) \\ &= 1 - Q\left(\frac{(s_4 - 0.6016\sqrt{E_s}) |h|}{\sigma}\right). \end{aligned} \quad (\text{A.19})$$

The second probability in the right side of Eq.(A.18) can be obtained as

$$\begin{aligned} P(0 < r_I < 0.6016\sqrt{E_s}) &= P(r_I > 0) - P(r_I > 0.6016\sqrt{E_s}) \\ &= Q\left(\frac{(0 - s_4) |h|}{\sigma}\right) - Q\left(\frac{(0.6016\sqrt{E_s} - s_4) |h|}{\sigma}\right) \\ &= 1 - Q\left(\frac{s_4 |h|}{\sigma}\right) - Q\left(\frac{(0.6016\sqrt{E_s} - s_4) |h|}{\sigma}\right). \end{aligned} \quad (\text{A.20})$$

By substituting (A.19) and (A.20) in (A.18), conditional probability of correctly decoding the transmitted symbol s_4 can be expressed as:

$$P(c|h, s_4) = [1 - Q(0.3716\sqrt{\frac{2E_s|h|^2}{N_o}})][1 - Q(0.23\sqrt{\frac{2E_s|h|^2}{N_o}}) - Q(0.3716\sqrt{\frac{2E_s|h|^2}{N_o}})]. \quad (\text{A.21})$$

Taking the R-4QAM symbols equiprobable, average SER for M -QAM can be expressed as:

$$\bar{P}_s = \frac{1}{M} [4P_{out} + 4(\sqrt{M} - 2)P_B + (\sqrt{M} - 2)^2 P_{in}] \quad (\text{A.22})$$

where P_{out} is the error probability of four corner symbol points, P_{in} is the error probability of $(\sqrt{M} - 2)^2$ inner symbol points and for $4(\sqrt{M} - 2)$ border symbol points error probability is denoted by P_B . Because of the symmetry, for all constellation points one of these three error probabilities is valid. Finally, conditional probability of correctly decoding for the SISO system can be calculated as

$$P(c|h) = \frac{1}{16} (4P(c_r|h, s_5) + 4P(c_r|h, s_3) + 8P(c_r|h, s_4)) \quad (\text{A.23})$$

and $P(e|h) = 1 - P(c|h)$ where $P(e|h)$ is the total (CSEP). Substituting (A.11), (A.16) and (A.21) in (A.23) and after some calculation, total conditional SISO error probability can be expressed as

$$P(e|\gamma) = 2Q(\sqrt{2g_1\gamma}) - Q^2(\sqrt{2g_1\gamma}) + Q(\sqrt{2g_2\gamma}) - \frac{1}{4}Q^2(\sqrt{2g_2\gamma}) - Q(\sqrt{2g_1\gamma})Q(\sqrt{2g_2\gamma}) \quad (\text{A.24})$$

where $\gamma = |h|^2 \frac{E_s}{N_o}$ is the exponentially distributed r.v., $g_1 = (0.3716)^2$ and $g_2 = (0.23)^2$. The term $Q(\sqrt{2g_1\gamma})Q(\sqrt{2g_2\gamma})$ in (A.24) could be ignored with respect to the other terms.

0.4 Maximum Likelihood (ML) Decoding

ML decision rule from [17] for symbols x_1 and x_2 is calculated in the following. The received signal at PR after combining and de-interleaving for symbol x_1 is given as

$$r = c_1 x_1^R + j c_2 x_1^I + n \quad (\text{A.25})$$

where $a = c_1$, $b = c_2$. We already calculated the pdf of n as

$$P(n) = \frac{1}{2\pi\sigma^2\sqrt{c_1 c_2}} \exp\left(-\frac{n_R^2}{2c_1\sigma^2}\right) \exp\left(-\frac{n_I^2}{2c_2\sigma^2}\right). \quad (\text{A.26})$$

Applying ML rule and taking $Ln(\cdot) = \log_e(\cdot)$ in (A.26), x_1 can be decided from

$$\hat{x}_1 = \underset{x_1^R, x_1^I}{\operatorname{argmin}} (b|r^R - a x_1^R|^2 + a|r^I - b x_1^I|^2). \quad (\text{A.27})$$

After combining and deinterleaving the received signal at PR for the symbol x_2 is obtained as

$$r = c_2 x_2^R + j c_1 x_2^I + n \quad (\text{A.28})$$

where $a = c_1$, $b = c_2$. We already calculated the pdf of n as

$$P(n) = \frac{1}{2\pi\sigma^2\sqrt{c_1c_2}} \exp\left(-\frac{n_R^2}{2c_2\sigma^2}\right) \exp\left(-\frac{n_I^2}{2c_1\sigma^2}\right). \quad (\text{A.29})$$

By applying ML rule and taking $\text{Ln}(\cdot) = \log_e(\cdot)$ in (A.29) x_2 can be decided from

$$\hat{x}_2 = \underset{x_2^R, x_2^I}{\text{argmin}} (a|r^R - bx_2^R|^2 + b|r^I - ax_2^I|^2). \quad (\text{A.30})$$

0.5 Conditional Pairwise Error Probability (CPEP) Calculation

Here, CPEP for symbols $x_1 = x_1^R + x_1^I$ and $x_2 = x_2^R + x_2^I$ is calculated. Considering the symbol x_1 , CPEP can be expressed as:

$$P(x_1 \rightarrow \hat{x}_1 | h) = P[b|\hat{y}_{PR1}^R - a\hat{x}_1^R|^2 + a|\hat{y}_{PR1}^I - b\hat{x}_1^I|^2 < b|\hat{y}_{PR1}^R - ax_1^R|^2 + a|\hat{y}_{PR1}^I - bx_1^I|^2] \quad (\text{A.31})$$

where $h \in \{h_1, h_3, h_{31}, h_{32}\}$, respectively. By substituting (4.47) and (5.25) in (A.31) we have

$$\begin{aligned} P(x_1 \rightarrow \hat{x}_1 | h) &= P[b|ax_1^R + u_1^R - a\hat{x}_1^R|^2 + a|bx_1^I + u_1^I - b\hat{x}_1^I|^2 \\ &< b|ax_1^R + u_1^R - ax_1^R|^2 + a|bx_1^I + u_1^I - bx_1^I|^2]. \end{aligned} \quad (\text{A.32})$$

By simplifying we obtain the CPEP of x_1 as

$$\begin{aligned} P(x_1 \rightarrow \hat{x}_1 | h) &= P[b|a(x_1^R - \hat{x}_1^R) + u_1^R|^2 + a|b(x_1^I - \hat{x}_1^I) + u_1^I|^2 < b|u_1^R|^2 + a|u_1^I|^2] \\ &= P[b|a(x_1^R - \hat{x}_1^R) + u_1^R|^2 - b|u_1^R|^2 < +a|u_1^I|^2 - a|b(x_1^I - \hat{x}_1^I) + u_1^I|^2] \\ &= P[b(|a(x_1^R - \hat{x}_1^R) + u_1^R|^2 - |u_1^R|^2) < +a(|u_1^I|^2 - |b(x_1^I - \hat{x}_1^I) + u_1^I|^2)] \\ &= P[b(|a\Delta_R + u_1^R|^2 - |u_1^R|^2) < a(|u_1^I|^2 - |b\Delta_I + u_1^I|^2)] \\ &= P[b(a^2\Delta_R^2 + |u_1^R|^2 + 2a\Delta_R u_1^R - |u_1^R|^2) \\ &< a(|u_1^I|^2 - b^2\Delta_I^2 - |u_1^I|^2 - 2b\Delta_I u_1^I)] \\ &= P[ba(a\Delta_R^2 + 2\Delta_R u_1^R) < ab(-b\Delta_I^2 - 2\Delta_I u_1^I)] \\ &= P[(a\Delta_R^2 + 2\Delta_R u_1^R) < (-b\Delta_I^2 - 2\Delta_I u_1^I)] \\ &= P[(2\Delta_R u_1^R + 2\Delta_I u_1^I) < (-a\Delta_R^2 - b\Delta_I^2)] \end{aligned} \quad (\text{A.33})$$

where $\Delta_R = x_1^R - \hat{x}_1^R$ and $\Delta_I = x_1^I - \hat{x}_1^I$. CPEP for x_2 can be expressed as:

$$P(x_2 \rightarrow \hat{x}_2 | h) = P[a|\hat{y}_{PR2}^R - b\hat{x}_2^R|^2 + b|\hat{y}_{PR2}^I - a\hat{x}_2^I|^2 < a|\hat{y}_{PR2}^R - bx_2^R|^2 + b|\hat{y}_{PR2}^I - ax_2^I|^2]. \quad (\text{A.34})$$

where $h \in \{h_1, h_3, h_{31}, h_{32}\}$, respectively. Substituting (4.48) and (5.26) in (A.34) we could write

$$\begin{aligned} P(x_2 \rightarrow \hat{x}_2 | h) &= P[a|bx_2^R + u_2^R - b\hat{x}_2^R|^2 + b|ax_2^I + u_2^I - a\hat{x}_2^I|^2 \\ &< a|bx_2^R + u_2^R - bx_2^R|^2 + b|ax_2^I + u_2^I - ax_2^I|^2]. \end{aligned} \quad (\text{A.35})$$

After some calculation, CPEP can be expressed as

$$\begin{aligned}
P(x_2 \rightarrow \hat{x}_2|h) &= P[a|b(x_2^R - \hat{x}_2^R) + u_2^R|^2 + b|a(x_2^I - \hat{x}_2^I) + u_2^I|^2 < a|u_2^R|^2 + b|u_2^I|^2] \\
&= P[a|b(x_2^R - \hat{x}_2^R) + u_2^R|^2 - a|u_2^R|^2 < +b|u_2^I|^2 - b|a(x_2^I - \hat{x}_2^I) + u_2^I|^2] \\
&= P[a(|b(x_2^R - \hat{x}_2^R) + u_2^R|^2 - |u_2^R|^2) < b(|u_2^I|^2 - |a(x_2^I - \hat{x}_2^I) + u_2^I|^2)] \\
&= P[a(|b(\Delta_R) + u_2^R|^2 - |u_2^R|^2) < b(|u_2^I|^2 - |a(\Delta_I) + u_2^I|^2)] \\
&= P[a(b^2\Delta_R^2 + |u_2^R|^2 + 2b\Delta_R u_2^R - |u_2^R|^2) \\
&< b(|u_2^I|^2 - |u_2^I|^2 - a^2\Delta_I^2 - 2a\Delta_I u_2^I)] \\
&= P[ba(b\Delta_R^2 + 2\Delta_R u_2^R) < ba(-a\Delta_I^2 - 2\Delta_I u_2^I)] \\
&= P[b\Delta_R^2 + 2\Delta_R u_2^R < -a\Delta_I^2 - 2\Delta_I u_2^I] \\
&= P[2\Delta_R u_2^R + 2\Delta_I u_2^I < -b\Delta_R^2 - a\Delta_I^2] \tag{A.36}
\end{aligned}$$

where $\Delta_R = x_2^R - \hat{x}_2^R$ and $\Delta_I = x_2^I - \hat{x}_2^I$.

CURRICULUM VITAE

Name Surname: Mohammadreza Babaei

Place and Date of Birth: Tabriz/Iran

Address: Maslak/Istanbul

E-Mail: babaei@itu.edu.tr

B.Sc.: University of Tabriz, Telecommunication Engineering (2011)

M.Sc.: Istanbul Technical University, Telecommunication Engineering (2016)

Professional Experience and Rewards:

Researcher in TÜBİTAK Project No.114E607 (Cooperative Spatial Modulation Systems)

List of Publications and Patents:

PUBLICATIONS/PRESENTATIONS ON THE THESIS

- **Babaei M.** and Aygözü Ü. 2015: Spectral efficient and interference-free spectrum sharing in cognitive radio using signal space diversity. *IEEE International Black Sea Conference on Communication and Networking*, May 18-21, 2015 Constanta, Romania.
- **Babaei M.** and Aygözü Ü. 2016: A Cooperative Spectrum Sharing Protocol for Cognitive Radio Based on Space Diversity. *IEEE Conference on Signal Processing and Communication Applications-SIU*, May 16-19, 2016 Zonguldak, Turkey.
- **Babaei M.** and Aygözü Ü. 2016: Interference-free Spectrum Sharing in Cognitive Radio Based on Combined CIOD and STBC. *International Wireless Communication and Mobile Computing Conference- IWCMC*, Sept 05-09, 2016 Paphos, Cyprus.

